

EFFECTS OF WEATHERING ON PERFORMANCE OF  
INTUMESCENT COATINGS FOR STRUCTURE FIRE PROTECTION  
IN THE WILDLAND-URBAN INTERFACE

by

Babak Bahrani

A thesis submitted to the faculty of  
The University of North Carolina at Charlotte  
in partial fulfillment of the requirements  
for the degree of Master in  
Fire Protection and Administration

Charlotte

2015

Approved by:

---

Dr. Aixi Zhou

---

Dr. Stephen L. Quarles

---

Prof. Jeffrey T. Kimble



## ABSTRACT

BABAK BAHRANI. Effects of weathering on performance of intumescent coatings for structure fire protection in the wildland-urban interface  
(Under the direction of DR. AIXI ZHOU)

The objective of this study was to investigate the effects of weathering on the performance of intumescent fire-retardant coatings on wooden products. The weathering effects included primary (solar irradiation, moisture, and temperature) and secondary (environmental contaminants) parameters at various time intervals.

Wildland urban interface (WUI) fires have been an increasing threat to lives and properties. Existing solutions to mitigate the damages caused by WUI fires include protecting the structures from ignition and minimizing the fire spread from one structure to another. These solutions can be divided into two general categories: active fire protection systems and passive fire protection systems. Passive systems are either using pre-applied wetting agents (water, gel, or foam) or adding an extra layer (composite wraps or coatings). Fire-retardant coating treatment methods can be divided into impregnated (penetrant) and intumescent categories. Intumescent coatings are easy to apply, economical, and have a better appearance in comparison to other passive fire protection methods, and are the main focus of this study.

There have been limited studies conducted on the application of intumescent coatings on wooden structures and their performance after long-term weathering exposure. The main concerns of weathering effects are: 1) the reduction of ignition resistance of the coating layer after weathering; and 2) the fire properties of coatings after weathering since coatings might contribute as a combustible fuel and assist the fire growth after ignition.

Three intumescent coatings were selected and exposed to natural weathering conditions in three different time intervals. Two types of tests were performed on the specimens: a combustibility test consisted of a bench-scale performance evaluation using a Cone Calorimeter, and a thermal decomposition test using Simultaneous Differential Scanning Calorimetry (DSC) and Thermogravimetric Analysis (TGA) method (also known as SDT). For each coating type and weathering period, three different radiative heat flux levels were used in the combustibility tests. Data obtained from the tests, including flammability and thermal properties, were gathered, analyzed, and compared to non-weathered specimens.

The results revealed visible effects of weathering on pre (and up to)-ignition flammability and intumescent properties, especially decreases in Time-to-Ignition (TTI), Time-to-Intumescence ( $t_{\text{intu.}}$ ), and (maximum) Intumescence Height ( $H_{\text{intu.}}$ ) values in weathered specimens. These results showed that the ignition resistance of the coating layers decreased after weathering exposure. On the other hand, the obtained results from weathered specimens for the post-ignition flammability properties, especially Peak Heat Release Rate (PHRR) and Effective Heat of Combustion (EHC) did not show a noticeable difference in comparison to the non-weathered samples. These results demonstrated that the weathered coating layer would not likely to act as an additional combustible fuel to increase fire spread. In addition, results showed that the heat flux level increase greatly affected the intumescence mechanism in weathered specimens, where the mechanism did not follow the formation sequence and was stopped at a certain step. However, the threshold in which the sequence of intumescence mechanism was changed is not known yet.

## DEDICATION

To mom,

*Fereshteh Mostafavi Sabet,*

who taught me not only how to read and write, but also the alphabet of life.

To dad,

*Hassan Ali Bahrani,*

who passed on a great respect for education, and for all his supports.

## ACKNOWLEDGEMENTS

The preparation of this proposal was not possible without the guidance and consideration of my advisor, Dr. Aixi Zhou. He provided a motivating and friendly environment to conduct the research. I, hereby, give him my greatest appreciation not only for being a knowledgeable advisor, but also for being a great friend.

Besides, I would like to thank Dr. Stephen L. Quarles, my committee member and the senior scientist of the project, and other staff at the Insurance Institute for Business and Home Safety (IBHS) Research Center, for all their significant helps, and giving access to the research facilities. I thank Professor Jeffrey T. Kimble for serving as a committee member, and for his insightful comments. I also thank Dr. Katherine Weaver, the Material Characterization Laboratory (MCL) manager, for her valuable advices during the thermal analysis tests, and Dr. Tara L. Cavalline, the assistant professor in the Department of Engineering Technology and Construction Management, for her helpful comments. I also thank Mr. Parks Davidson, the research operation manager, and Mr. Eric Larson, the field service engineer at GBH International, for their assistance with the cone calorimeter maintenance.

My sincere thanks goes to my dear friend, Dr. Ning Tian, the former doctoral student at UNC Charlotte and current post-doctoral researcher at Ulster University, for all his help during this research.

Additionally, I thank the Engineering Technology and Construction Management Department and the Graduate School at UNC Charlotte, and the IBHS Research Center for providing the financial support for this research through grants and research assistantship opportunities.

Last but not the least, I express the deepest gratitude to my family for being helpful and patient, and for giving their endless love during my graduate study.

## TABLE OF CONTENTS

LIST OF TABLES	xiii
LIST OF FIGURES	xv
LIST OF SYMBOLS	xix
LIST OF ABBREVIATIONS	xxi
CHAPTER 1: INTRODUCTION	1
1.1 Problem Statement	1
1.1.1 Fire Basics	2
1.1.2 WUI Fire Problem	3
1.1.3 Structure Ignition in WUI Fires	6
1.1.3.1 Structure Ignition due to Radiation	6
1.1.3.2 Structure Ignition due to Convection	7
1.1.3.3 Structure Ignition due to Firebrands	7
1.1.4 Structure Survival against WUI Fires	8
1.1.4.1 Active Fire Protection Systems	10
1.1.4.2 Passive Fire Protection Systems	10
1.2 Objectives and Scope	11
1.3 Organization of the Thesis	13
CHAPTER 2: LITERATURE REVIEW	14
2.1 Fire Retardants	14
2.1.1 Fire Retardant Coatings	15

2.2 Intumescent Coatings	16
2.2.1 History and Development	17
2.2.2 Composition	17
2.2.3 Intumescence Mechanism	20
2.2.3.1 Chemical Mechanism	20
2.2.3.2 Physical Mechanism	23
2.3 Weathering Durability	27
2.3.1 Accelerated Natural Weathering	28
2.3.2 Laboratory Accelerated (Artificial) Weathering	28
2.3.3 Natural Weathering	28
2.3.3.1 Solar Energy	29
2.3.3.2 Temperature	30
2.3.3.3 Moisture	30
2.3.3.4 Atmospheric Contaminants	31
2.4 Effects of Weathering on Coatings	31
2.4.1 Material Degradation	32
2.4.2 Fire Performance	33
2.5 Significance of the Literature Review	36
CHAPTER 3: RESEARCH METHODOLOGY	37
3.1 Experiment Design	37
3.1.1 Samples	37

3.1.2 Intumescent Coatings	39
3.1.2.1 Dry Film Thickness and Wet Film Thickness	39
3.1.2.2 Preparation of Coatings	40
3.1.3 Weathering	41
3.1.4 Cone Calorimetry	44
3.1.5 Thermal Analysis	47
3.1.5.1 Simultaneous DSC and TGA (SDT)	48
3.2 Fire Test	48
3.2.1 Specimen Preparation	48
3.2.2 Cone Calorimeter Calibration	49
3.2.3 Testing and Data Collection	50
3.2.4 Collectible Parameters	54
3.3 Thermal Test	57
3.3.1 Sample Preparation	57
3.3.2 Testing and Data Collection	57
3.4 Preliminary Data and Data Analysis	58
3.5 Image Processing	58
<b>CHAPTER FOUR: RESULTS AND DISCUSSION</b>	<b>60</b>
4.1 Observations	60
4.1.1 Coating A	60
4.1.1.1 During the Weathering Period	60

4.1.1.2 During the Fire Test	61
4.1.1.3 During the Thermal Test	61
4.1.2 Coating B	61
4.1.2.1 During the Weathering Period	61
4.1.2.2 During the Fire Test	62
4.1.2.3 During the Thermal Test	62
4.1.3 Coating C	62
4.1.3.1 During the Weathering Period	62
4.1.3.2 During the Fire Test	63
4.1.3.3 During the Thermal Test	63
4.2 Flammability Properties	63
4.2.1 Time to Intumescence	63
4.2.1.1 Coating A	63
4.2.1.2 Coating B	67
4.2.1.3 Coating C	69
4.2.2 Maximum Intumescence Height	70
4.2.2.1 Coating A	70
4.2.2.2 Coating B	73
4.2.2.3 Coating C	74
4.2.3 Time to Ignition (TTI)	76
4.2.3.1 Coating A	78

4.2.3.2 Coating B	79
4.2.3.3 Coating C	82
4.2.4 Average Heat Release Rate (AHRR)	84
4.2.4.1 Coating A	84
4.2.4.2 Coating B	86
4.2.4.3 Coating C	88
4.2.5 Peak Heat Release Rate (PHRR)	89
4.2.5.1 Coating A	90
4.2.5.2 Coating B	91
4.2.5.3 Coating C	92
4.2.6 Effective Heat of Combustion	93
4.2.6.1 Coating A	94
4.2.6.2 Coating B	95
4.2.6.3 Coating C	96
4.3 Intumescence Mechanism during Combustibility Tests	97
4.4 SDT Thermal Tests	101
4.4.1 Coating A	102
4.4.2 Coating B	103
4.4.3 Coating C	104
CHAPTER FIVE: CONCLUSIONS AND RECOMMENDATIONS	107
5.1 Conclusions	107

5.2 Significance of Research	108
5.3 Recommendations for Future Research	109
REFERENCES	111
APPENDIX A: PRELIMINARY DATA	119
APPENDIX B: FIRE TEST DIAGRAMS	123
APPENDIX C: SIMULTANEOUS DSC/TGA DIAGRAMS	140
APPENDIX D: SAMPLE CONE CALORIMETER REPORT	146
APPENDIX E: THE MATLAB CODE	148

## LIST OF TABLES

TABLE 1: Largest wildland fires in the U.S. up to 2012	5
TABLE 2: Additive flame retardants vs. reactive flame retardants	14
TABLE 3: Flame spread classification	15
TABLE 4: Acrylic-based vs. epoxy-based intumescent coatings	17
TABLE 5: Common substances for catalysts, carbonifics, and spumifics	18
TABLE 6: Coating systems overview	40
TABLE 7: Preparation of the coatings	41
TABLE 8: Time intervals for the weathering tests	44
TABLE 9: Collected parameters in TGA and DSC tests	48
TABLE 10: Calibration gases	50
TABLE 11: Collectible flammability parameters	56
TABLE 12: $t_{\text{intu}}$ . average decrease/increase percentage during tests	64
TABLE 13: Effects on $t_{\text{intu}}$ .- coating A	66
TABLE 14: Effects on $t_{\text{intu}}$ .- coating B	68
TABLE 15: Effects on $t_{\text{intu}}$ .- coating C	70
TABLE 16: $H_{\text{intu}}$ . average decrease/increase percentage during tests	71
TABLE 17: Effects on $H_{\text{intu}}$ .- coating A	72
TABLE 18: Effects on $H_{\text{intu}}$ .- coating B	73
TABLE 19: Effects on $H_{\text{intu}}$ .- coating C	75
TABLE 20: TTI average decrease/increase percentage during tests	77

TABLE 21: Effects on TTI- coating A	79
TABLE 22: Effects on TTI- coating B	81
TABLE 23: Effects on TTI- coating C	83
TABLE 24: AHRR average decrease/increase percentage during tests	85
TABLE 25: Effects on AHRR- coating A	86
TABLE 26: Effects on AHRR- coating B	87
TABLE 27: Effects on AHRR- coating C	88
TABLE 28: Average PHRR decrease/increase percentage during tests	89
TABLE 29: Effects on PHRR- coating A	90
TABLE 30: Effects on PHRR- coating B	91
TABLE 31: Effects on PHRR- coating C	92
TABLE 32: EHC average decrease/increase percentage during tests	93
TABLE 33: Effects on EHC- coating A	94
TABLE 34: Effects on EHC- coating B	95
TABLE 35: Effects on EHC- coating C	96
TABLE 36: Results obtained from the SDT tests	102
TABLE 37: Raw data from the fire tests for uncoated specimens	119
TABLE 38: Raw data from the fire tests for coating A	120
TABLE 39: Raw data from the fire tests for coating B	121
TABLE 40: Raw data from the fire tests for coating C	122
TABLE 41: Guideline for plotted comparison diagrams	123
TABLE 42: AMLR average decrease/increase percentage during tests	125

## LIST OF FIGURES

FIGURE 1.1: The fire triangle	2
FIGURE 1.2: Structural ignition sources in WUI	6
FIGURE 1.3: Structural ignition assessment model (SIAM)	9
FIGURE 1.4: Structural survival chart	9
FIGURE 2.1: Steps in chemical mechanism of intumescent systems	21
FIGURE 2.2: Dehydration synthesis in presence of phosphoric acid	22
FIGURE 2.3: Intumescence formation mechanism chart	23
FIGURE 2.4.A: Step (1) heating started	24
FIGURE 2.4.B: Step (2) polymer softening, acid release, bubbles appear	25
FIGURE 2.4.C: Step (3) carbonization, pyrolysis, char appears	25
FIGURE 2.4.D: Step (4) foaming, solidification, intumescence appears	26
FIGURE 2.4.E: Step (5) ignition, release of combustion gases	26
FIGURE 2.5: Physical and chemical processes in flaming combustion of polymers	27
FIGURE 2.6: Absorption/desorption cycle	31
FIGURE 2.7: Apparent placement of the sun in the northern hemisphere	33
FIGURE 3.1: The plywood panel before cutting	38
FIGURE 3.2.A: Weathering fence schematic	42
FIGURE 3.2.B: Weathering fence, December 2014	42
FIGURE 3.2.C: Weathering fence, January 2015	43
FIGURE 3.2.D: Lateral schematic of the weathering fence	43

FIGURE 3.2.E: Weathering fence at noon sunlight- August 2015	43
FIGURE 3.3: A cone calorimeter schematic	45
FIGURE 3.4: Main calibration process stages	49
FIGURE 3.5: Exhausted and unused desiccants	51
FIGURE 3.6: Desiccant holder cap after testing	52
FIGURE 3.7: Cone calorimeter in the UNC Charlotte MFL	55
FIGURE 3.8: Sample collection for SDT tests- coating C	57
FIGURE 3.9: Image processing snapshot to obtain the intumescence height	59
FIGURE 4.1: Visible weathering effects on coating A	60
FIGURE 4.2: Visible weathering effects on coating B	62
FIGURE 4.3: Visible weathering effects on coating C	62
FIGURE 4.4.A: Average $t_{intu.}$ comparison bar-chart for coating A	65
FIGURE 4.4.B: Average $t_{intu.}$ comparison diagram for coating A	65
FIGURE 4.5.A: Average $t_{intu.}$ comparison bar-chart for coating B	67
FIGURE 4.5.B: Average $t_{intu.}$ comparison diagram for coating B	68
FIGURE 4.6.A: Average $t_{intu.}$ comparison bar-chart for coating C	69
FIGURE 4.6.B: Average $t_{intu.}$ comparison diagram for coating C	69
FIGURE 4.7: Maximum $H_{intu.}$ comparison bar-chart for coating A	72
FIGURE 4.8: Maximum $H_{intu.}$ comparison bar-chart for coating B	73
FIGURE 4.9: Maximum $H_{intu.}$ comparison bar-chart for coating C	74
FIGURE 4.10: Initial steps of intumescence formation for coating C	75

FIGURE 4.11.A: TTI comparison bar-chart for coating A	78
FIGURE 4.11.B: TTI comparison diagram for coating A	78
FIGURE 4.12.A: TTI comparison bar-chart for coating B	80
FIGURE 4.12.B: TTI comparison diagram for coating B	80
FIGURE 4.13.A: TTI comparison bar-chart for coating C	82
FIGURE 4.13.B: TTI comparison diagram for coating C	83
FIGURE 4.14: AHRR comparison bar-chart for coating A	84
FIGURE 4.15: AHRR comparison bar-chart for coating B	86
FIGURE 4.16: AHRR comparison bar-chart for coating C	88
FIGURE 4.17: AHRR comparison bar-chart for coating C	90
FIGURE 4.18: PHRR comparison bar-chart for coating B	91
FIGURE 4.19: PHRR comparison bar-chart for coating C	92
FIGURE 4.20: EHC comparison bar-chart for coating A	94
FIGURE 4.21: EHC comparison bar-chart for coating B	95
FIGURE 4.22: EHC comparison bar-chart for coating C	96
FIGURE 4.23: Main steps in intumescence mechanism	97
FIGURE 4.24: Coating A- south- 3-months weathered- HF=50 kW/m <sup>2</sup>	98
FIGURE 4.25: Coating A- south- 3-months weathered- HF=70 kW/m <sup>2</sup>	98
FIGURE 4.26.A & B: Coating B- south- 3-months weathered- HF=30 kW/m <sup>2</sup>	99
FIGURE 4.27: Coating B- south- 3-months weathered- HF=50 kW/m <sup>2</sup>	99
FIGURE 4.28.A & B: Coating C- north- 6-months weathered- HF=70 kW/m <sup>2</sup>	100

FIGURE 4.29: SDT result for coating A	103
FIGURE 4.30: SDT results for coating B	104
FIGURE 4.31: SDT results for coating C	105
FIGURE 4.32: Collected coatings from surface of the specimens	105
FIGURE 4.33: Comparison of the specimens at the end of the fire test	106

## LIST OF SYMBOLS

$A_S$	Nominal specimen exposed surface area	[m <sup>2</sup> ]
$C$	Calibration constant for oxygen consumption analysis	[m <sup>1/2</sup> kg <sup>1/2</sup> K <sup>1/2</sup> ]
$D$	Dry film thickness	[Mil]
$H_{intu.}$	Intumescence height	[mm]
$\Delta h_c$	Net heat of combustion	[kJ/kg]
$\Delta h_{c,eff}$	Effective heat of combustion	[kJ/kg]
$m$	Specimen mass	[kg]
$m_f$	Final specimen mass	[kg]
$m_i$	Initial specimen mass	[kg]
$\dot{m}$	Specimen mass loss rate	[kg/s]
$\dot{m}_e$	Exhaust duct mass flow rate	[kg/s]
$P$	Percentage of solids by volume	[-]
$q''_{tot}$	Total heat release rate	[kJ/m <sup>2</sup> ]
$\dot{q}$	Heat release rate	[kW]
$\dot{q}''$	Heat release rate per unit area (heat flux)	[kW/m <sup>2</sup> ]
$\dot{q}''_{max}$	Maximum heat release rate per unit area	[kW/m <sup>2</sup> ]
$t$	Time	[s]
$t_{ig}$	Time to sustained flaming	[s]
$t_{intu.}$	Time to intumescence	[s]
$t_p$	Time to peak heat release rate	[s]
$\Delta P$	Orifice meter pressure differential	[Pa]
$\Delta t$	Sampling time interval	[s]
$W$	Wet film thickness	[Mil]
$X_{CO_2^0}$	Initial CO <sub>2</sub> reading, mole fraction	[-]
$X_{CO^0}$	Initial CO reading, mole fraction	[-]
$X_{O_2^0}$	Initial O <sub>2</sub> reading, mole fraction	[-]
$X_{O_2^a}$	Ambien oxygen mole fraction	[-]

$X_{CO_2}$	CO <sub>2</sub> reading after delay time correction, mole fraction	[-]
$X_{CO}$	CO reading after delay time correction, mole fraction	[-]
$\rho$	Density	[kg/m <sup>3</sup> ]
$\varphi$	Oxygen depletion factor	[-]

## LIST OF ABBREVIATIONS

AHRR	average heat release rate
AMLR	average mass loss rate
ANOVA	analysis of variance
ASTM	American society for testing and materials
DSC	differential scanning calorimetry
DFT	dry film thickness
EHC	effective heat of combustion
FIGRA	fire growth rate
FPI	fire performance index
FTT	fire testing technology
HF	heat flux
HRR	heat release rate
HRRPUA	heat release rate per unit area
IBC	international building code
IBHS	insurance institute for business and home safety
ICAL	intermediate-scale calorimeter
ICC	international council code
ICTAC	international confederation for thermal analysis and calorimetry
ISO	international organization for standardization
MCC	microscale combustion calorimeter
MCL	materials characterization laboratory
MFL	materials flammability laboratory
ML	mass loss
MLR	mass loss rate

NFPA	national fire protection association
NIFC	national interagency fire center
NIST	national institute of standards and technology
NPS	national park service
NWCG	national wildland coordinating group
PHRR	peak heat release rate
SDT	simultaneous DSC and TGA
SIAM	structure ignition assessment model
SPR	smoke production rate
STA	simultaneous thermal analyzer
TGA	thermogravimetric analysis
THR	total heat released
TTI	time-to-ignition
USDA	United States department of agriculture
USFA	United States fire administration
USFS	United States fire service
WFT	wet film thickness
WUI	wildland-urban interface

## CHAPTER 1: INTRODUCTION

### 1.1 Problem Statement

Many structures have been damaged due to Wildland-Urban Interface (WUI) fires during the past years. Based on NFPA reports, the frequency and severity of wildland fires has continued to increase (NFPA, 2008).

Different methods have been used in order to prevent and/or delay the ignition in structures exposed to such fires. One way to increase the time-to-ignition (TTI) in the structures is applying fire-retardant coatings on the exterior surfaces. Although this method is not new, there are still many unknown parameters which affect the coatings' performance. Coatings are directly exposed to humidity, temperature difference, sunlight, and other weathering parameters, and their performance in different time intervals is not consistent. Studying the effects of these parameters during a certain period has been a main issue which has to be resolved.

This chapter serves as an introduction and presents the WUI fire problem together with fire prevention and fire protection procedures. Afterwards, passive fire protection systems with focus on intumescent coatings will be reviewed. The mechanism of action and important combustibility properties for the intumescent coating systems will come in the next step. The previous works related to intumescent coatings will be explained in the following. As the main goal, the effects of weathering on intumescent fire retardant coatings will be discussed in this thesis.

### 1.1.1 Fire Basics

Three main elements to initiate a fire are a heat source, a combustible fuel, and a sufficient amount of oxygen. These components are usually illustrated as the Fire Triangle (Figure 1.1).

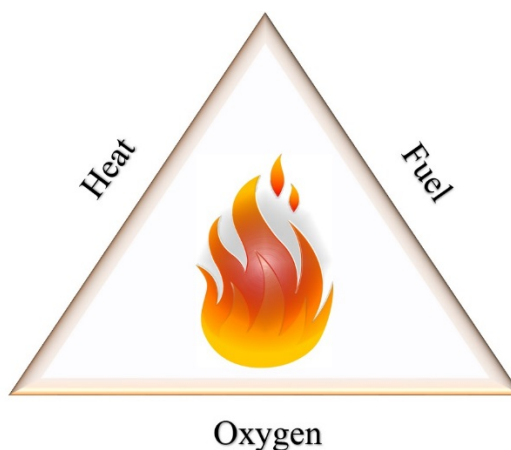


Figure 1.1. The fire triangle

In order to suppress or control a fire, at least one of the three bases on the fire triangle should be blocked. These three legs are discussed in detailed in the following.

Heat is transferred by three mechanisms: conduction, convection, and radiation. In wildland fires, convection (direct flame contact to the structures) and radiation (from flames to structures) occur. In some cases, the temperature rise caused by radiation is so high that combustibles (including vegetation and structures) can ignited before a direct flame contact or spotting (fire from burning embers) occurs.

In the WUI –based on location of the fuel- many materials can be fuels, including (but not limited to) structures, grasses, needles, leaves, brush and shrubs, trees, roots, branches, and hanging moss. Four key elements affect the fuel side (NIFC, 2015a), including: 1) the moisture content (which affects ignitibility of the fuel); 2) size and shape of the fuel; 3) quantity of combustible fuel; and 4) vertical arrangement of fuel. Note that there are four categories of fuels in term of vertical arrangement: 1)

ground fuels (combustibles below the ground); 2) surface fuels (combustibles at the ground level); 3) ladder fuels (combustibles just above the ground); and 4) aerial fuels (combustibles with more elevation from the ground) (NIFC, 2015a).

The other leg of the fire triangle is oxygen, which is necessary for oxidation process and burning continuation. Dry air in the atmosphere consists of 21 percent oxygen. Fire needs only 16 percent to burn (Wright and Singer, 2014). In addition to the three main elements, a set of self-sustained exothermic chemical chain reactions must occur. Oxygen supports such processes during a wildland fire. Note that chain chemical reaction can also be considered as a component to the other present elements. In this case, the fire triangle becomes the fire tetrahedron.

#### 1.1.2 WUI Fire Problem

WUI fires have threatened buildings worldwide for more than a century, and became more prominent in recent years. Wildland is defined as a region that except the roads, railroads, power lines, and similar transportation facilities, no significant development has occurred (NWCG, 2015). Following this definition, wildland fires are those non-structural fires that take place in vegetation or natural fuels (Masys, 2015). According to the United States Fire Administration (USFA), WUI is defined as a zone where structures and other human-development facilities meet the undeveloped wildland or vegetative fuels in nature (USFA, 2014).

WUI fires can be destructive, especially to those structures which are not treated or resistant to ignition and fire spread. In other words, structures with combustible exteriors and other vulnerable features, can be weaker against the WUI fires. These fires can have two different sources: natural ignition sources (like lava or lightning), and man-made ignition sources. According to the National Park Service (NPS) and National Interagency Fire Center (NIFC) reports, a great number of wildland fires in

the United States are human-caused. These include (but not limited to) unattended campfires left behind, acts of arson, and discarded cigarettes (NPS, 2012; NIFC, 2014).

Moreover, NFPA reports illustrate that although most of the wildland fires have an initial human reason, the most burnt areas are those where a natural reason (lightening and barely lava) has a significant role in such incidents. Near 16 percent of reported forest, woods, or wildland fires and 4 percent of natural vegetation fires between 2007 and 2011 were caused by lightening (Ahrens, 2013).

According to a NFPA report, of the top 10 fire-loss incidents in the last 100 years, 6 were WUI fires, all of which occurred within the last 20 years and in the western US (all but one in California). The overall adjusted loss in 2012 for these 10 wildland fires is nearly 11.5 billion dollars (NFPA, 2008). Some examples are the 1991 Oakland Hills fire, the 1998 fire in Florida, the 2003, 2007, and 2014 fires in southern California (San Diego area), and the 2012 Waldo Canyon Fire. The ten largest loss wildland fires in the U.S. up to 2013 are shown in Table 1.

Beside the elements previously mentioned for a fire initiation, three other parameters should be considered for fire's behavior in WUI fires: 1) fuel; 2) weather conditions (including wind, temperature, and humidity); and 3) the topography of the region (including shape, elevation, slope, and amount of shade and sunlight) (NIFC, 2015a). Even the steepness and the slope direction of hills have a significant role in WUI fire intensity. For instance, one side can be drier and the other side have vegetation with more moisture content based on the sunlight direction. Interaction between the basic elements and these components determines the probability of occurrence, intensity, duration, and magnitude of a WUI fire incident.

Table 1. Largest wildland fires in the U.S. up to 2012 (NFPA, 2013; NIFC, 2015b)

Year	Incident Name	Location	Significance
October 1918	Forest Fire	Cloquet, Minnesota	38 communities destroyed, 450 lives lost
June 1990	"Paint Fire" Goleta (Wildland/Urban Interface)	Santa Barbara, California	641 structures destroyed
October 1991	Oakland Fire Storm (Wildland/Urban Interface)	Oakland, California	25 lives lost and 2,900 structures destroyed
October 1993	Laguna Beach Fire (Wildland/Urban Interface)	Orange County, California	366 structures destroyed in 6 hours
May–June, 1998	Wildland Fire	Florida	Forced the evacuation of thousands of residents
May 2000	Cerro Grande Wildland Fire (Wildland/Urban Interface)	Los Alamos, New Mexico	235 structures destroyed and Los Alamos National Laboratory damaged
October 2003	"Cedar" Wildland Fire	Julian, California	2,400 structures destroyed, 15 lives lost
October 2003	"Old" Wildland Fire	San Bernardino, California	280 homes and more than 60 structures destroyed
October 2007	The Southern California Firestorm	San Diego County, California	1,600 homes, 800 outbuildings, and 253 structures destroyed
November 2008	Southern California Wildfires	Sacramento, CA	1958 structures destroyed
June 2012	Waldo Canyon Fire	Waldo Canyon, Colorado	346 homes burned, 2 lives lost
August 2013	Rim Fire	Rim, California	112 structures destroyed

Despite all mentioned above about the WUI fires destructive aspects, they are inevitable and essential for nature. Vegetation can be accumulated during time, and this

stack may prevent the growth of new plants. WUI fires can be beneficial and help the growth or re-growth of some plants.

### 1.1.3 Structure Ignition in WUI Fires

The three fundamental sources for the fire spread into and within the WUI fires are radiant exposure, direct flame contact, and burning firebrands. Two important factors should be considered to have a wildfire-safe residential structures (Quarles, et al., 2010): 1) wise selection of building materials and design; and 2) consider an adequate defensible space based on near-home vegetation. It is generally accepted that a structure's potential to ignite increases as the radiative, convective, and firebrand exposure increases (Cohen and Butler, 1996). Figure 1.1 shows a schematic of different structure ignition sources in WUI.

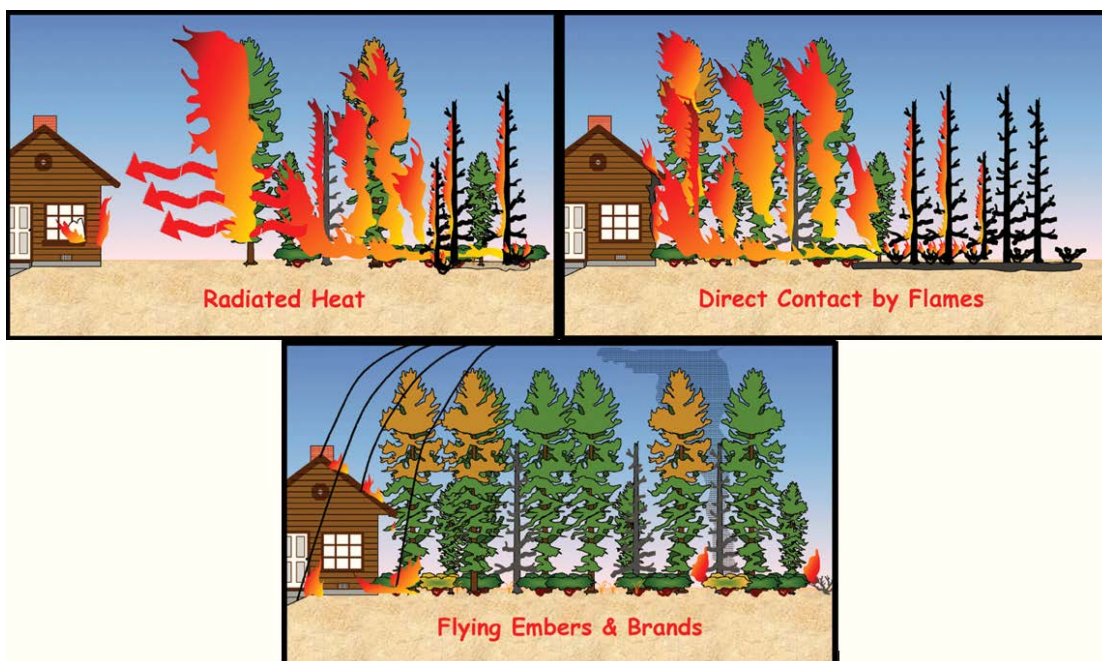


Figure 1.2. Structural ignition sources in WUI (Firewise, 2012)

#### 1.1.3.1 Structure Ignition due to Radiation

If the distance of a vegetation is more than 40 meters to a structure, ignition from flame radiation is unlikely to occur (Cohen and Butler, 1996). Although the effect

of radiation cannot be thoroughly neglected, a proper selection of vegetation helps to reduce it (Calkin, et al., 2014).

When the separation distance between fire and the structure increases, the radiant exposure decreases. In other words, the greater the distance between fuels, the less the ignition due to radiation. Note that regard to the nature of wood, if the radiant heat level is not high enough, and the exposure period to the radiation is not long enough, combustible structures will not ignite (Quarles, et al., 2010).

#### 1.1.3.2 Structure Ignition due to Convection

Catching fire through direct flame contact is how a structure gets ignited by convection. Direct flame is considered as a secondary source of ignition, not a primary one (Gollner, et al., 2015). This form of ignition could be either because of structure ignition itself, or direct contact of flame with combustible items near the building.

#### 1.1.3.3 Structure Ignition due to Firebrands

Firebrands (also known as burning embers) are generated by a main fire, a nearby flammable material, or nearby burning structures (Cohen, 2000b). Firebrands dispersed in the atmosphere and carried by the wind to several locations are the reason of spot fires which lead to urban fires (Manzello, et al., 2008). The magnitude of a fire caused by firebrands is directly related to the quantity, shape, size, and mass distribution of the embers. The amount of firebrands depends on the fire intensity and magnitude. Firebrands can ignite a structure in two ways: 1) accumulation on the outer surface of the structure; and 2) reach into the structure through a vent and ignite a combustible fuel (Hurley, et al., 2015).

There are three main mechanisms for firebrand spotting: generation, transport, and ignition of fuel at the landing position (Koo, et al., 2010). Regarding their study, burning embers may ignite the combustible construction material, the nearby plants, or

combustible items in a building. One thing to be considered is as the firebrands ignite a vegetation fuel, they make the fuel to another source of firebrand generation.

#### 1.1.4 Structure Survival against WUI Fires

WUI fire disasters depend on the amount of structures ignited during wildfires (Cohen, 2010). In other words, the WUI problem is a structural ignition problem. There are numerous factors which affect the fire spread rate and fire behavior during a wildland fire; such as vegetation (either near structures or nearby wildland vegetation), exterior materials of buildings exposed to the fire (especially decks and attics), topography, weather conditions, number of buildings at the time of fire spread, etc. It is important to know that the likelihood of a structure ignition depends on its physical attributes and fire exposure conditions (Mell, et al., 2010).

The question is, how do structures survive during a wildland-urban interface fire? The Structure Ignition Assessment Model (SIAM) was developed by the United States Department of Agriculture (USDA) Forest Service Fire Research, and can help to answer this question (Cohen, 1995). This model uses several components to calculate an index ignition risk for a structure, including the structure's general descriptions, potential fire characteristics around the structure, and the topography at the building site. The model go through several processing steps to compute the final risk index value, and the main components for the calculation comes in Figure 1.3.

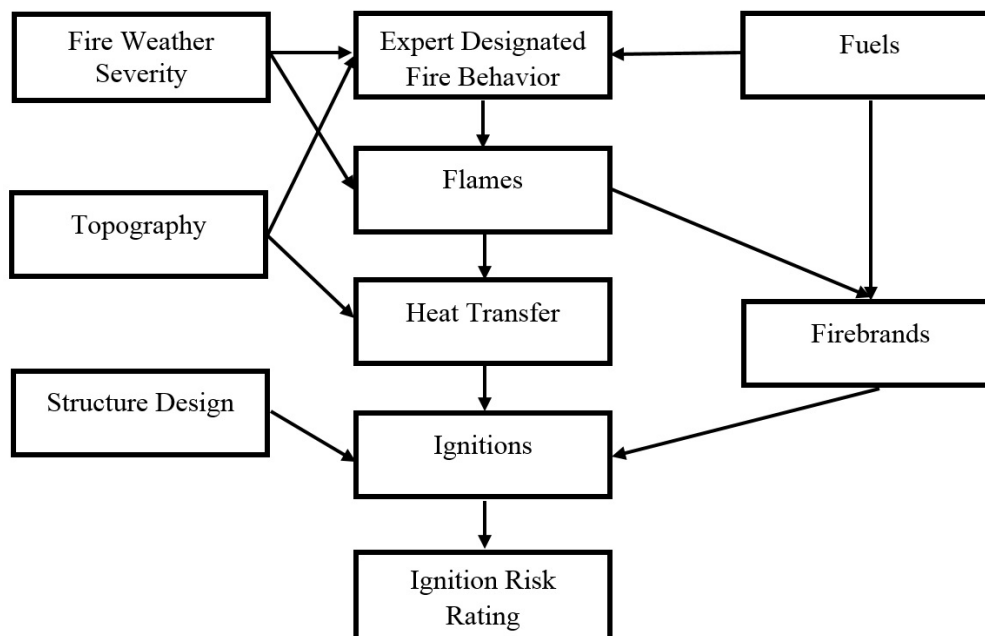


Figure 1.3. Structural ignition assessment model (SIAM) (Cohen, 1995)

Some experimental studies were also performed in order to validate the SIAM model, including window breakage tests and wall ignition tests in case of WUI fires. Cohen and Butler also developed the following flowchart for the structural survival:

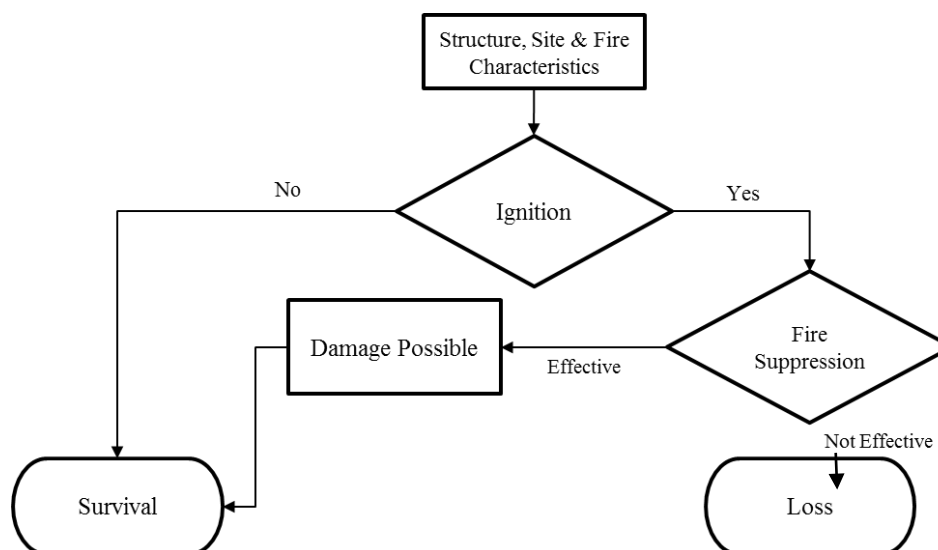


Figure 1.4. Structural survival chart (Cohen, 2000)

From the chart, damage to structures starts when ignition occurs. There will be less damage in case of effective fire suppression, as well. In conclusion, the lower a

structure's ignitibility, the lower the chance of occurring an effective ignition (Cohen, 2000).

Existing solutions to mitigate the structure damages caused by WUI fires (protect the structures from ignition, and minimize the fire spread from one structure to another) can be divided into two methods: 1) active fire protection; and 2) passive fire protection. The best result will obtain when there is a collaboration between active and passive fire protection systems.

#### 1.1.4.1 Active Fire Protection Systems

Active fire protection systems are those which distinguish, control, suppress, and/or extinguish a fire (Roach, 2014). The first step in such systems are detection through the presence of heat, smoke, and/or flames. Active fire protection systems can be operated automatically or manually, and include (but not limited to) fire extinguishers, sprinklers, fire and smoke alarm systems, and fire fighters. As mentioned before, a proper design of active fire protection systems along with maintained means of egress and well-treated constructions with fire resistant materials contributes bring a great level of financial saving and life (both for occupants and fire fighters) protection (Diamentes, 2010).

#### 1.1.4.2 Passive Fire Protection Systems

Passive fire protection systems do not interact with their surroundings, and need no external work. These systems provide an interface between the substrate (e.g. a structure exterior wall) and the fire. The main goal of using passive systems is to prevent/delay the ignition, and decelerate the fire growth and fire spread.

Passive fire protection system examples include using the pre-applied wetting agents (water, gel, or foam), adding an extra layer (composite wraps or coatings), and using fire dampers, fire doors, and fire walls.

In case of WUI fires, and to protect structures and their surroundings from three potential ignition sources (embers, surface fires, and crown fires), a fire protection concept was developed by Jack Cohen in late 1990's named the "Home Ignition Zone" (Firewise, 2014). According to this method, different zones around a structure are defined based on the structures characteristics and ignitability. Home surroundings divided into three zones based on distance (structure ignition, firebreak, and reduced fuel), and each zone has a certain preparation criteria.

Passive fire protection systems should be used in these zones to prevent/delay the fire growth and fire spread. Fire-retardant coatings (both impregnated-treated and intumescent-treated) are good products of choice in such cases.

## 1.2 Objectives and Scope

The objective of this research project was to evaluate the effect of weathering on the performance of intumescent coatings when applied to wood used on the exterior parts of residential structures. There are two main concerns, included: (a) the reduction of ignition resistance of the coating layer due to weathering, and (b) the fire behavior of the coating after weathering since it might become a combustible material that assists the fire spread or results in ignition and loss of the building.

In order to address the concerns, a set of wooden specimens were coated with intumescent fire retardant coatings and were exposed to natural weathering conditions in different time intervals. These specimens were tested with both a combustibility performance test using a cone calorimeter to evaluate the ignition potential, and a thermal degradation test using simultaneous TGA/DSC to evaluate the pyrolysis kinetics.

The intumescent paint-coated samples were provided by the Insurance Institute for Business and Home Safety (IBHS), including three intumescent fire retardant

coatings. Initially, controlled samples (which have not been exposed to weathering conditions) were tested, and results were considered as the baseline data. The next two set of specimens were weathered for 3-months and 6-months, respectively. Fire tests were performed following procedures set forth in ASTM E1354, and the results were analyzed and compared to the baseline data. In addition, thermal tests using thermogravimetric analysis (TGA) and differential scanning calorimetry (DSC) methods were performed on samples, and results are compared to examine the effects of weathering on decomposition kinetics of the coatings.

Based on demanded flammability properties for this study, the performance of coatings were evaluated in a bench-scale test method using the Cone Calorimeter at three different heat flux levels, 30 kW/m<sup>2</sup>, 50 kW/m<sup>2</sup>, and 70 kW/m<sup>2</sup>. Each of these heat flux level represent a certain condition: 30 kW/m<sup>2</sup> for low radiation exposures, 50 kW/m<sup>2</sup> representing the medium with heat flux level in corresponding to the developing fires (Schartel and Hull, 2007), and 70 kW/m<sup>2</sup> for higher heat flux levels which are possible to occur both in the WUI fires and burning buildings.

Compared to small-scale tests, such as Cone Calorimeter, large-scale methods are more expensive and/or demand more time to evaluate (Urbas and Shaw, 1993). Other calorimetry methods such as Microscale Combustion Calorimetry (MCC) and Intermediate-Scale Calorimeter (ICAL) have limitations to be used in this study. Examples of limitations are specimen mass range (for MCC) and vertical orientation of samples (for ICAL). Since intumescence height is one of the key parameters which needs to be measured in this study (in order to evaluate the performance of coatings after weathering), it is desirable that the specimens are tested in horizontal orientation to observe the intumescence growth more thorough.

### 1.3 Organization of the Thesis

There are five chapters in this thesis. This chapter provides an introduction, a brief background, and the problem statement. The second chapter is a comprehensive literature review which shows the necessity and significance of this research study, previous works, and existing gaps. The third chapter covers the experimental design for this research, i.e. the set-up, samples, standards, preparation, and preliminary data. The fourth chapter discusses the observations and results obtained in the study. In the fifth and final chapter, conclusions and recommendations are presented.

In addition, five appendices are also included. Raw data obtained from fire tests are presented in appendix A (following the format of ASTM E1354). Plotted comparison and bar-chart diagram for those flammability properties, which are not in the main body, come in appendix B. In appendix C, diagrams obtained from thermal degradation tests (TGA and DSC) are presented. Appendix D shows a sample report created by the cone calorimeter software, ConeCal 5.6. Finally, the Matlab code used for image processing to measure the intumescence height comes in appendix E.

## CHAPTER 2: LITERATURE REVIEW

### 2.1 Fire Retardants

Fire retardants are compounds added to materials such as surface finishes, textiles, and coatings that limit, suppress, or delay the production of flame in order to mitigate the fire spread and fire growth (Community, 2015). Note that flame and fire have different definitions; fire is a chemical reaction, and flame is the visible form of that reaction (NIFC, 2015). There is also a difference between a flame-resistant material and a flame-retardant material. Flame-resistant materials are inherently resistant to fire, but flame retardants are chemically treated materials which are added to various substrates (e.g. wood, steel, etc.) in order to decrease the flame spread and increase the time-to-ignition simultaneously. In general, there are two types of flame-retardants: additive, and reactive.

Table 2. Additive flame retardants vs. reactive flame retardants (SpecialChem, 2015)

<b>Additive Flame Retardants</b>	<b>Reactive Flame Retardants</b>
Added to polymer through physical mixing	Added to polymer via chemical reactions
Do not undergo any chemical reactions	Bind chemically (become a permanent part of the polymer after the reaction)
Can be combined into the polymeric mixture at any stage	Only can be combined during the early stages of manufacturing

As said before, there are two types of fire protection systems: passive fire protection (which is a heat barrier against the fire), and active fire protection (using an extinguishing agent). Fire retardant coatings are classified in the passive fire protection category.

### 2.1.1 Fire Retardant Coatings

Fire retardant coatings are used for three main purposes during the early stages of a fire: 1) Delay the time-to-ignition (TTI); 2) Reduce the heat release rate (HRR) during combustion; and 3) Limit the surface spread of flames (through controlling the flammability properties of combustible items).

In other words, fire retardant coatings are used to save lives by delaying the fire growth by means of modifying the fire kinetics at the early stages of a fire. On the other hand, fire-resistant materials limit the physical progression of fire by acting as a fire barrier during all stages of the fire (i.e., from early stages to post-flashover) (SpecialChem, 2015). According to NFPA 101, the flame spread index is divided into Class A, Class B, and Class C. The ranges for each flame spread class, as defined in NFPA 101, is shown in Table 3. Note that the flame spread index value is presented in Chapter 8 of the International Building code (IBC), as well (section 801).

Table 3. Flame spread classification (NFPA 101, 2015)

Class	Flame Spread Index
A	0-25
B	26-75
C	76-200

Previous studies have shown that adequately applied fire-retardant coatings will reduce the flame spread as well as decrease the fire growth period (Saxena and Gupta, 1990). Based on chemical composition and weathering exposure conditions, fire retardant coatings will be effective in certain heat flux ranges. In other words, each coating is designed for specific conditions and range.

Fire retardant coatings could be either coated on the surface (intumescent coatings), or impregnated into the wood (penetrant coatings). Intumescent coatings are more economical and easy to apply. Penetrant type of coatings require impregnated

chemicals which usually involves full-scale pressure treatment and can be expensive to prepare (NII, 2009).

## 2.2 Intumescent Coatings

Intumescent coatings (also known as reactive coatings) are thermal-resistant chemical compounds that can be applied to common building materials (such as wood and steel) in order to increase the time-to-ignition and maintain the strength of the structures during a fire. When the heat exposure reaches to a certain level, the coatings swell 20 to 50 times their as-applied dry film thickness and produce a carbonaceous protection layer on the material's surface. This char foam is an insulating barrier for the heat and oxygen, and will be effective until the layer is consumed by ignition (Lawrence, 2014).

While applying the coating, there is a base coat (primer) which provides a strong bond to the substrate, and a top coat which provides a durable finished surface (FPS, 2011). Intumescent coatings can be either Acrylic-based or Epoxy-based. The latter is used both for interior and exterior applications, and is more durable. Epoxy-based intumescent coatings are known to have better performance in corrosive environments (Bhatnagar, 1996). Acrylic intumescent coatings are either water-based or solvent based.

The main materials usually used in water-based intumescent coatings are amino formaldehyde resins, vinyl acetate, vinyl chloride copolymer, or acrylic latexes. On the other hand, solvent-based intumescent coatings usually consist of epoxies, polyurethanes, phenolic, alkyds, vinyl toluene-acrylate copolymers, and chlorinated rubbers (Pearce, 2012). Table 4 shows applications and differences between these two types.

Table 4. Acrylic-based vs. epoxy-based intumescent coatings (Boake, 2015)

Type		Description
Acrylic-based	Water-Based	<ul style="list-style-type: none"> <li>- Greener</li> <li>- Mostly used for interior applications</li> <li>- Takes more time to dry (in higher relative humidity and lower temperature)</li> <li>- Applied when relative humidity is between 40% and 60%</li> </ul>
	Solvent-Based	<ul style="list-style-type: none"> <li>- Mostly used for exterior applications</li> <li>- Dry sooner (may also dissolve prior layers if no adequate time between layers is considered)</li> <li>- More robust</li> <li>- Can be applied in a relative humidity up to 85%</li> </ul>
Epoxy-based		<ul style="list-style-type: none"> <li>- Appropriate for steel structures</li> <li>- More effective in corrosive environments (e.g. offshore and petrochemical industries)</li> <li>- Categorized as organic coatings</li> </ul>

### 2.2.1 History and Development

The word “Intumescent” is taken from the Latin word “intumescēns” and “intumescō”, which means “I rise”. The first intumescent systems were used in early 1980’s with a combination of melamine, ammonium polyphosphate, and melamine (Green, 1997). The first patent about intumescent coatings was published in 1938, but it took years to use them as a passive fire protection method, in late 1970’s (Bourbigot and Duquesne, 2007).

### 2.2.2 Composition

Intumescent flame retardant systems consist of three basic, active ingredients:

1) A carbon source (carbonific), which is the main component in char formation,

- 2) An acid source (a catalyst), which expands simultaneously and makes the intumescent reaction kinetically feasible (Bisschoff, 2000), and
- 3) A blowing agent (spumific), which produces gas and helps in foam formation.

In addition, a resin (binder) system is present. The binder helps to keep the compounds in contact with each other (Labuschagné, 2001). These four components act together to form the intumescent layer after certain chemical reactions have occurred. The common substances used as catalyst, carbonific, and blowing agent are shown in the following table:

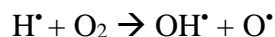
Table 5. Common substances for catalysts, carbonifics, and spumifics (Bourbigot and Duquesne, 2007)

<b>Catalyst (Acid Source)</b>	<b>Carbonific (Carbon Source)</b>	<b>Blowing Agent (Spumific)</b>
<ul style="list-style-type: none"> <li>- Ammonium Salts</li> <li>- Phosphates of amine or amide</li> <li>- Organophosphorus compounds</li> </ul>	<ul style="list-style-type: none"> <li>- Starch</li> <li>- Dextrins</li> <li>- Sorbitol, mannitol</li> <li>- Phenol-formaldehyde resins</li> <li>- Charring former polymers</li> <li>- Pentaerythritol, monomer, dimer, trimer</li> <li>- Methylol melamine</li> </ul>	<ul style="list-style-type: none"> <li>- Amines/amides</li> <li>- Melamine</li> <li>- Urea-formaldehyde resins</li> <li>- Polyamides</li> <li>- Dicyandiamide</li> </ul>

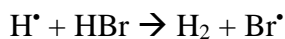
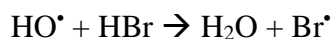
Several compounds can be used as intumescent coatings base, including (but not limited to) halogenated (bromine/chlorine) compounds, phosphorus compounds, organic nitrogen compounds, boron-based compounds, and antimony-based compounds (Visakh and Arao, 2015).

#### 1) Halogenated Compounds

The halogenated compounds reduce the combustion process through eliminating the radicals. The following reactions take place (Mouritz and Gibson, 2007):



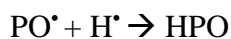
The mechanism for a bromine component (considering  $M^\bullet$  as the residue of organic molecule) will continue as below (Georlette, 2001):

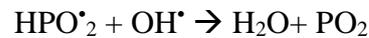
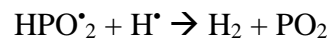
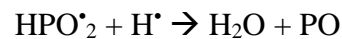
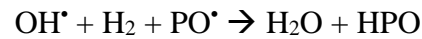


Among halogens, bromine and chlorine compounds are usually being used. Iodides are thermally unstable and fluoride compounds' effectiveness is too low (SpecialChem, 2015). Bromine compounds are also more reactive than the chlorine ones. However, a growing concern is the high level of toxicity in halogenated intumescent coatings.

## 2) Phosphorus Compounds

Similar to the halogenated intumescent coatings, "hydrogen and hydroxy radicals are replaced by less effective radicals or are rendered harmless by radical recombination in the gas phase" (Schartel, 2010). The main mechanism for phosphorus compounds was defined by Hastie and Bonnell (Hastie and Bonnell, 1980) and comes as following (Morgan and Wilkie, 2007):





### 3) Nitrogen Compounds

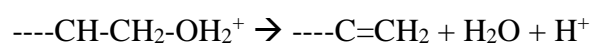
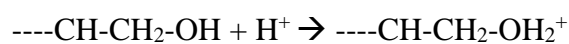
Nitrogen-based intumescent coatings are used widely regard to their environmental aspects. They produce less smoke and fewer toxic gases; in fact, the released gases of nitrogen-based compounds are ammonia and nitrogen. Cross-linking reactions occur in condensed phase in presence of melamine and prevents the formation of combustible gases (Kilinc, 2013). The polymer residue is easier to dispose and the smoke is less toxic (Horacek and Grabner, 1996).

#### 2.2.3 Intumescence Mechanism

Intumescence mechanism has both chemical and physical aspects. As the fire retardant coatings are exposed to a heat source, a series of chemical and physical reactions are initiated. These mechanism are described in detail in the following sections.

##### 2.2.3.1 Chemical Mechanism

Chemical reactions in intumescent coatings takes place in two phases: condensed phase and gas phase. As the heating begins, the binder/polymer starts to soften. The polymer starts to break down, and the acid releases from the acid source in a temperature below the polymer and carbonizing agent decomposition temperatures (Dasari, et al., 2013). These steps are known as depolymerization (Mount, 1994):



The chemical section consists of a series of reactions, comes in Figure 2.1.

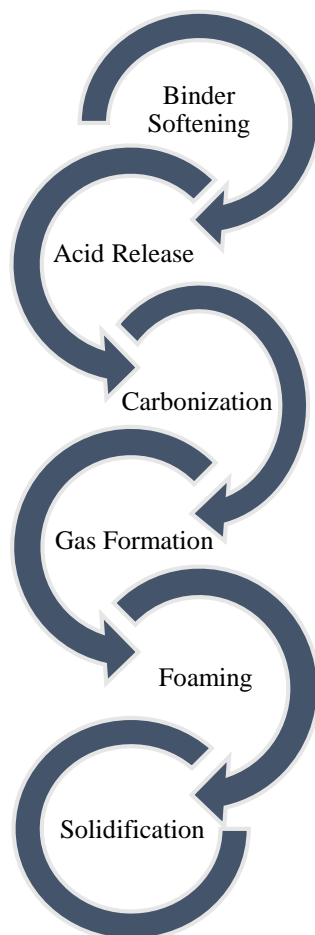


Figure 2.1. Steps in chemical mechanism of intumescent systems

Depolymerization process often occurs in high temperatures, and an increase of entropy. At the acid presence, the dehydration synthesis occurs; where monomers bind to remove water molecules. The producing acid reacts with the carbonific agent. Figure 2.2 shows dehydration in presence of phosphoric acid.

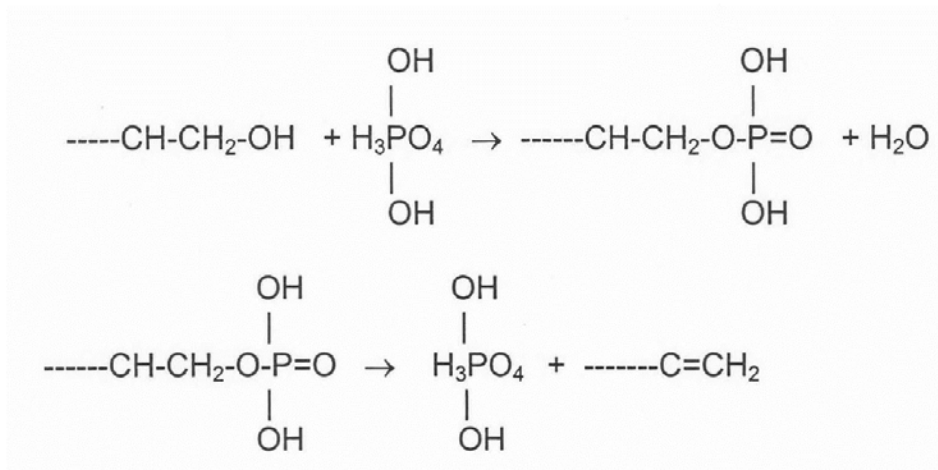
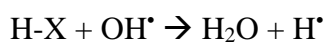
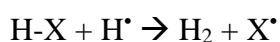
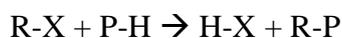


Figure 2.2. Dehydration synthesis in presence of phosphoric acid (Labuschagné, 2001)

In both reactions, a  $\text{---C=CH}_2$  fragment is produced in the polymer chain. These fragments are the reason of carbon-rich chars in the next steps (Labuschagné, 2001). Through an esterification process, a carbon residue (carbonaceous char) produces. Note that the char formation is not always a good option. The solid-phase combustion of char can cause sustained smoldering combustion (Beyler and Hirschler, 2002). Meanwhile, gases ( $\text{CO}_2$ / ammonia/ water vapor) are released by the blowing agent. The released gases are the reason of the foam forming. The final step is solidification, where the foam becomes solid through cross-linking and cyclizing reactions.

As described above, a chemical mechanism is present in the gas phase. The radical substitution reactions of the combustion products are being affected by the flame retardant degradation products. This means, the active radicals in the gas phase tend to combine with those radicals released from the flame retardant. The less the radicals, the less the created combustion is. These are the main reactions occur in the gas phase (SpecialChem, 2015):



A schematic of the process is shown in Figure 2.3.

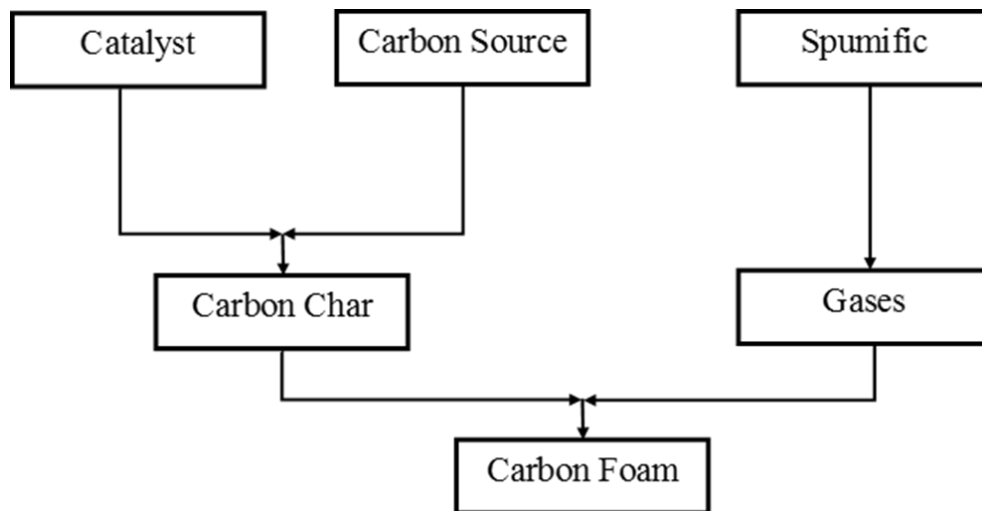


Figure 2.3. Intumescence formation mechanism chart (Stevens, 1999)

In other words, intumescent char has the following main functions:

- 1) Retarding the heat transfer and act as a thermal barrier (regard to its lower heat conductivity),
- 2) Limiting the access of oxygen from the atmosphere,
- 3) Maintain the structural integrity.

### 2.2.3.2 Physical Mechanism

In the physical aspect, the heat transfer from the heat source to the sample is being decreased due to the fire retardant's presence. Char formation lowers the rate of surface temperature increase beneath the char and decreases the oxygen diffusion to the site of combustion (Labuschagné, 2001). In between, the fuel flow (which is the pyrolysis gas from the material degradation) release is also decreased (SpecialChem, 2015). There are three main physical mechanisms for the fire retardant coatings:

1. Cooling Effect: The substrate cools down to a temperature below the required temperature to sustain the combustion process regard to the presence of the additives

2. Dilution: The gas mixture's lower ignition limit is not reached as the presence and reaction of the additives and inert substances dilutes the fuel in both solid and gas phases.

3. Protective Layer Formation: Due to exposure to heat, the coating layer swells. Combustible gases and tars transform to a low thermal conductive carbon protective layer which act as a barrier between heat source and the substrate. As mentioned before, this process decreases the polymer's degradation rate along with fuel flow reduction (Bourbigot and Duquesne, 2007).

The step-by-step progress of the intumescence forming (including both chemical and physical mechanisms) can be seen in Figures 2.4.a to 2.4.e.

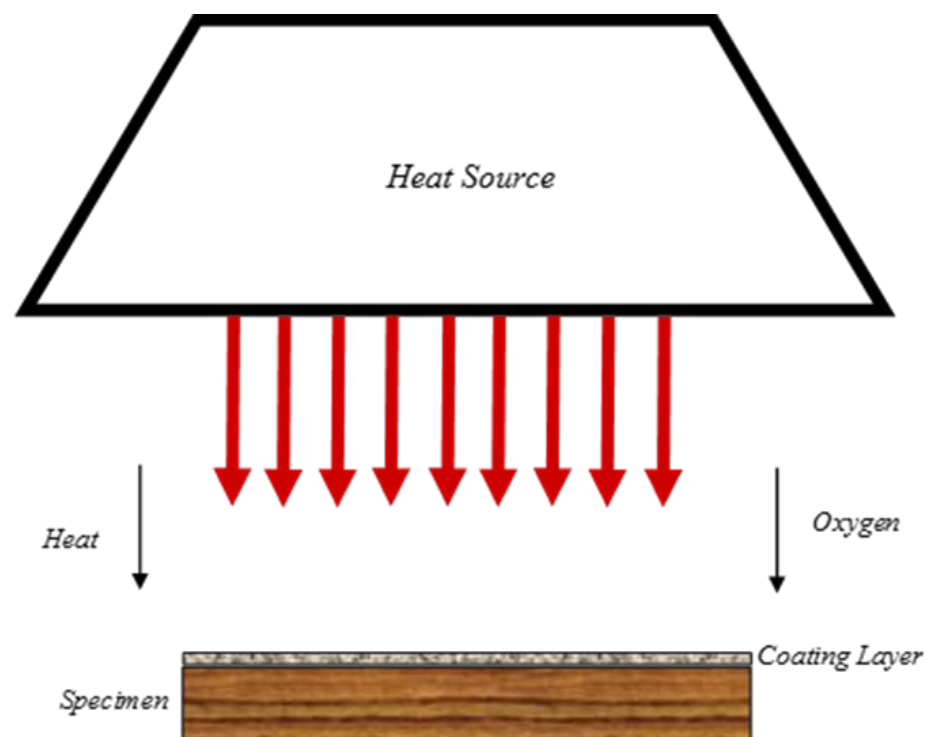


Figure 2.4.a. Step (1) heating started

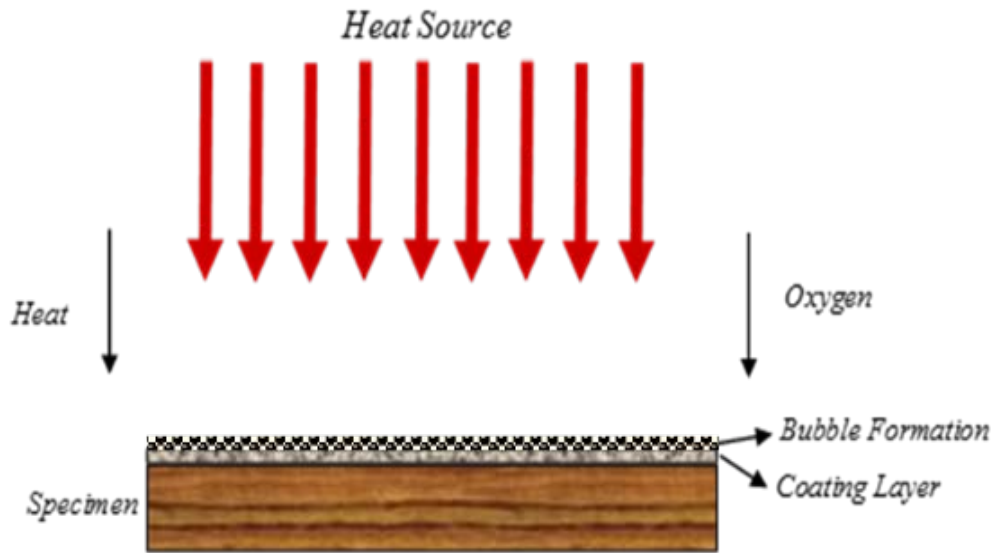


Figure 2.4.b. Step (2) polymer softening, acid release, bubbles appear

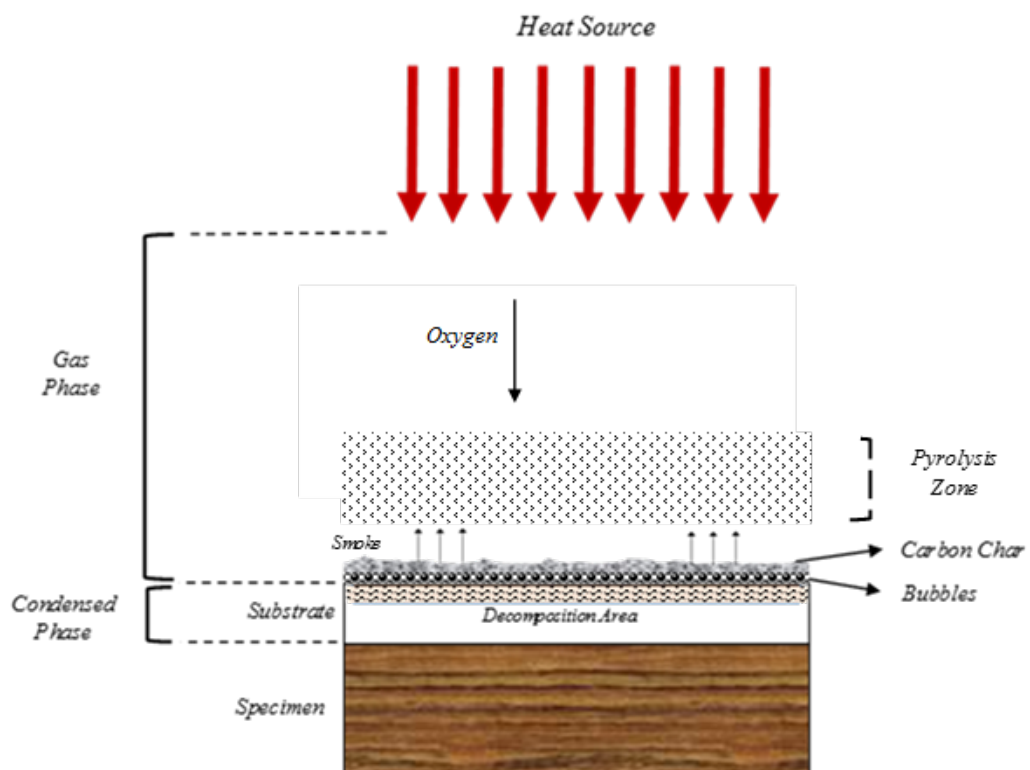


Figure 2.4.c. Step (3) carbonization, pyrolysis, char appears

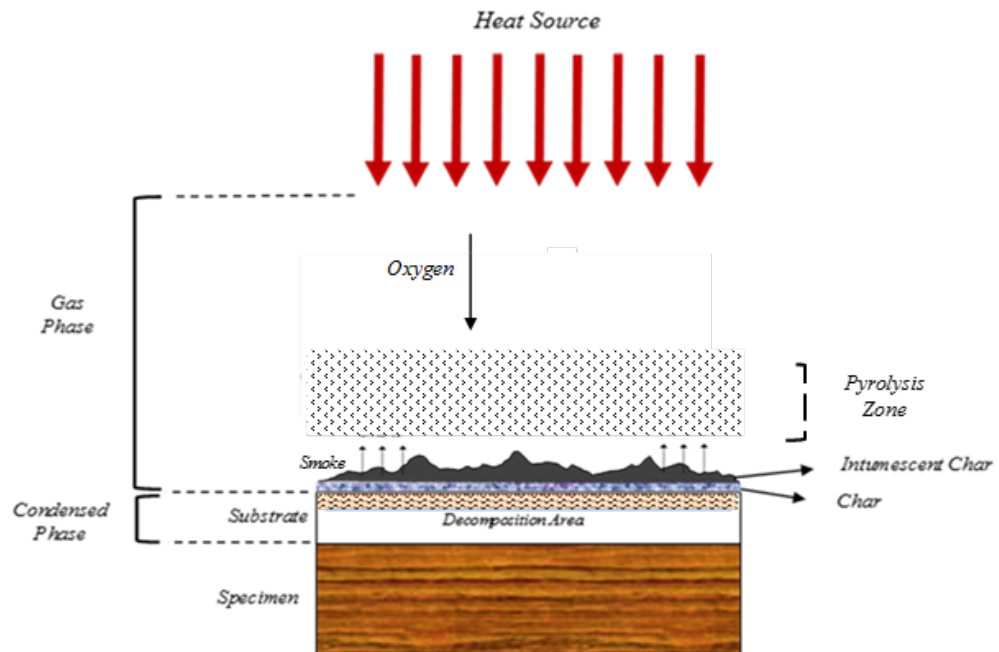


Figure 2.4.d. Step (4) foaming, solidification, intumescence appears

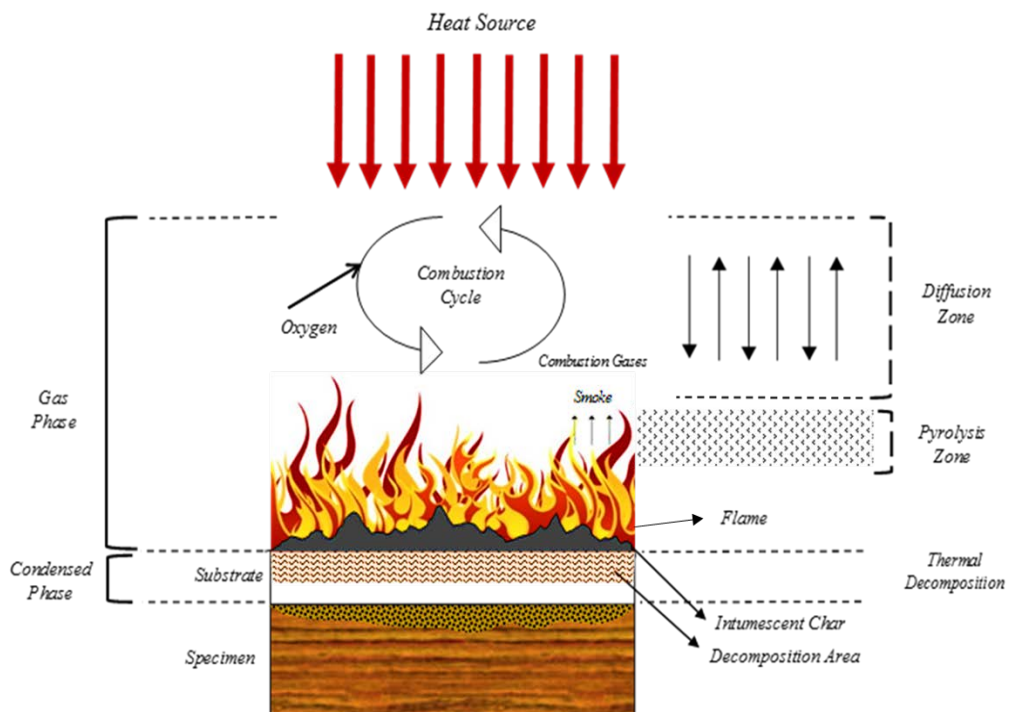


Figure 2.4.e. Step (5) ignition, release of combustion gases

Comparison between chemical and physical mechanisms in polymers is summarized in Figure 2.5. The mesophase in the physical section (left) is an interface between the gas and condensed phase during burning (Lyon and Jassens, 2005).

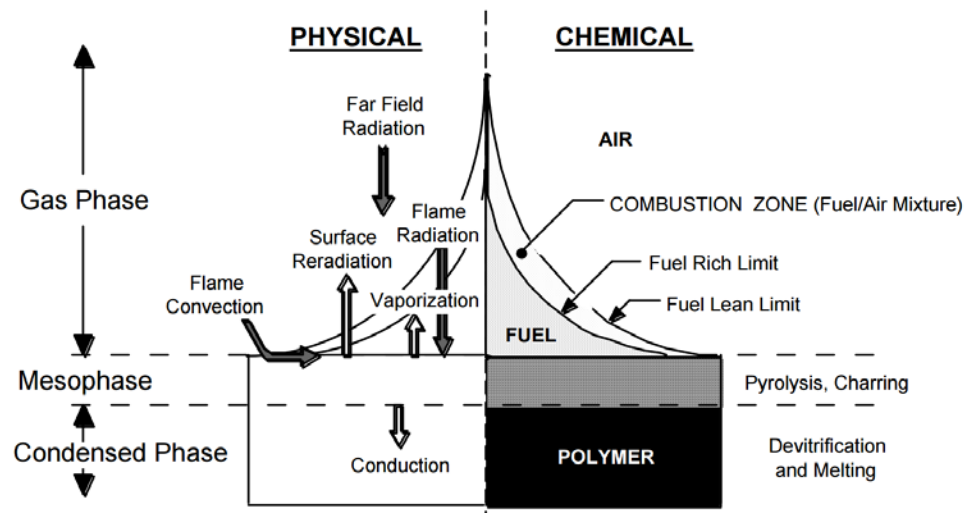


Figure 2.5. Physical and chemical processes in flaming combustion of polymers (Lyon and Jassens, 2005)

### 2.3 Weathering Durability

Weathering tests are used to evaluate the durability and degradation rate of coatings and materials under natural or laboratory conditions. The key weathering parameters are solar energy, temperature, and moisture. Environmental exposure methods are generally divided into three tests: natural weathering test, accelerated natural weathering test, and accelerated laboratory weathering test. The results of such test give a better understanding of the material in order to monitor the changes in material properties during weathering (Corrosionpedia, 2015).

Ignition-resistant building materials should maintain their performance required for weathering parameters (temperature, moisture, and ultraviolet radiation in accordance with the current available standards, including 1) ASTM D2898 (Method A) for fire-retardant-treated wood, wood-plastic composites, and plastic lumber

materials, 2) ASTM D7032 for wood-plastic composite materials, and 3) ASTM D6662 for plastic lumber materials (ICC, 2015).

### 2.3.1 Accelerated Natural Weathering

According to ASTM G113, accelerated weathering is an outdoor weathering using the sun as the source of irradiance, and to shorten the testing time, some parameters can be intensified by using other equipment (e.g. mirror to intensify the UV radiation) (ASTM G113, 2014). As an example, if weathering effects of a certain period needs to be simulated, an accelerated weathering test can be performed to accelerate the process.

### 2.3.2 Laboratory Accelerated (Artificial) Weathering

Exposing samples in outdoor tests for a long period of time does not always give a desirable result. Sometimes there is a need to obtain the results faster. In such cases, an artificial weathering test is the best option.

Specially designed weathering chambers using gas-discharge (xenon) lamps, electric (carbon) arc, or fluorescent lamps to simulate or accelerate the sunlight are used in laboratory accelerated weathering tests. Other weathering parameters including temperature and moisture can be manipulated in artificial weathering tests (McGreer, 2001). The main advantage of this method is the repeatability and reproducibility of tests, although the artificial weathering does not necessarily represent the natural conditions completely (Schulz, 2009).

### 2.3.3 Natural Weathering

According to ASTM G113, natural weathering is outdoor exposure of materials to non-concentrated sunlight in order to examine the environmental effects on other visual and functional parameters of the specimens (ASTM G113, 2014).

Natural weathering tests are generally performed outdoors on fixed-angle racks or fences in those locations with pre-defined orientations (e.g. northern and southern) to evaluate the effects of weathering components, particularly solar radiation (Searle, 2009). Three primary natural weathering factors are 1) solar energy, 2) temperature, and 3) moisture, along with secondary parameters such as atmospheric containments. Note that tests are normally designed so that the weathering effects are maximized for further evaluations. Usually it takes longer to see significant results in natural weathering testing conditions in comparison to other weathering testing methods.

#### 2.3.3.1 Solar Energy

The solar energy impact is consist of two parts: daylight (which is the absorbed energy directly from the sunlight beams), and skylight (the reflected diffusion from atmosphere). Solar irradiance is known to have the most impact among the four factors (solar energy, moisture, temperature, and atmospheric contaminants) on coatings; effects such as fading, color change, surface erosion, and loss of gloss (Quill and Fowler, 2015). Note that irradiance is defined as the radiant power per unit area incident on a receiver (ASTM G113, 2014).

There are several parameters which determines the impact of solar energy on the coatings; including intensity, exposure angle, elevation, and wavelength. Radiant energy from the sun is made up of photons that travel through space as waves (McGreer, 2001). The proportion of photon's energy and wavelength is inverse; means the longer the wavelength is, the lower the relative photon energy is. Radiation absorption leads to photochemical reaction on the surface of coatings. Based on the Grotthus-Draper law (known as the first law of photochemistry), only radiation absorbed in a system can produce a chemical change (Matafonova and Batoev, 2012).

### 2.3.3.2 Temperature

Either temperature rise or temperature drop have their own impacts on coatings. If the temperature drops below the dew point, dew forms and affect the coatings (comes in the next section). In case of temperature rise, the hydrolysis reaction quickens. Note that the hydrolysis resistance is an important criterion for good weathering properties of a paint film (Daniliuc, et al., 2012). As the temperature goes higher, the photochemical reactions occur faster and easier. Based on the Arrhenius equation, secondary (non-thermochemical) reactions (along with primary photochemical reactions) occur, which are subsequent reaction steps. The reaction rate approximately doubles with each 10 °C rise in material temperature (McGreer, 2001). The surface absorptivity varies based on the color; the darker the color, the more the absorption is. The amount of heat absorption (and consequently, temperature rise) depends on thermal conductivity and heat capacity of the surface.

### 2.3.3.3 Moisture

Based on location, atmospheric condition, and ambient temperature, there are various forms in which moisture can affect the coatings. These forms including (but not limited to) rain, hail, snow, dew, humidity, and frost (Searle, 2009). The night condensation-day solar drying cycle which repeats every day results in mechanical stress increase for exposed specimens. The exerted stress of this repetitive cycle (swelling-drying) can cause cracking, bond separation between the coating and substrate, and deformation (Searle, 2009). In addition, if moisture seats on the coatings for a notable period, it may act as a solvent. In contrast to water absorption, layers can also lose water. This loss leads to contraction tendency in layers and the surface, and finally cracks and fractures appear on the surface. The last effect of moisture on the coatings is the freeze-thaw cycle (McGreer, 2001). Water in the inner layers of

specimens can freeze, and cause expansion. This expansion exert stress to the outer layers, and contribute to cracking and peeling. The absorption/desorption process simply comes in Figure 2.6.

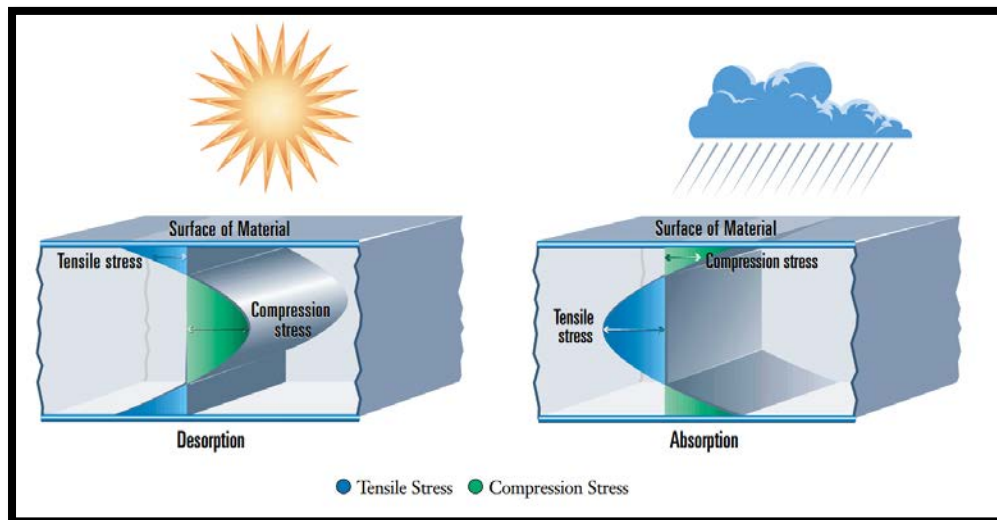


Figure 2.6. Absorption/desorption cycle (McGreer, 2001)

#### 2.3.3.4 Atmospheric Contaminants

There are numerous contaminants and pollutants presented in the atmosphere. Generally, these pollutants can be divided into two parts: first, the industrial pollutants (such as NOX, Sulphur oxides, and hydrocarbons), and second, particulates (such as dirt, soot, sand, and dust) (Searle, 2009). Each of these pollutants can individually or in combination with another weathering factor (like moisture) affect the coatings. Those combination which forms an acid (like acid rains) can react rapidly with polymeric compounds and cause cross-linking (Wu, 1982) and embrittlement (Ripling, et al., 1971) along with changes in color.

#### 2.4 Effects of Weathering on Coatings

Several passive fire protection systems are currently used to protect industrial/residential structures. However, exposure to different environmental conditions may affect the performance of such systems. Different weathering parameters such as sunlight radiation, moisture, temperature, and being in a corrosive

environment are all the reasons for the change in behavior of such systems. Fire retardant coatings take the aforesaid influences as one of the most applicable passive fire protection systems.

There are two main concerns regard to the effects of weathering on the performance of the fire retardant coatings:

- 1) Being exposed to weathering conditions may reduce the ignition resistance of the coating,
- 2) The coating layer may become a combustible fuel itself for the structure ignition and increase the fire growth after ignition, and the fire may spread to nearby structures.

#### 2.4.1 Material Degradation

Material degradation under weathering starts by the direct sunlight radiation. Azwa and others stated that this radiation breaks the organic bonds in the polymers, and come with many circumstances such as color fading, weight loss, surface roughening, mechanical property deterioration, and embrittlement (Azwa, et al., 2013). Degradation starts when the amount of absorbed energy exceed the bond energy. Note that the resistibility of an intumescent coating is determined when the foam layer is stable and there is no sign of cracks in it (Thewes, 2009).

Considering the orientation, objects located toward south to north in the northern hemisphere, absorb more sunlight beam in the southern part rather than the north. This is caused by the sun path during different seasons. The apparent placement of the sun in the northern hemisphere is shown in Figure 2.7. Note that a weathering fence (which is used in this research) has been added to the original figure.

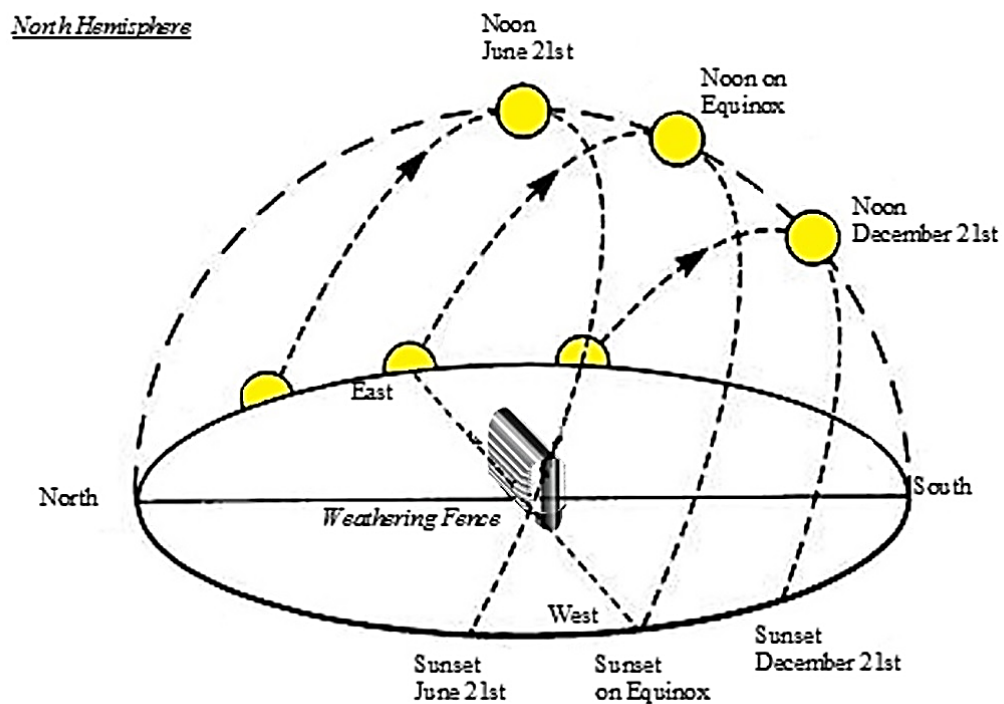


Figure 2.7. Apparent placement of the sun in the northern hemisphere (Foundation, 2012)

#### 2.4.2 Fire Performance

It should be mentioned that the synergy of all aforementioned weathering effects leads to degradation of the intumescent coatings. There are very limited studies on the effects of weathering fire performance of intumescent coatings. Harada and others conducted research on impregnated fire retardant coatings, using four different kind of specimens to examine combustibility, weatherability, and retaining fire-retardant chemicals against leaching after 2000 hours of accelerated weathering. Their study showed that pigmented and penetrated coatings had the best performance in the fire test (Harada, et al., 2009).

Another study conducted by Vahabi and colleagues determined the effects of ageing on the fire behavior of flame-retarded polymers. They considered six parameters as the most important ones to modify the fire behavior: temperature, moisture, UV radiation, ionizing radiation, chemical solvent, and physical stress. Their main

suggestion was using stabilizers to limit the influence of ageing on flame retardancy. They also discussed the above parameters one by one, and pointed out that radiation ageing and the effect(s) of recycling on the fire performance of coatings should be studied more concisely as there were not adequate literature in these areas (Vahabi, et al., 2015).

Roberts and others conducted a 10-year study on six epoxy intumescent and one cementitious PFP product for steel structures. Although the focus of the study was on offshore structures, and considering corrosion as the main problem of such structures, the results are significant and in some cases, their recommendations are similar to the wood-based studies, including proper treatment of edges and proper preparation of the substrate (Roberts, et al., 2010).

Holmes (Holmes and Knispel, 1981) also conducted a 5-year study on wood shingles and shakes. The significant and acceptable results for his study were obtained after two years of exposure, except the reference pyrestone treatment. They tested the specimens by burning brand and modified Schlyter. The Schlyter test is a method to measure the vertical flame-spread characteristics of a material, and useful for fire-retardant coating evaluation (Pearce, 2012). All systems showed weakness in the Schlyter test.

Daniliuc and others (Daniliuc, et al., 2012) conducted a comparison study on exterior coatings in which the polyester composition was the investigated parameter. They performed hydrolysis resistance tests, UV synthesis tests, and TGA tests on various samples, including weathered QUV (accelerated weathering) ones after 2016 hours of weathering. They also exposed specimens to natural weathering for 15 months. The results showed visual damage (at later stages), and decrease of performance. In addition, they tested specimens painted with intumescent coatings, and artificially

weathered for 240 hours. In this test, “Pentaerythritol (PER) was brought by encapsulation of ammonium polyphosphate (APP) to its immediate proximity” in order to increase the fire retardant performance. Their results showed that the absence of inorganic salts can be replaced by applying a topcoat. However, based on their fire tests, the topcoat reduced the fire-protection performance. Finally, they suggested that increasing the filling grade of intumescent additives can lead to a better fire-retardant performance.

A 10-year study on the effectiveness of fire-retardant treatment for shingle was conducted by LeVan and Holmes. Coatings were either pressure-impregnated or coated on the surface of the shingles. They examined the effectiveness of fire-retardant treatment in four different time intervals: non-weathered, after 2, 5, and 10 years. They performed two tests: a Class C burning-brand test (based on ASTM E108), and a Schlyter flame-spread test. The results showed that most specimens passed the Class C burning test after 10 years, but they did not have an acceptable performance in the Schlyter test (LeVan and Holmes, 1986).

Jimenez et al. (2013) conducted a study on ageing effects on an epoxy-based intumescent coating which was applied on steel coatings. They exposed one set of samples to accelerated weathering conditions at 80% moisture content and 70°C for 2 months, and immersed the other set in a bath with and without NaCl (5 g/L) at 20°C for one month. Both sets were tested with a small-scale furnace (heat flux level = 35 kW/m<sup>2</sup>), and results showed a decrease in failure temperature for steel specimens, and no intumescence formation after immersion and weathering exposure.

## 2.5 Significance of the Literature Review

Summarizing all the previous sections in this chapter and reviewing the previous studies, it is important to point out that the weathering and ageing effects on intumescent fire retardant coatings with wooden substrates have not been thoroughly studied.

Although some remarkable studies were conducted on the impregnated fire retardant coatings, there is no such study for intumescent coatings. In addition, the effect of heat flux level rise on physical and chemical mechanism of intumescence is not completely known. The objective of this study is to fulfill the current gap in intumescent systems performance evaluation, and provide a better understanding on the effects of various HF levels on intumescent coatings.

## CHAPTER 3: RESEARCH METHODOLOGY

### 3.1 Experiment Design

To examine the weathering effects on intumescent coatings, three different coatings with different weathering capabilities (claimed by manufacturers) were selected. Prepared specimens (with plywood substrates and intumescent coatings) were placed on an aluminum-frame fence and exposed to natural weathering conditions. To examine the fire performance and thermal degradation rate of the specimens after different weathering periods, bench-scale combustibility tests using a cone calorimeter and thermal analysis degradation test using SDT method were performed.

#### 3.1.1 Samples

Both substrate and fire retardant coatings were prepared for tests, plywood samples as base (substrate) and intumescent coatings as fire retardants. In general, plywood is made out of three or more layers. Based on quality, layers are graded by different letters (in sequence from best quality to the worst): A, B, C, and D. Note that these veneer grade letters only show the visual characteristics of the wood, not the structural and/or applications. Where there is a combination of letters, the first letter shows the exposed face grading, and the second one is the reverse face (Crooks, 2011). The middle layers in plywood are not graded.

The wooden samples used in this research were made of AC grade southern yellow pine 4-ply plywood. Samples came in three 98"×46" (2490 mm × 1170 mm) panels. Each panel was cut into eleven 88"×4" (2235 mm × 100 mm), and 121 of 8"×4"

(200 mm × 100 mm) pieces afterward. Finally, a total of 363 specimens out of 3 panels became ready (121 specimens per panel). Samples were prepared and cut in the IBHS research center. Note that the top and the right edges of the wooden panels -which are illustrated in a darker color in Figure 3.1- represent those specimens which were discarded. Consequently, no tested specimen has the following numbers:

- Panel (1): 1 to 11, 12, 23, 34, 45, 56, 67, 78, 89, 100, 111;
- Panel (2): 122 to 132, 133, 144, 155, 166, 177, 188, 199, 210, 221, 232;
- Panel (3): 243 to 253, 254, 265, 276, 287, 298, 309, 320, 331, 342, 353.

A schematic of aforesaid panel is shown in Figure 3.1.



Figure 3.1. The plywood panel before cutting

The initial measuring of the specimens were 8'' (200 mm) longitudinal × 4'' (100 mm) lateral, and each cut in half after the accelerated weathering period. Therefore, they are measuring 4'' (100 mm) longitudinal × 4'' (100 mm) lateral × ¼'' (12.5mm) vertical for the fire test. The specimens were selected using a random allocation process in the IBHS research center, where each 4'' × 8'' (100 mm × 200 mm) sample was given a number base on: 1) weathering orientation; 2) radiant heat exposure level; and 3) exposure weathering time (comes in Table 8). Based on the number of available

samples, the average of 32 specimens were considered for each weathering period. All specimens were finished with one of the coatings presented in Table 6.

### 3.1.2 Intumescent Coatings

As mentioned before, fire retardant coatings could be either coated on the surface (intumescent coatings), or impregnated into the wood (penetrant coatings). The three coatings used in this study are intumescent type, including TPR<sup>2</sup> Fireshell Ultra F1EP (Structure Saver<sup>®</sup>), FirePoly<sup>™</sup> FP100, and FireSheath<sup>™</sup>.

#### 3.1.2.1 Dry Film Thickness and Wet Film Thickness

There are two different types of film thickness for coatings: dry film thickness (DFT) and wet film thickness (WFT). The difference is in the solid content, which is represented in weight (or volume). DFT is the thickness of a coating which is applied on the surface, and WFT is the thickness of wet paint or any liquid-based coating. It can be a single layer or multiple layers; based on the manufacturer recommendation and/or the research need. If more than one layer is applied, adequate timing should be considered before applying the next layer so that the first layer have adequate time to become dry (normally provided by the manufacturer). DFT is the most important parameter which determines the durability of a coating (Francis, 2009). The thickness should be measured after the coatings gets dry. The unit for measuring the dry film thickness is Mil, which is equal to 1/1000 of 1 inch.

The solid content represents the amount of material remaining on the surface after the coating treated (Hinojosa, 2009). The following equations show the relation between wet film thickness and dry film thickness:

$$D = W \times P, W = D / P \quad \text{Equation (1)}$$

where:

D = Dry film thickness [Mil]

W = Wet film thickness [Mil]

P= Percentage of solids by volume

The percentage of solids by volume (P) should be expressed as a decimal less than 1 (CEI International, 2012). Having the WFT, the coverage of each layer of the coatings can also be calculated as the following (consider each gallon equals 231 cubic inches):

$$\text{Coverage [ft}^2\text{/gal]} = 1604.17 / W \text{ [Mil]} \quad \text{Equation (2)}$$

### 3.1.2.2 Preparation of Coatings

The C-grade side (along the four edges) was painted with one layer of regular, semi-gloss white paint and primer. The purpose to paint the edges along the C-grade surface was to protect them from the weathering effects, and prevent fire propagation from them since only the exposed surface to the heat should be tested. The front faces (A-grade side) of the specimens were finished with one out of three available intumescent coatings: (A), water-based, non-flammable, non-toxic coating, (B), latex-based coating, and (C), water-based, non-combustible coating. Specimens finally cut into two 4"×4" (100 mm × 100 mm) pieces; one labeled and stayed in the research center, and the other was used for the fire test.

Table 6. Coating systems overview

Coating System	Description (Per Manufacturer's Instructions)	Primer	Coating	Coating
		Number of Layers	Number of Layers	Dry Film Thickness [Mil]
A	Water-based intumescent coating (w/formaldehyde, non-flammable)	2	1	4
B	Latex-based intumescent coating	0	1	9
C	Water-based intumescent coating, non-combustible	2	2	12 to 18

There are three ways to apply intumescent coatings on a wood specimen: brush, roller, or an airless spray. In this experiment, a regular brush was used. Table 5 shows

the application of the coatings in detail. The table was prepared based on information initially prepared by the IBHS Research Center.

Table 7. Preparation of the coatings

Label	Mfg. Application Rate [ft <sup>2</sup> /gal]	Sample Area [ft <sup>2</sup> ]	Weight / gallon [lb]	Application Rate to each 4"x 8" Sample [g]	Dry Film Thickness [Mils]	Notes
A	120	0.25	12.1	11.4	4	3 layers of coating
B	150	0.25	10.4	7.9	9	1 layer of coating
C	125	0.25	11	10	12 to 18	1 to 2 layers of coating

### 3.1.3 Weathering

All the specimens (coated and uncoated) stood on a metal weathering test fence in order to expose the natural weathering conditions (Figure 3.2(a)). The fence can hold a total of 1232 specimens, divided equally in the northern and southern sections. Specimens were prepared to be weathered in 9 different time intervals; including: non-weathered, 3-months weathered, 6-months weathered, 12-months weathered, 18-months weathered, 24-months weathered, 30-months weathered, 48-months weathered, and 60-months weathered. Note that this study was planned for 5 years, but interim results may modify the original research design in term of duration. Figures 3.2(a) and 3.2(b) show a schematic of the weathering fence:

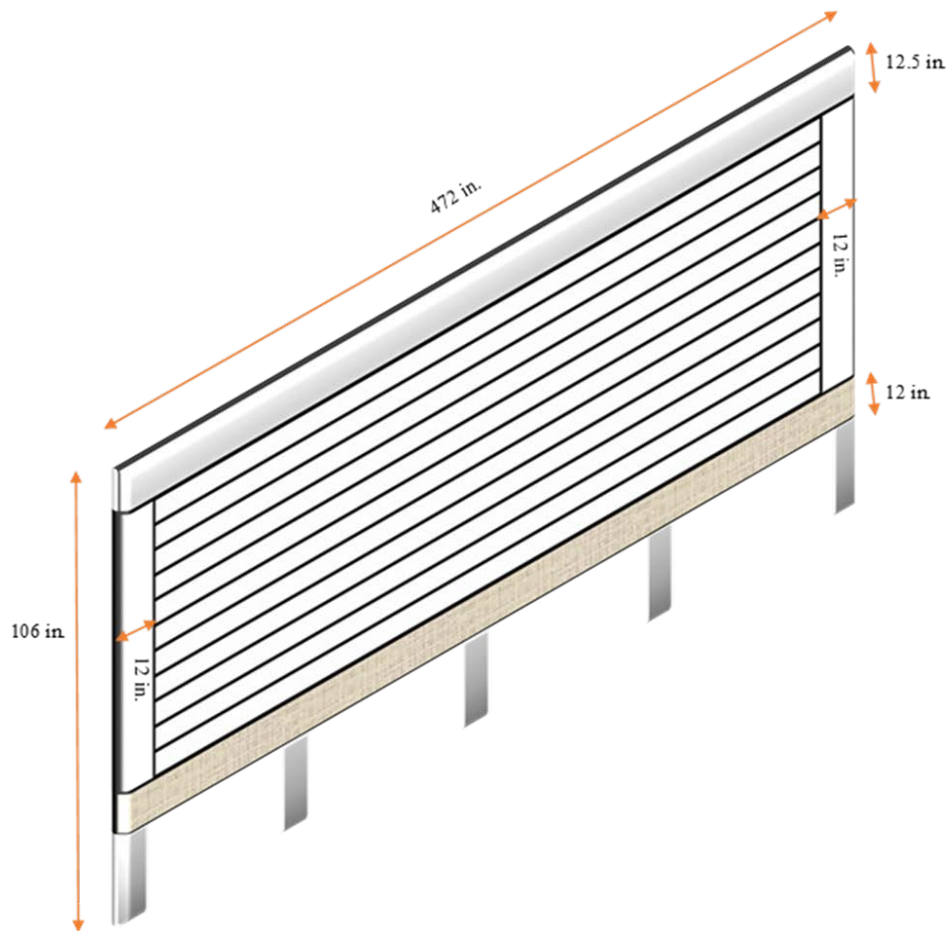


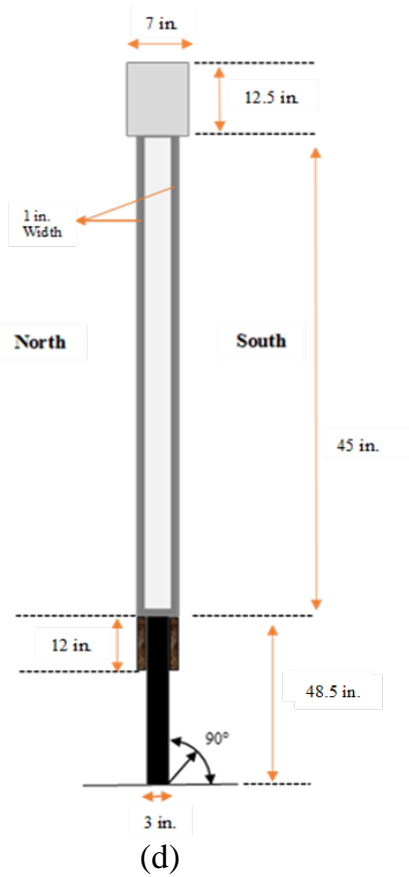
Figure 3.2.a. Weathering fence schematic



Figure 3.2.b. Weathering fence, December 2014



Figure 3.2.c. Weathering fence, January 2015



(d)



(e)

Figure 3.2.d Lateral schematic of the weathering fence

Figure 3.2.e. Weathering fence at noon sunlight- August 2015

Table 6 summarizes the time weathering periods for this study. The first set of specimens (non-weathered) have been tested. This data set was considered as the baseline data. Two other sets (3-months and 6-months) were tested and analyzed.

Table 8. Time intervals for the natural weathering tests

Series	Time Interval (Months)	Weathering Period
1	0	January 2015
2	3	January 2015 – April 2015
3	6	January 2015 – July 2015
4	12	January 2015 – January 2016
5	18	January 2015 – July 2016
6	24	January 2015 – January 2017
7	36	January 2015 – January 2018
8	48	January 2015 – January 2019
9	60	January 2015 – January 2020

#### 3.1.4 Cone Calorimetry

Cone Calorimeter is a fire testing tool that works based on a simple principle: the heat release rate from a combustion process is directly related to the amount of consumed oxygen during the burning (Davis, 2014). Specimens used in the test using this equipment should be of uniform or composite construction, and may be tested in a horizontal, face-up orientation (Babrauskas, 1984). The main parameters to be measured in order to obtain the heat release rate of a full scale item are ignitability, surface spread flame rate, and the heat release rate per unit area.

Cone calorimetry is reported to be the most accurate method to obtain the heat release rate; one of the most important factors to determine a fire hazard (Babrauskas and Peacock, 1992). A schematic of a cone calorimeter is shown in Figure 3.3.

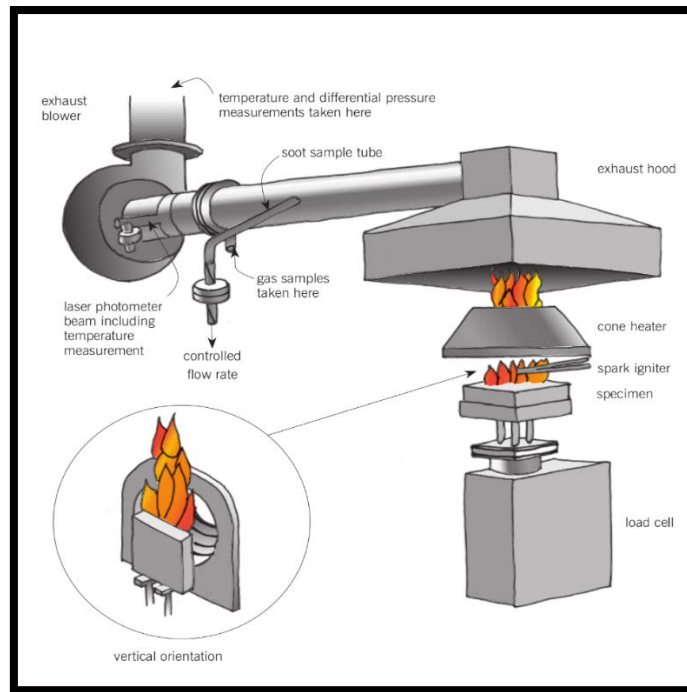


Figure 3.3. A cone calorimeter schematic (Davis, 2014)

The governing equations for the cone calorimeter were obtained from the ASTM E1354 (15-a).

The C-Factor was determined based on a methane burner set at 5kW, and was used for the heat release calibration. According to the Cone Calorimeter Standard Operating Procedure (FTT and GBH International, 2014), the C-factor should be in a range of 0.40 to 0.046. C-factor calibration was run every day, and the difference between the C-Factor values in two days in a row should not be more than 0.002. The C-Factor is in fact the uncertainty associated with HRR calculation, as shown in Equation (4) (Enright and Fleischmann, 1999).

$$C = \frac{5.0}{1.10 \times (12.54 \times 10^3)} \sqrt{\frac{T_e}{\Delta P}} \times \frac{1.105 - 1.5X_{O_2}}{X_{O_2}^0 - X_{O_2}^0} \quad \text{Equation (3)}$$

$$\dot{Q}(t) = \left(\frac{\Delta h_c}{r_0}\right) \times (1.10) C \sqrt{\frac{\Delta P}{T_e}} \frac{(X_{O_2}^0 - X_{O_2}(t))}{(1.105 - 1.5X_{O_2}(t))} \quad \text{Equation (4)}$$

Where:

$\dot{q}$  = Rate of heat release

$C$  = Orifice plate coefficient ( $\text{kg}^{1/2} \cdot \text{m}^{1/2} \cdot \text{K}^{1/2}$ )

$\Delta P$  = Pressure drop across the orifice plate (Pa)

$T_e$  = Gas temperature at the orifice plate (K)

$X_{O_2}$  = Measured mole fraction of  $O_2$  in the exhaust air (dimensionless)

$$\left(\frac{\Delta h_c}{r_o}\right) = 13.1 \times 10^3 \text{ kJ/kg } O_2$$

To obtain the heat release rate per unit area, the following equation (5) is used:

$$\dot{q}''(t) = \frac{\dot{q}(t)}{A_s} \quad \text{Equation (5)}$$

Where:

$A_s$  = Initial exposed area =  $0.0088 \text{ m}^2$  (in this study)

To determine the average effective heat of combustion, the following equation (6) is used:

$$\Delta h_{c,eff} = \frac{\sum_i \dot{q}_i(t) \cdot \Delta t}{m_i - m_f} \quad \text{Equation (6)}$$

In case CO and  $CO_2$  are also measured, the heat release rate is determined as follow:

$$\dot{q} = 1.10 \left(\frac{\Delta h_c}{r_o}\right) X_{O_2}^a \left[ \frac{\varphi - 0.172(1-\varphi)X_{CO}/X_{O_2}}{(1-\varphi) + 1.105\varphi} \right] \dot{m}_e \quad \text{Equation (7)}$$

The Oxygen depletion factor ( $\varphi$ ), exhaust rate flow ( $\dot{m}_e$ ), and the oxygen ambient mole fraction ( $X_{O_2}^a$ ) are as follow:

$$\varphi = \frac{X_{O_2}^0(1-X_{CO_2}-X_{CO})-X_{O_2}(1-X_{CO_2}^0)}{X_{O_2}^0(1-X_{CO_2}-X_{CO}-X_{O_2})} \quad \text{Equation (8)}$$

$$\dot{m}_e = C \sqrt{\frac{\Delta P}{T_e}} \quad \text{Equation (9)}$$

$$X_{O_2^a} = (1 - X_{H_2O^o})X_{O_2^o} \quad \text{Equation (10)}$$

As stated in ASTM 1354, the average net heat of combustion for a large set of materials is equal to  $13.1 \times 10^3$  kJ/ 1 kg O<sub>2</sub>. This value is known as “Huggett’s Constant” (Huggett, 1980). The heat release rate (HRR) is measured by the amount of oxygen consumed, as determined by the oxygen concentration and flowrate. The effective heat of combustion (EHC) is determined based on the mass loss rate (MLR) and smoke development.

### 3.1.5 Thermal Analysis

Based on the definition of the International Confederation for Thermal Analysis and Calorimetry (ICTAC), thermal analysis cover a group of techniques in which a property of the sample is monitored against time or temperature while the temperature of the sample is programmed. The sample is kept in a specified atmosphere (Brown, 2001). Among numerous available techniques, two of them have been used for this research study, namely Thermogravimetric Analysis (TGA) and Differential Scanning Calorimetry (DSC). Based on the properties which need to be measured, the proper method should be chosen. Thermal analysis tests gave a better understanding of the effects of weathering on pyrolysis kinetics for this study.

#### 1) Thermogravimetric Analysis (TGA)

In this test method, the mass evolution of a sample (with respect to time/temperature) is measured. This change can be caused by thermal degradation, oxygen adsorption, and/or other heterogeneous reactions (Beyler and Hirschler, 2002).

#### 2) Differential Scanning Calorimetry (DSC)

In this test method, the heat flow rate of a sample (with respect to time/temperature) was measured. DSC was used to measure the phase changes of materials.

### 3.1.5.1 Simultaneous DSC and TGA (SDT)

Using a simultaneous thermal analyzer (STA), the heat flow rate and mass change could be measured at the same time. This method is known as Simultaneous DSC and TGA (SDT). The main parameters which can be collected by each of the aforesaid methods come in Table 7 (Brown, 2001):

Table 9. Collected parameters in TGA and DSC tests

Thermal Test Method	Property
TGA	Heterogeneous Reaction/ Thermal Degradation Kinetics, Temperature Stability, Pyrolysis Temperature Range
DSC	Specific Heat Capacity, Conversion Enthalpy, Melting Enthalpy/Point, Solid-Solid Transitions, Enthalpy of Reaction/ Thermal Degradation, Compositional Analysis

## 3.2 Fire Test

Fire test consisted of three main stages: specimen preparation, cone calorimeter calibration, and evaluation by a cone calorimeter. The flammability parameters in can be obtained within either measurement of the air flow through system, or oxygen concentration in the exhaust stream (FTT, 2015).

### 3.2.1 Specimen Preparation

Specimens are prepared in comply with section 8 (Test Specimens) of ASTM E1354. All specimens were dried before the fire test under a hood in the Materials Flammability Lab (MFL) for at least 200 hours in order to meet the conditioning criteria stated in ASTM E 1354.

The main reason for conditioning was to assure there was no mass reduction (due to moisture content loss) in the specimens before testing. Specimens were wrapped in heavy duty aluminum foil, with the shiny side towards the sample. The aluminum wrap had the minimum possible coverage on the specimen edges, and it covered the

sides and bottom of the specimens. The testing surface meant to expose the heat during the test. The average temperature in the MFL is between 20°C to 22°C (68°F to 72°F), and average relative humidity is between 48 to 51 percent.

A fiber blanket and two non-combustible, 4"×4" (100 mm × 100 mm) ceramic boards seated beneath the sample in the holder. Before testing each day, the fiber blanket was placed in an oven and heated at 150°C for at least two hours. This helped minimize the moisture content of the fire blanket and the related effect to the test.

### 3.2.2 Cone Calorimeter Calibration

A calibration must be performed each day before testing. Prior to starting the calibration, all the valves, pipes, filters, and the drying agents must be checked. The process includes four main steps, as shown in Figure 3.4. The calibration procedure followed the standard operating procedure provided by the Fire Testing Technology (FTT) and GBH International companies.

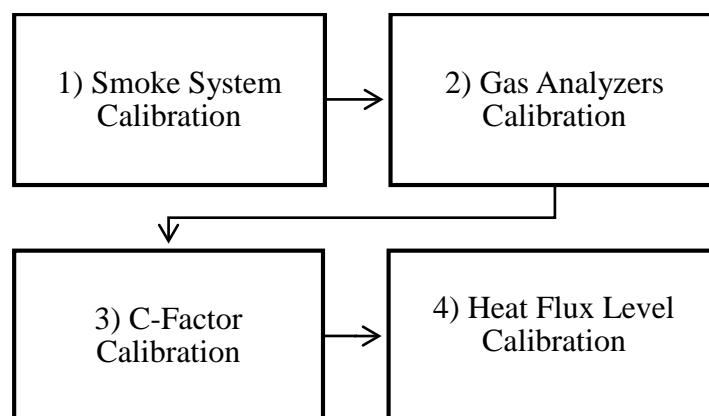


Figure 3.4. Main calibration process stages

Three gases get calibrated during the process; oxygen, carbon monoxide, and carbon dioxide. Flow, lower, and upper limits of each gas were zeroed and spanned during the calibration as shown in Table 10.

Table 10. Calibration gases

Gas	Gas used for Calibration	Flow Range (l/s)	Lower Limit (Volume %)	Upper Limit (Volume %)
Oxygen (O <sub>2</sub> )	Nitrogen (N <sub>2</sub> )	3 – 3.5	0.000	20.95
Carbon Monoxide (CO)	Calibration Gas (N <sub>2</sub> /CO/CO <sub>2</sub> )	3 – 3.5	0.000	0.69
Carbon Dioxide (CO <sub>2</sub> )	Calibration Gas (N <sub>2</sub> /CO/CO <sub>2</sub> )	3 – 3.5	0.000	7.08

Methane (CH<sub>4</sub>) was used as a fuel for the C-factor calibration. Radiant heat flux exposure levels were set to be 30 kW/m<sup>2</sup> (as a low heat flux level), 50 kW/m<sup>2</sup> (equals to a heat flux level from a fully-developed room fire to the wall), or 70 kW/m<sup>2</sup> (to simulate a high heat flux levels which are possible in the WUI fires). The equivalent temperature for the determined heat fluxes (obtained from the heat flux calibration) are 636 °C for 30 kW/m<sup>2</sup>, 769 °C for 50 kW/m<sup>2</sup>, and 863 °C for 70 kW/m<sup>2</sup>.

### 3.2.3 Testing and Data Collection

The gas scrubbing chemicals were checked every day before the tests started. Two types of desiccants were use in this study (Drielite™): a regular, white, anhydrous calcium sulfate (which can also be regenerated for reuse), and an indicating, blue desiccant impregnated with cobalt chloride. The exhausted, blue desiccant turned to purple after the moisture absorption. Both desiccants had the size of 8 mesh (0.093”). A mixture of two desiccants (half and half) were used in the combustibility tests. Figure 3.5 shows a desiccant tube containing unused (right) and partially-exhausted (left).



Figure 3.5. Exhausted and unused desiccants

Note that the desiccant tube and the tube cap were cleaned after the scrubbing chemicals were exhausted since the threads in the cap were filled with chemical's residues. Figure 3.6 shows a desiccant tube cap after a couple of fire tests.



Figure 3.6. Desiccant holder cap after testing

Prepared specimens were placed horizontally under the cone. For each coating, at least three replicates were tested for each heat flux. Tests were operated based on procedures described in the ASTM E1354. For this study, the latest version of the standard (2015-a) was used.

A spark igniter was used during the tests in order to ignite the mixture of pyrolysis gases and air (Urbas and Luebbbers, 1995), consequently all the tests were piloted ignition (elsewise the ignition was not seen). The spark igniter was positioned 25 mm under the cone. This space was measured and ensured by a 25 mm metal spacer. Collected parameters come in the next section. All tests were recorded using two video recorders, one in a horizontal position in front of the cone, and the other with a 45° to the horizon in order to record the intumescence growth from above. Recording continued until shortly after flaming and ignition, and the videos were used to obtain the expansion ration and the maximum height of the intumescence for each specimen.

Three replicates were tested for each coating at each heat flux level. Specimens were placed on a 4"× 4" (100 mm×100 mm) pre-heated fiber blanket and two 4"× 4" (100 mm×100 mm) ceramic boards in a steel specimen holder (which remained in the room temperature), and the holder's edge frame (with 2mm thickness) seated around them. Afterward, the specimen holder was placed on the load cell, under the cone, with closed shutters. The shutters were opened and video recording was started after a 60-second baseline data was collected by the cone calorimeter's software, ConeCal 5.6.

During each test, three parameters were constantly monitored on the computer, using the ConeCal 5.6 Software: smoke production rate (SPR), heat release rate (HRR), and mass loss (ML). All specimens weighted after wrapping, using an electronic scale with a sensitivity of 0.01 gram increments.

The initial procedure for the first set of specimens (non-weathered) was to continue the test and collecting all the data up to flameout. Later on, for the second and third sets of tests, a new procedure was considered. Tests were stopped 3 minutes (180 seconds) after the peak heat release rate (PHRR) was seen through the monitoring, or (as stated in the ASTM E1354, section 14 for reporting) 10 minutes after starting the test (in case no ignition was observed). There were two reasons to change the procedure: 1) required data to analyze for this research were gathered up to ignition point; and 2) running tests up to flameout were markedly time-consuming. Note that changing the procedure did not affect the obtained results used for analysis and conclusion.

Based on the reporting section in ASTM E1354 standard, data collected for the heat release rate (HRR) should be presented in 60s, 180s, and 300s. For this study, as some of the tests lasted less than 5 minutes, the data collected in 3 minutes (180s) is used to analyze and plot the heat release rate diagrams.

### 3.2.4 Collectible Parameters

The main four parameters that are constantly being recorded by the cone calorimeter are heat release rate, smoke production, ignitability, and mass loss. A wide range of data were collected during the fire test using the cone calorimeter. These data included (but not limited to): total heat released ( $HRR_T$ ), time-to-ignition (TTI), time to flameout ( $t_{fo}$ ), average specific mass loss rate ( $m_{A,10-90}$ ), initial and final mass of specimens, total smoke production, and soot mass sampling.

Additionally, the peak heat release rate (PHRR) and average heat release rate 180s ( $AHRR|_{180s}$ ), effective heat of combustion (EHC), mass loss rate (MLR), specific extinction area (SEA), plus the expansion ratio, and concentrations of toxic gases such as carbon monoxide (CO) and carbon dioxide (CO<sub>2</sub>) have been collected. The (maximum) intumescence height ( $H_{intu.}$ ) and time-to-intumescence ( $t_{intu.}$ ) parameters, which are directly related to the intumescent coating, were also collected.

Right before each test, the environmental parameters including ambient temperature ( $T_a$ ), ambient pressure ( $P_a$ ), and relative humidity (RH) were recorded using a thermohygrometer. A brief overview of the parameters comes in Table 11. Definitions were obtained mostly from the ASTM E1354-15a standard, otherwise another reference was cited.

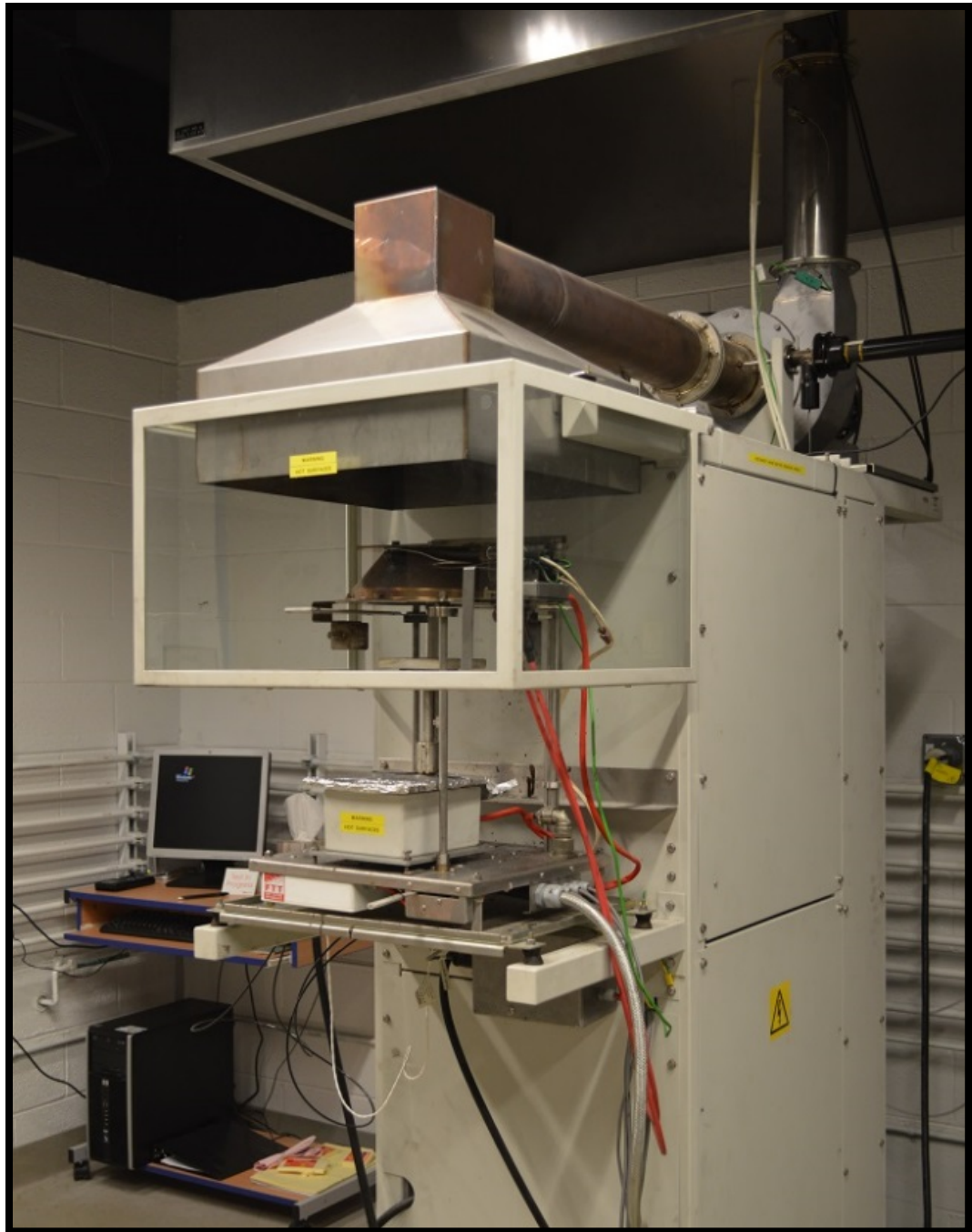


Figure 3.7. Cone calorimeter in the UNC Charlotte MFL

Table 11. Collectible flammability parameters

Number	Parameter (Abbreviation)	Symbol [Unit]	Definition
1	Effective Heat of Combustion (EHC)	$\Delta h_{c,eff}$ [kJ/kg]	The amount of heat generated per unit mass lost by a material, product or assembly, when exposed to specific fire test conditions (contrast gross heat of combustion*).
2	Time to Ignition (TTI)	$t_{ig}$ [s]	Time between the start of the test and the presence of a flame on or over most of the specimen surface for a period of at least 4 seconds (ASTM E1354, 2015).
3	Heat Release Rate (HRR)	$\dot{q}$ [kW]	The heat evolved from the specimen, per unit of time.
4	Heat Flux	$\dot{q}''$ [kW/m <sup>2</sup> ]	Heat transfer to a surface per unit area, per unit time.
5	Average Heat Release Rate, per Unit Area,	$\dot{q}''$ [kW/m <sup>2</sup> ]	The average heat release rate per unit area, over the time period starting at time-to-ignition and ending 180 seconds later, as measured in ASTM E 1354 (NFPA 130, 2014).
6	Total Heat Released (THR)	$\dot{q}''_{tot}$ [kJ/m <sup>2</sup> ]	The cumulative heat release (area under the heat release curve) through the duration of the test. ** Note that kJ $\equiv$ kW·s
7	Fire Performance Index (FPI)	[s.m <sup>2</sup> /kW]	1) Ratio of the time-to-ignition to the peak heat release rate (NFPA 556, 2011). 2) The propensity of a material to support fire propagation beyond the ignition zone in terms of the chemical heat release rate during upward fire propagation and thermal response parameter (TRP) (NFPA 287, 2012).
8	Fire Growth Rate (FIGRA)	[W/s]	Rate of change of the heat release rate. Some factors that affect the fire growth rate are exposure, geometry, flame spread, and fire barriers (NFPA 130, 2014). <b>Note:</b> FIGRA is defined as the growth rate of the burning intensity and heat release rate during a test. It is calculated as the maximum value of the function heat release rate over the elapsed test time (Sundström, 2007).
9	Specific Extinction Area (SEA)	[M <sup>2</sup> /kg]	A measure of the amount of smoke produced during the combustion (Hull and Kandola, 2009)

\* Gross Heat of Combustion: The maximum amount of heat per unit mass that theoretically can be released by the combustion of a material, product, or assembly; it can be determined experimentally and only under conditions of high pressure and in pure oxygen (contrast effective heat of combustion).

\*\* THR depends on MLR, EHC of volatiles, and combustion efficiency in the flame zone (Papaspyrides and Kiliaris, 2014).

### 3.3 Thermal Test

Thermal analysis tests for this study were performed using a TA Q600 SDT at the UNC Charlotte's Materials Characterization Laboratory (MCL).

#### 3.3.1 Sample Preparation

Samples were collected from the surface of 4"×4" (100 mm ×100 mm) coated specimens, including non-weathered, 3-months weathered, and 6-months weathered ones. A micro stainless steel spatula was used to scrap off the intumescent coating from the specimens. The spatula got cleaned with ethanol after each sample collection.



Figure 3.8. Sample collection for SDT tests- coating C

#### 3.3.2 Testing and Data Collection

Two replicates for each coatings were tested in the temperature range of ambient (30°C) to the temperature equivalent to heat flux=50 kW/m<sup>2</sup> (769°C). The residues of specimens were also collected after each test. Note that for Coating A, collecting sample from the surface was impossible as the coating lost its glossiness, and almost

completely disappeared from the surface of the plywood in the 3-months and 6-months weathered specimens. Consequently, the only sample tested for Coating A was the non-weathering one. In this case, two replicates were tested.

Reports were prepared using the TA Instruments's software, "TA Universal Analysis". Complete plotted diagrams for thermal tests are presented in appendix C of this thesis.

### 3.4 Preliminary Data and Data Analysis

Raw data collected from tests are presented in the format of ASTM E1354 standard, and are presented in the appendix A. A sample output report printed by the FTT's cone calorimeter software, ConeCal 5.6 is also available in appendix D.

The expected results of this research includes two main features. The first one is the performance, durability, and effectiveness of the tested fire-retardant coatings. The results are presented as comparison charts and diagrams in regard to different time intervals and heat fluxes. The second will be a set of recommendations to optimize the performance of coatings under similar conditions.

### 3.5 Image Processing

A customized MATLAB code was used to obtain the expansion rate and the maximum intumescence height for each sample. The code was written so that a framework could be defined around the sample holder, using the frame-by-frame images captured from the previously recorded videos. Afterwards, the sample holder's height (53 mm), number of columns (between 5 and 10) and rows (between 20 and 25), and the time interval were defined. Using a 1-second time interval, the intumescence height was observed and recorded in the most possible concise way.

Figure 3.9 shows a captured image in the image processing tool in MATLAB. The image is from a non-weathered specimen with Coating A at radiant heat flux level of 50 kW/m<sup>2</sup>.

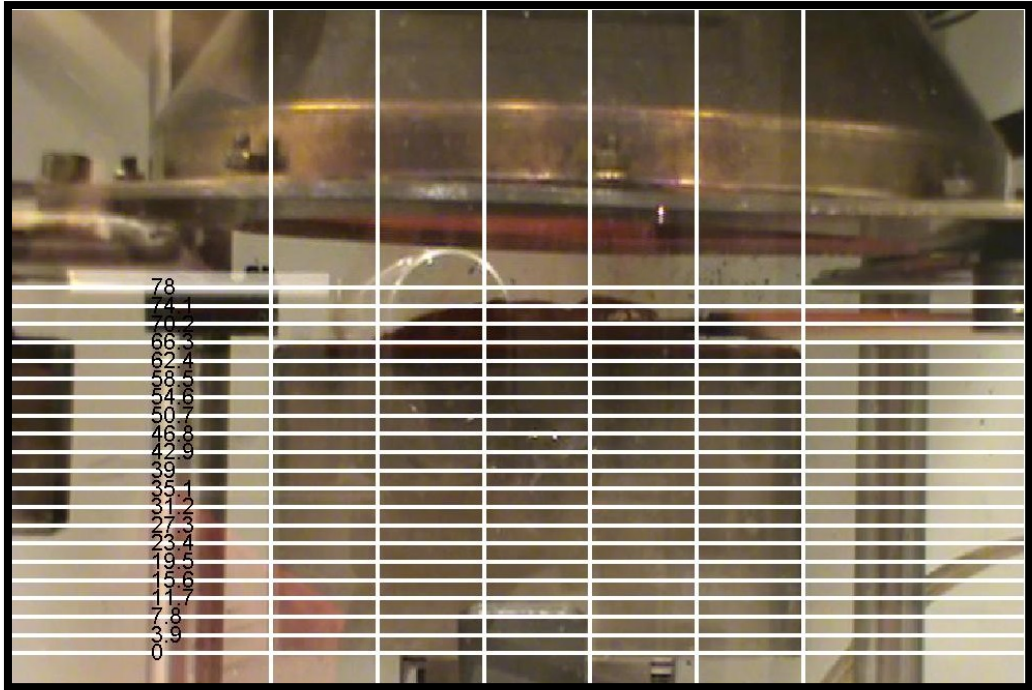


Figure 3.9. Image processing snapshot to obtain the intumescence height

Note that in obtaining the intumescence height, the sample holder's height was considered to be 53mm. The thickness of the edge frame (which is 2mm) was added to the calculated intumescence height in the end.

## CHAPTER FOUR: RESULTS AND DISCUSSION

A total of 193 fire tests were performed using the cone calorimeter for this study. In addition, total of 37 thermal analysis tests were evaluated in the MCL, using the TA Q600 SDT.

### 4.1 Observations

This section was written based on the notes taken during observations during the tests and reviewing the videos recorded for each test.

#### 4.1.1 Coating A

##### 4.1.1.1 During the Weathering Period

Coating A lost the surface glossiness during the weathering period (3 months and 6 months). In addition, a noticeable amount of mold was seen after weathering, while collecting the specimens from the weathering fence. No visible cracks or deformation were observed. The visual effects for Coating A can be seen in Figure 4.1.



Figure 4.1. Visible weathering effects on coating A

#### 4.1.1.2 During the Fire Test

Coating A was the only coating of three where flameout was seen, even using the new procedure (which was used for 3-months and 6-months weathered specimens). In the new testing procedure, tests were stopped 3 minutes after the PHRR observation, or (based on ASTM E1354) 10 minutes after the test was started when no ignition was observed.

#### 4.1.1.3 During the Thermal Test

Aforesaid, as the coating disappeared from the surface of the plywood after weathering, collecting sample from the specimen surface was not possible for 3-months and 6-months weathered ones. The SDT test performed only for non-weathered specimens, using the procedure noted for Coating B.

### 4.1.2 Coating B

#### 4.1.2.1 During the Weathering Period

After the weathering period (3 months and 6 months), visible cracks appeared on the specimens' surface. These cracks on the surface were the main reason for many fractures formation during the specimen cutting (fractures can be seen on the right edge on 6-month weathered specimen in Figure 4.2). In order to prevent fire spread from the edges, especially for those specimens which had more fractures on the edge, such specimens were wrapped using excess heavy duty aluminum foil on the edges. Measurements showed that the initial testing surface of the specimens ( $A_s=0.0088 \text{ m}^2$ ) were decreased less than 5% when the excess aluminum was used. Consequently, it had a minor effect on final results. Some white/grain imperfections were also seen on the surface after weathering. Changes in the specimens' surface can be seen in Figure 4.2.



Figure 4.2. Visible weathering effects on coating B

#### 4.1.2.2 During the Fire Test

Weathering had a significant impact on intumescence forming for Coating B. Such effect will be discussed in sections 4.2.4.1 and 4.2.5.1.

#### 4.1.2.3 During the Thermal Test

The thermal test was performed in the temperature range associated with a heat flux of  $50 \text{ kW/m}^2$ , which was  $30^\circ\text{C}$  to  $769^\circ\text{C}$ . No intumescence was seen after the test, and the residue was grey ash.

### 4.1.3 Coating C

#### 4.1.3.1 During the Weathering Period

Minor cracks were seen after the weathering period (3 months and 6 months) for Coating C. There was no noticeable change in color/texture of the coating. Specimens during weathering period can be seen in Figure 4.3.

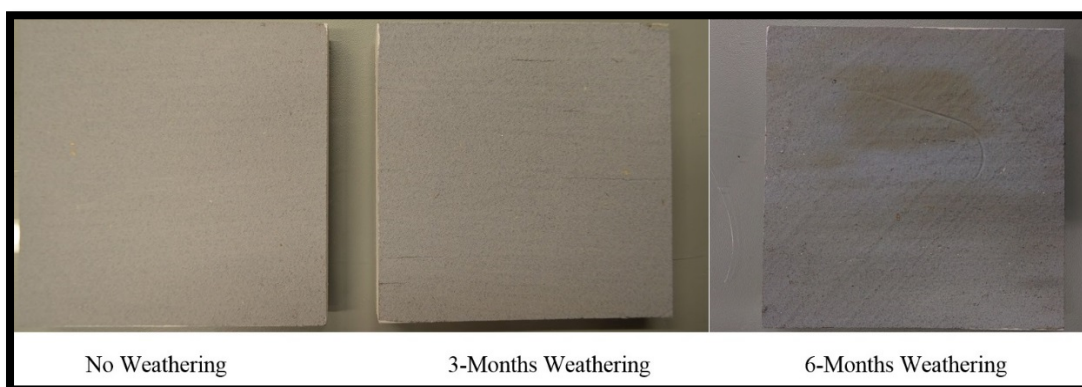


Figure 4.3. Visible weathering effects on coating C

#### 4.1.3.2 During the Fire Test

Coating C showed a different behavior in compared to the other two coatings in the fire tests, especially in heat flux level=50 kW/m<sup>2</sup>. It is discussed in section 4.2.2.2.

#### 4.1.3.3 During the Thermal Test

No intumescence was observed after the thermal test, and the residue was a dark gray ash. Tests were performed in the temperature range equivalent to heat flux=50 kW/m<sup>2</sup>, which is 30°C to 769°C.

### 4.2 Flammability Properties

In this section, each flammability property (variable) was discussed in terms of four parameters: coating type, weathering period, specimen's weathering orientation on the weathering fence, and exposed radiant heat flux level. Total comparison diagrams for the three sets of tests are shown below. Note that separate diagrams were plotted and come in Appendix B (for fire tests) and Appendix C (for SDT tests).

#### 4.2.1 Time to Intumescence

Two times were recorded for the “time-to-intumescence” parameter; one when the bubbling was initially observed, and one when the intumescence covered all the exposed testing surface. The values from the whole- surface covering time were used to plot the comparison diagrams as the performance of intumescence meant to be when they covered the whole specimen surface.

##### 4.2.1.1 Coating A

At heat flux levels higher than 30 kW/m<sup>2</sup>, the bubbling on the surface occurred faster (regardless of weathering period and weathering orientation). This did not necessarily mean that the testing surface of all the specimens exposed to the higher heat flux levels were covered more quickly or more completely.

The decrease (-) / Increase (+) Percentage in comparison to non-weathered specimens and baseline data for  $t_{intu}$  is shown in Table 12.

Table 12.  $t_{intu}$  average decrease/increase percentage during tests

Coating	HF [kW/m <sup>2</sup> ]	Change in Comparison to	3-Months		6-Months	
			North [%]	South [%]	North [%]	South [%]
A	30	Non-Weathered	+191	+161	+161	+183
	50	Non-Weathered	+53	+35	+41	+71
	70	Non-Weathered	+44	+33	+56	+66
B	30	Non-Weathered	NA*	NA	NA	NA
	50	Non-Weathered	+41	NA	+41	NA
	70	Non-Weathered	NA	NA	NA	NA
C	30	Non-Weathered	-9	+6	+9	+15
	50	Non-Weathered	-43	-38	-48	-54
	70	Non-Weathered	+9	+18	+9	+9

\*NA: Intumescence was not seen or it was not measurable.

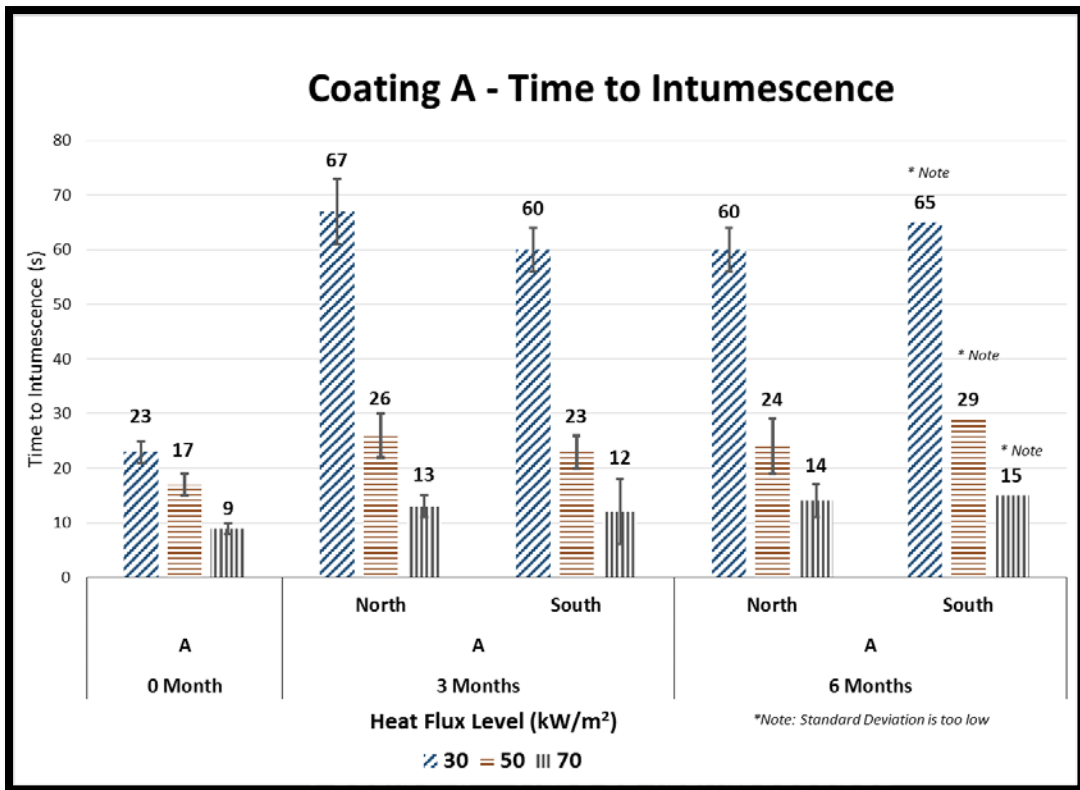


Figure 4.4.a. Average  $t_{intu.}$  comparison bar-chart for coating A

Non-weathered specimens are shown as the baseline data (dashed line) in Figure 4.4.b. All data-points related to weathered specimens were above the baseline, which clearly indicated the weathering effect on the intumescence.

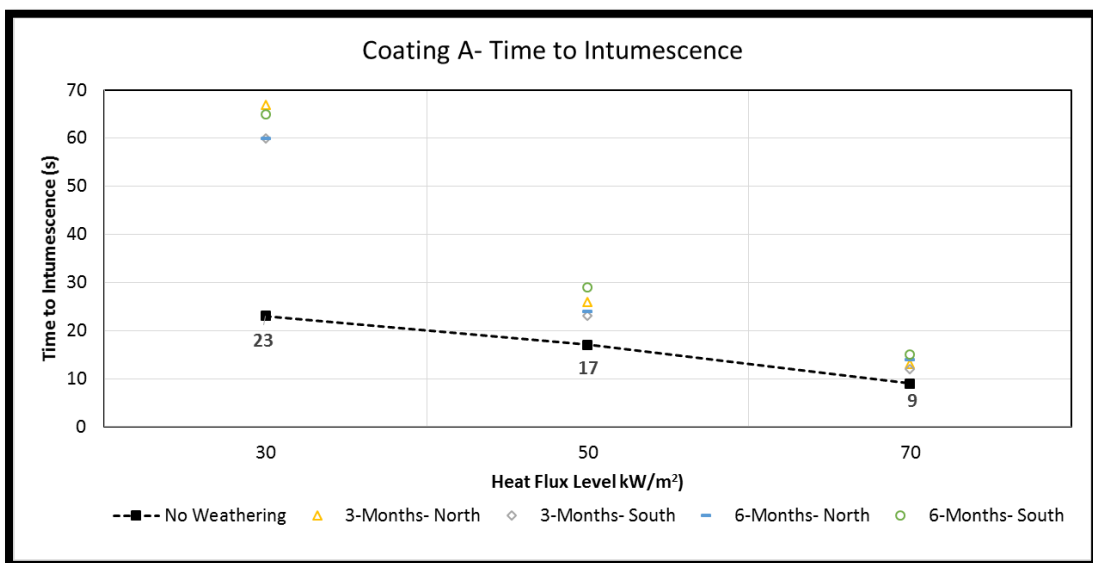


Figure 4.4.b. Average  $t_{intu.}$  comparison diagram for coating A

Table 13. Effects on  $t_{intu.}$ - coating A

Time-to-Intumescence	
Parameter	Effects
Weathering Period	From Figure 4.4.a, the weathering period had a notable role on $t_{intu.}$ . Specimens showed more resistance to intumescence formation as their surfaces were likely covered (up to 50% in 3-months weathered, and more than 50% in 6-months weathered) with mold. With regard to Figure 4.4.b, all the data-points for weathered samples are greater than the non-weathered line, which clearly shows the impact of weathering on $t_{intu.}$ .
Heat Flux Level	Heat flux level had the greatest impact on the formation of intumescence. The more the heat flux level, the less the time-to-intumescence was. Moreover, the difference between the $t_{intu.}$ value between heat flux levels 30 kW/m <sup>2</sup> and 50 kW/m <sup>2</sup> according to Table 12 (e.g 191% increase in 3-months weathered Coating A, HF of 30 kW/m <sup>2</sup> in northern section and 53% increase 3-months weathered Coating A, HF of 50 kW/m <sup>2</sup> in northern section in comparison to non-weathered specimens) was another evidence for the cases which intumescence mechanism does not follow the right sequence.
Weathering Orientation	The weathering orientation of specimens did not play an important role for $t_{intu.}$ . Note that base on the coating type, different results were seen according to the weathering orientation. For instance, regard to Table 12, $t_{intu.}$ for Coating A specimens in HF of 50 kW/m <sup>2</sup> increased more in southern section than the specimens located in northern section, but in the same HF level, Coating C specimens in northern section had a greater value (both in comparison to non-weathered samples). In conclusion, no uniform behavior was observed, and the weathering orientation in a function of coating type for $t_{intu.}$ .

## 4.2.1.2 Coating B

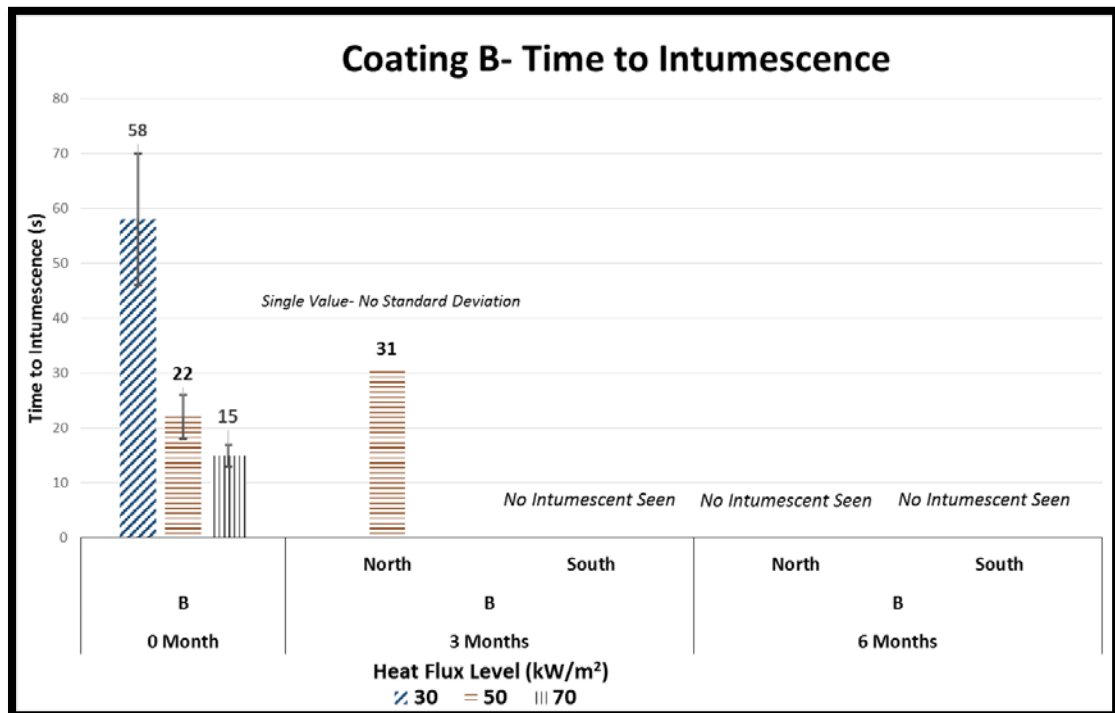


Figure 4.5.a. Average  $t_{\text{intu.}}$  comparison bar-chart for coating B

With regard to Figure 4.5.b, there was only a single-point data for weathered specimens, which was lower than the non-weathered samples. As intumescence was only seen in one specimen at HF=50 kW/m<sup>2</sup> (with the northern weathering orientation), there was no adequate data to compare other specimens in other heat flux levels to non-weathered samples. Further explanation for the mechanism failure will be provided in section 4.3.

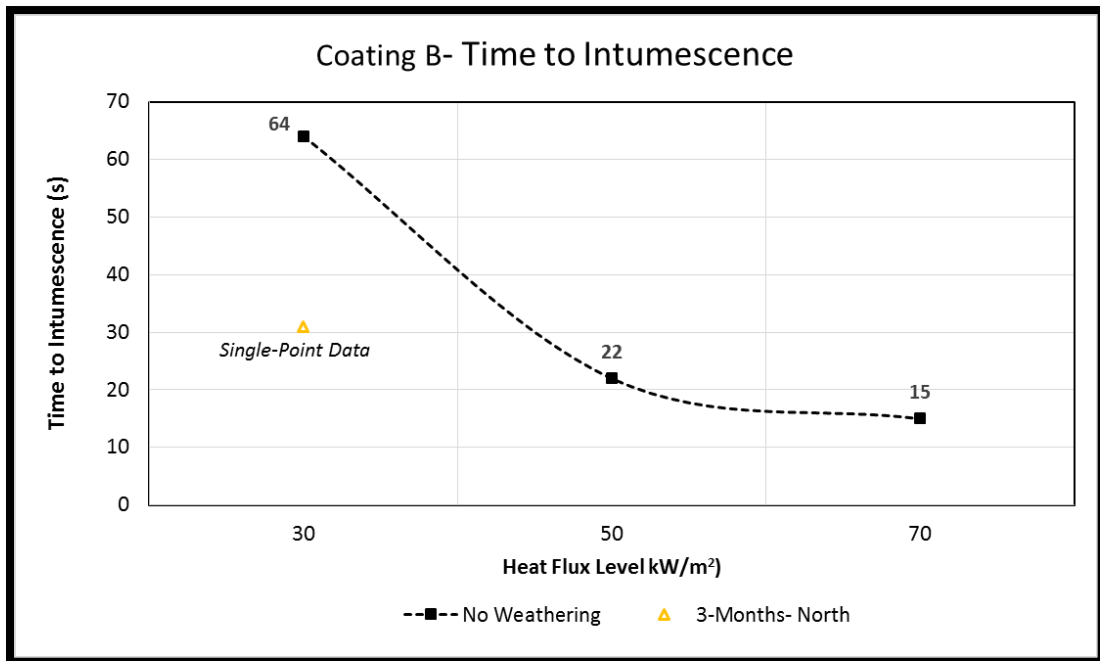


Figure 4.5.b. Average  $t_{intu.}$  comparison diagram for coating B

Table 14. Effects on  $t_{intu.}$ - coating B

Time-to-Intumescence	
Parameter	Effects
Weathering Period	As it seen in Figure 4.5.a, the weathering period came with a noticeable impact on Coating B. Among all weathered specimens which were tested, only one (3-month weathered) showed a complete intumescence at the surface. The rest of the samples (both for 3-months and 6-months weathered) only exhibited limited bubbling, and in some cases a narrow layer of intumescence which was not measurable as it did not swell higher than the specimen holder's frame edge (2 mm).
Heat Flux Level	For the non-weathered specimens, $t_{intu.}$ decreased as the heat flux level increased.
Weathering Orientation	As no intumescence was seen for the weathered specimens, the effect of weathering orientation cannot be discussed. Note that weathering orientation did not have a visible effect on bubble formation, as well.

### 4.2.1.3 Coating C

There were some cases in plotting the diagrams where the standard deviation values were too small to be shown (as in 6-months weathered, southern specimens in Figure 4.6.a).

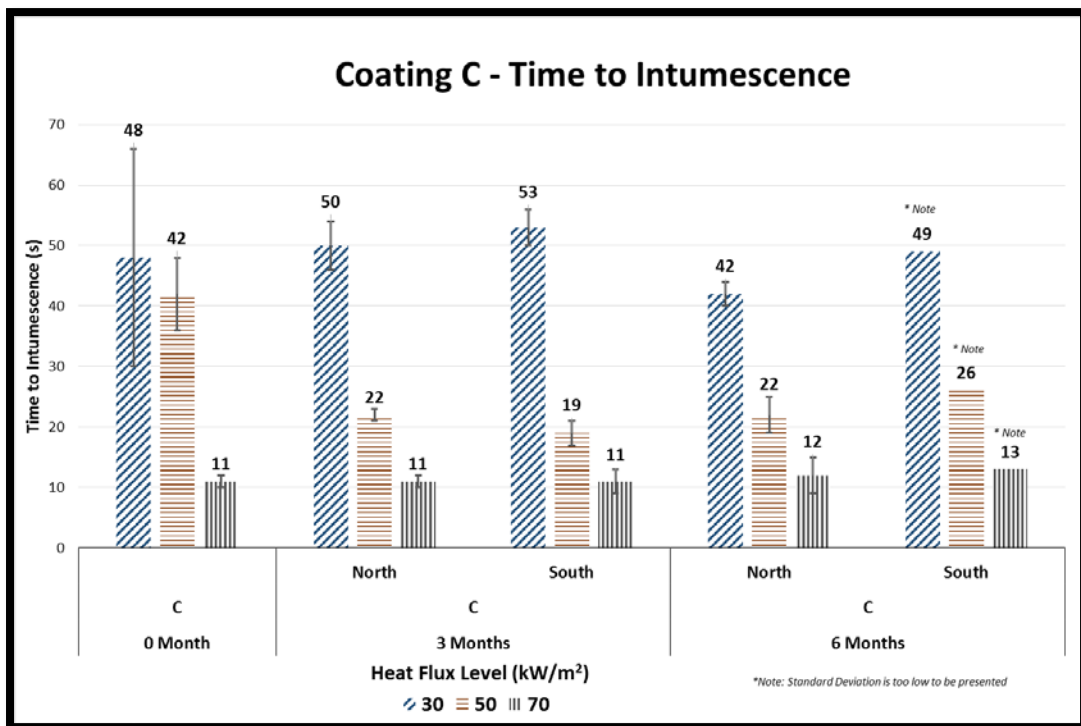


Figure 4.6.a. Average  $t_{intu.}$  comparison bar-chart for coating C

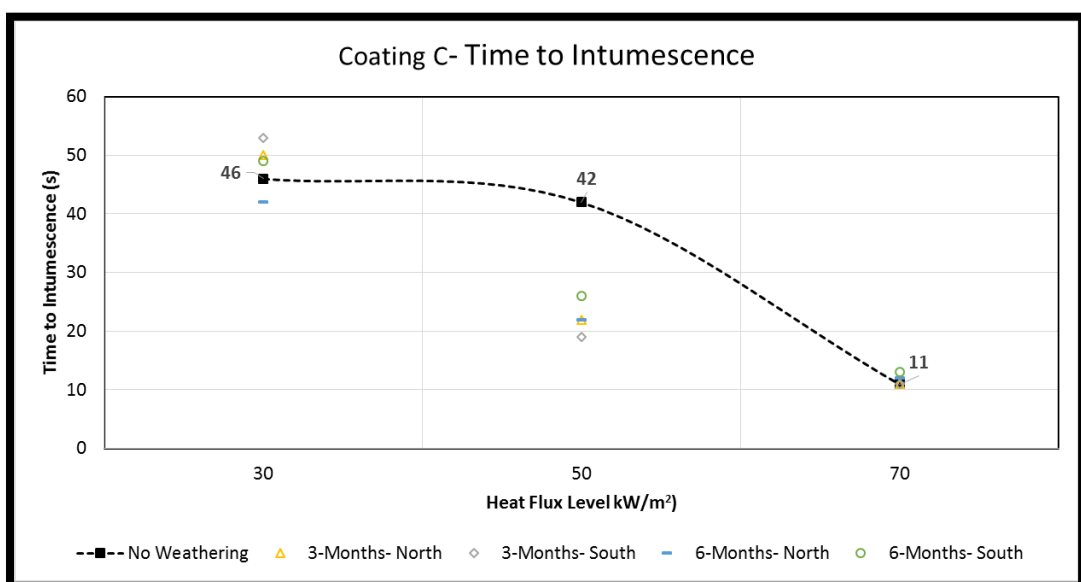


Figure 4.6.b. Average  $t_{intu.}$  comparison diagram for coating C

The results are shown in table 15.

Table 15. Effects on  $t_{intu.}$ - coating C

Time-to-Intumescence	
Parameter	Effects
Weathering Period	Regard to Figure 4.6.a, coating C showed a consistent behavior for heat fluxes 30 kW/m <sup>2</sup> and 70 kW/m <sup>2</sup> . For non-weathered specimens at heat flux level = 50 kW/m <sup>2</sup> , $t_{intu.}$ is higher in comparison to the values in the same heat flux, and different weathering periods. This shows the impact of weathering at this heat flux, for Coating C.
Heat Flux Level	Based on Figure 4.6.a, $t_{intu.}$ had a meaningful difference for heat flux = 70 kW/m <sup>2</sup> in comparison to the other two heat flux levels (intumescence mechanism sequence disorder). According to Figure 4.6.b, there was no significant difference in $t_{intu.}$ at heat flux level = 70 kW/m <sup>2</sup> for different weathering periods.
Weathering Orientation	For Coating C, weathering orientation did not have a noticeable role. According to Table 12, no uniform behavior was seen in terms of weathering orientation in different HF levels. For instance, in HF of 30 kW/m <sup>2</sup> , southern side specimens' percentage was increased, but it was increased in HF of 70 kW/m <sup>2</sup> .

## 4.2.2 Maximum Intumescence Height

### 4.2.2.1 Coating A

Intumescence was not seen in most of the weathered specimens. The data for  $H_{intu.}$  for weathered specimens were based on the single-point data observed. It is important to note that intumescence height was measured using a written code in Matlab which used the frame-by-frame captured snapshots (with 1-second time interval) from video recordings. The thickness of frame edge of the specimen holder was 2mm, and there were cases which bubbling started (in Coating A), but the height of the intumescence

did not surpass the edge frame. Measuring  $H_{intu}$  in such cases was difficult, and the height was negligible.

Decrease (-) / Increase (+) Percentage in comparison to non-weathered specimens and baseline data for  $H_{intu}$  is shown in Table 16.

Table 16.  $H_{intu}$  average decrease/increase percentage during tests

Coating	HF [kW/m <sup>2</sup> ]	Change in Comparison to	3-Months		6-Months	
			North [%]	South [%]	North [%]	South [%]
A	30	Non-Weathered	NA*	-84	NA	-82
	50	Non-Weathered	NA	NA	NA	NA
	70	Non-Weathered	NA	-72	-77	NA
B	30	Non-Weathered	NA	NA	NA	NA
	50	Non-Weathered	NA	NA	NA	-81
	70	Non-Weathered	NA	NA	NA	-81
C	30	Non-Weathered	+19	+30	+24	+22
	50	Non-Weathered	-10	-6	-2	-7
	70	Non-Weathered	-11	-12	-13	-11

\*NA: Intumescence was not seen or it was not measurable.

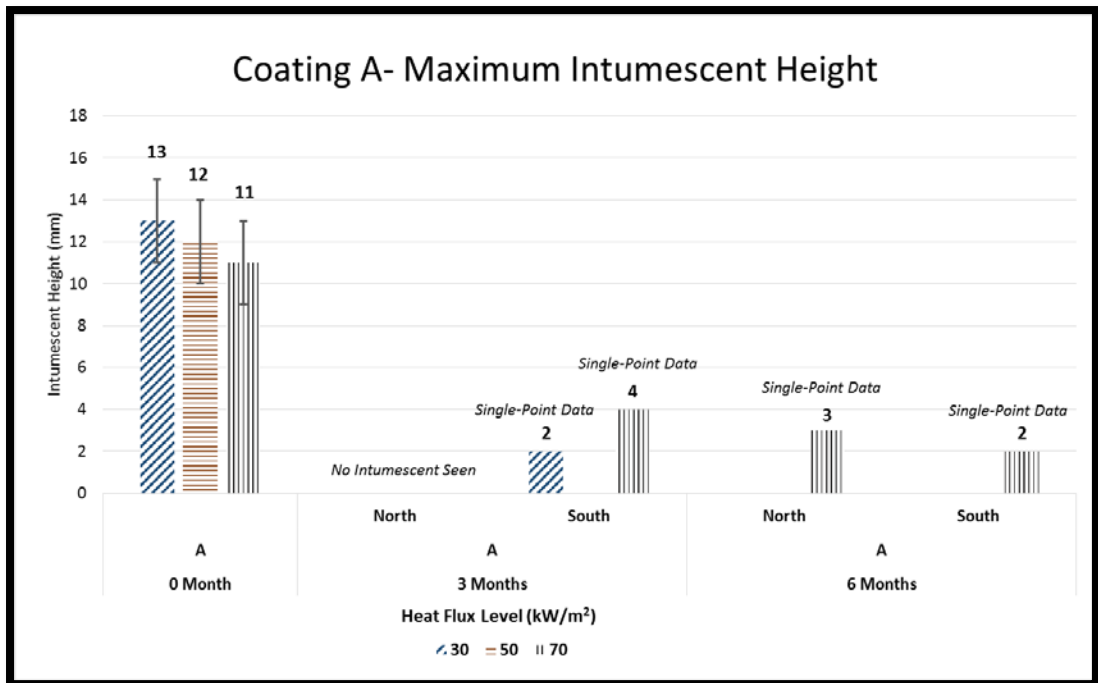


Figure 4.7. Maximum  $H_{intu.}$  comparison bar-chart for coating A

The result table comes as below:

Table 17. Effects on  $H_{intu.}$ - coating A

Intumescence Height	
Parameter	Effects
Weathering Period	As compared to the non-weathered (control) specimens, intumescence was seen for 1 (out of 3) tested specimens for 3-months and 6-months weathered samples.
Heat Flux Level	For non-weathered specimens, the intumescence height decreased as the heat flux level increased. There was insufficient data from weathered specimens to compare the $H_{intu.}$ values. Note that regardless of the weathering period, intumescence was formed at heat flux level of 70 kW/m <sup>2</sup> .
Weathering Orientation	There is no adequate gathered data to compare the effect of the weathering orientation on Coating A specimens.

#### 4.2.2.2 Coating B

For 3-months weathered Coating B specimens, coating was seen only in 1 (out of 3) tested specimens in heat flux level = 50 kW/m<sup>2</sup>. Bubbling, and in some cases char formation, on only one edge of the specimen was seen in the weathered specimens. The mechanism sequence will be discussed in section 4.3.

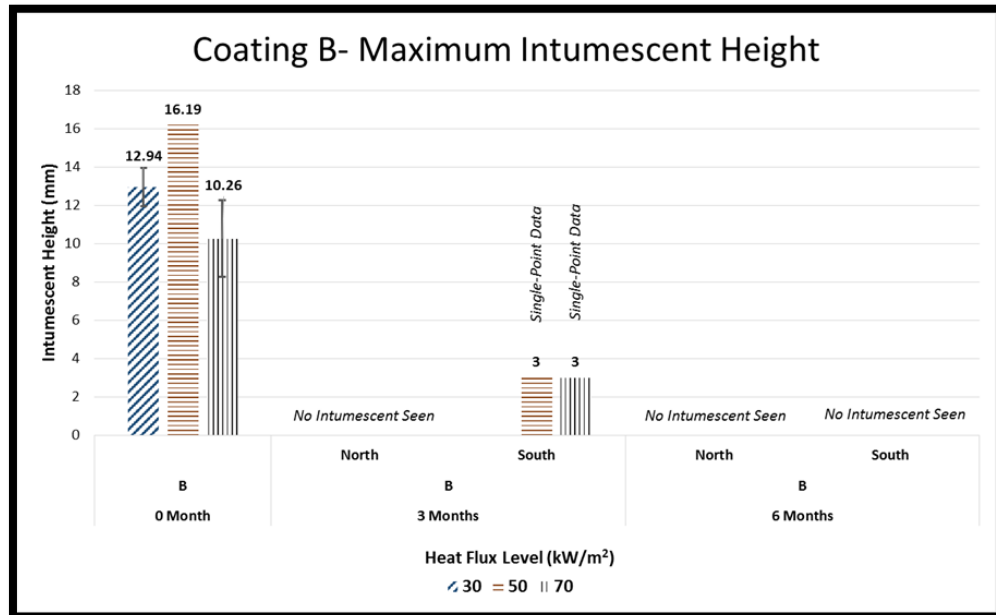


Figure 4.8. Maximum  $H_{intu.}$  comparison bar-chart for coating B

Table 18. Effects on  $H_{intu.}$ - coating B

Intumescence Height	
Parameter	Effects
Weathering Period	Intumescence height was not measurable for weathered samples as if there were bubbling and intumescence formation on one edge, the height was not more than the thickness of the frame edge (2mm).
Heat Flux Level	At heat flux level = 50 kW/m <sup>2</sup> , the greatest value for the intumescence height obtained (non-weathered specimens). Comparing this heat flux and heat flux level=70 kW/m <sup>2</sup> , more flameout/re-ignition seen for 50 kW/m <sup>2</sup> , and the intumescence was more likely to touch the spark igniter. For weathered specimens, only two single-point data gathered.
Weathering Orientation	Not enough available data to compare.

#### 4.2.2.3 Coating C

Coating C was the only coating among the three that intumescence was seen in all heat flux levels, and all weathering periods. According to Figure 4.12.a, and comparing the values to the other two, it showed the best performance, as well.

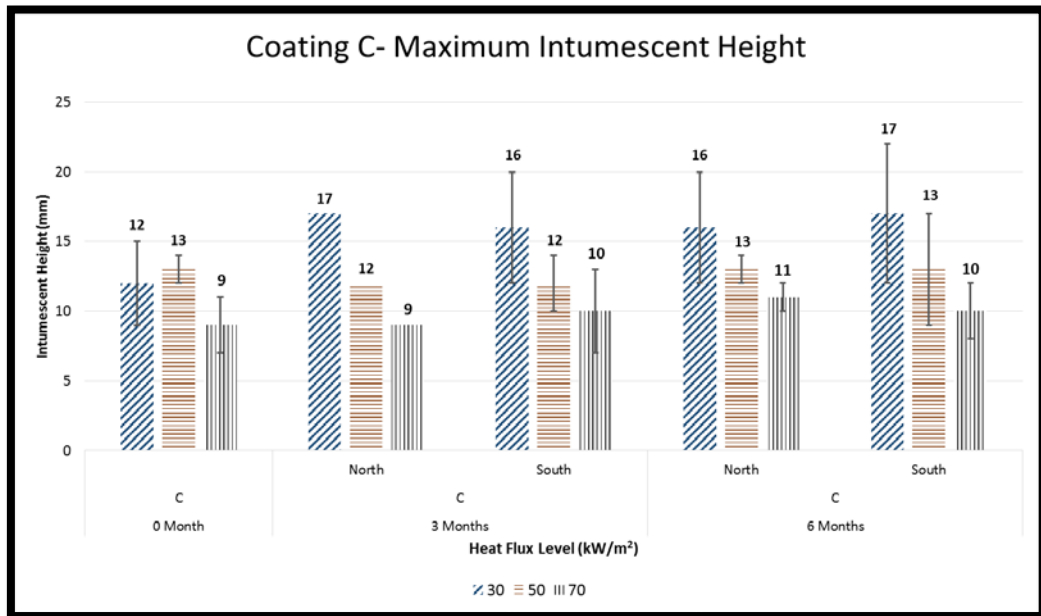


Figure 4.9. Maximum  $H_{intu.}$  comparison bar-chart for coating A

Multiple flameout/re-ignition was seen during testing the Coating C specimens. Since the intumescence swelled up to the spark igniter in some of the tests (mostly seen in non-weathered samples), the igniter must have been moved so that the intumescence did not touch it. According to this, some of the specimens had piloted re-ignition, and some (mostly 3-months and 6-months weathered) had non-piloted re-ignition.

Note that based on ASTM E1354 standard, in case no ignition was seen 10 minutes after a test was started, it has to be stopped. Results obtained from testing of the Coating C specimens are summarized in table 19.

Table 19. Effects on  $H_{intu.}$ - coating C

Intumescence Height	
Parameter	Effects
Weathering Period	According to Table 16, no remarkable difference was seen for various heat flux levels, comparing 0, 3, and 6 months weathered specimens. For example, the difference between the 3-months and 6-months weathered specimens at a HF level of $30 \text{ kW/m}^2$ was 5% (in comparison to non-weathered samples).
Heat Flux Level	In heat flux level= $30 \text{ kW/m}^2$ , no major difference was seen between non-weathered and weathered specimens. Except non-weathered specimens at heat flux level= $50 \text{ kW/m}^2$ (which several flameout/re-ignition was observed), intumescence height decreased as the heat flux level increased. Table 16 validates that in higher heat flux levels (more than $30 \text{ kW/m}^2$ ), the changes are negative. These results validate the effect of higher heat fluxes on intumescence mechanism sequence.
Weathering Orientation	Regard to Figure 4.9, weathering orientation did not have a major effect on intumescence height for Coating C.

Figure 4.10 shows the intumescence forming in Coating C at the initial steps. This specimen was 3-months weathered, had the north orientation, and was tested at heat flux level =  $50 \text{ kW/m}^2$ .

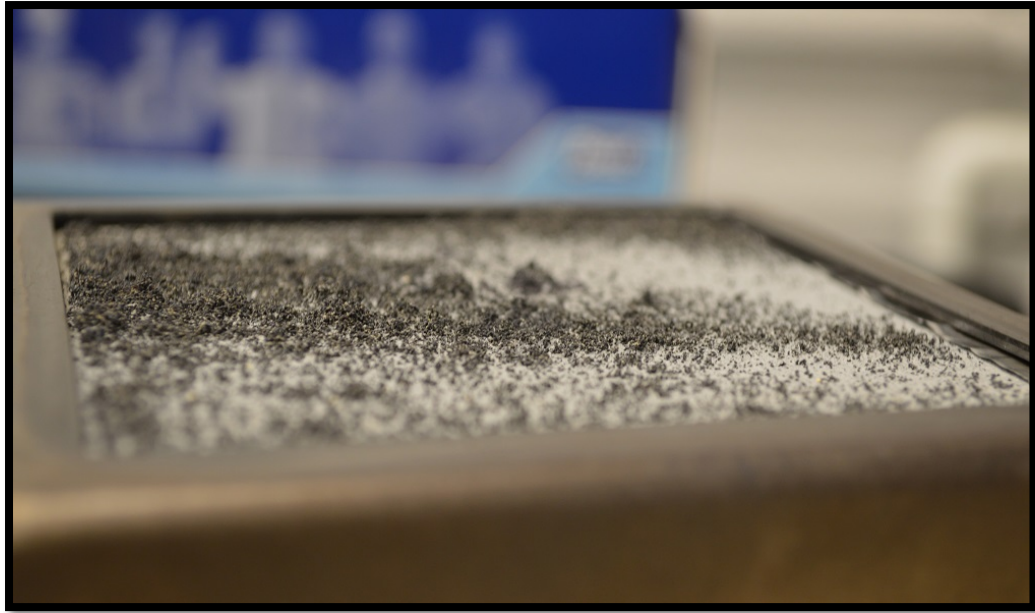


Figure 4.10. Initial steps of intumescence formation for coating C

Based on the coating type, heat flux level, and weathering period, the final mass (residue) of the samples was different. In addition, as the test procedure was reconsidered after the first set of testing (non-weathered specimens) from the “flameout observation” to “stop the test 3 minutes after the PHRR observation”, the final mass of specimens for same coatings at same heat flux level, but different weathering periods were not similar.

#### 4.2.3 Time to Ignition (TTI)

TTI is known as the primary factor for resistance evaluation of the coatings. The changes in TTI values in comparison to non-weathered specimens are summarized in Table 20.

Table 20. TTI average decrease/increase percentage during tests

Coating	HF [kW/m <sup>2</sup> ]	Change in Comparison to	0 Month [%]	3-Months		6-Months	
				North [%]	South [%]	North [%]	South [%]
A	30	Baseline	+309	+45	+40	+59	+48
		Non-Weathered	-	-64	-66	-61	-64
	50	Baseline	+245	+45	+40	+110	+100
		Non-Weathered	-	-58	-59	-39	-42
	70	Baseline	+225	+42	+33	+125	+58
		Non-Weathered	-	-56	-59	-31	-51
B	30	Baseline	+575	-12	-19	-12	-3
		Non-Weathered	-	-87	-88	-87	-86
	50	Baseline	+30	+110	+55	+110	-10
		Non-Weathered	-	+61	+19	+61	-31
	70	Baseline	+100	+17	+33	+17	+33
		Non-Weathered	-	-42	-33	-42	-33
C	30	Baseline	+323	+240	+181	+233	+165
		Non-Weathered	-	-20	-33	-21	-37
	50	Baseline	+1360	+180	+70	+140	+95
		Non-Weathered	-	-81	-88	-84	-87
	70	Baseline	+58	+133	+58	+8	+17
		Non-Weathered	-	+47	0	-32	-26

### 4.2.3.1 Coating A

As seen in Figure 4.11.a, TTI for Coating A decreased as the heat flux level increased.

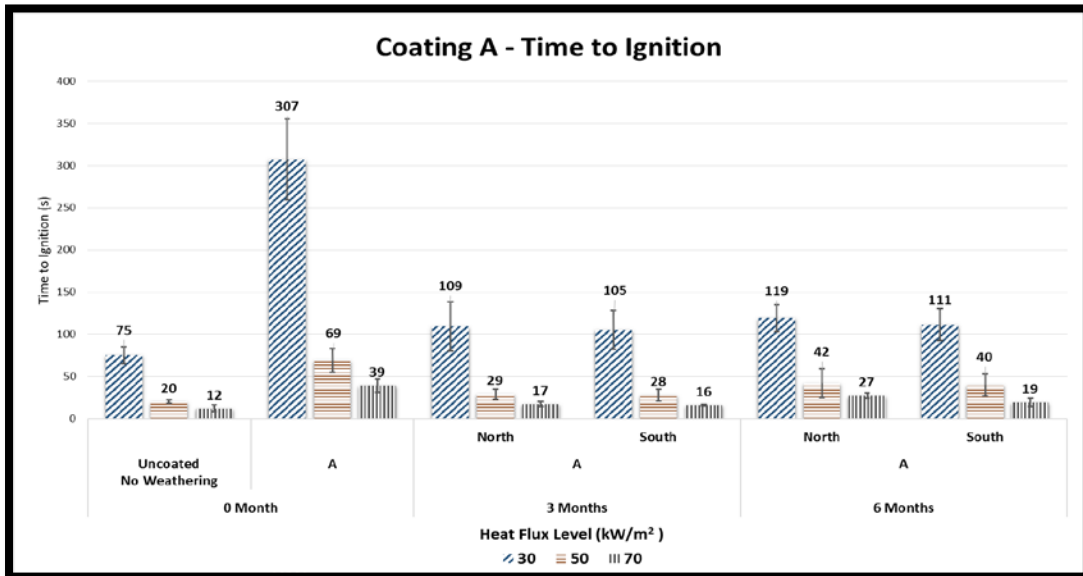


Figure 4.11.a. TTI comparison bar-chart for coating A

The comparison of coated specimens' data with the baseline data in Figure 4.11.a clearly shows the impact of coating application on the TTI.

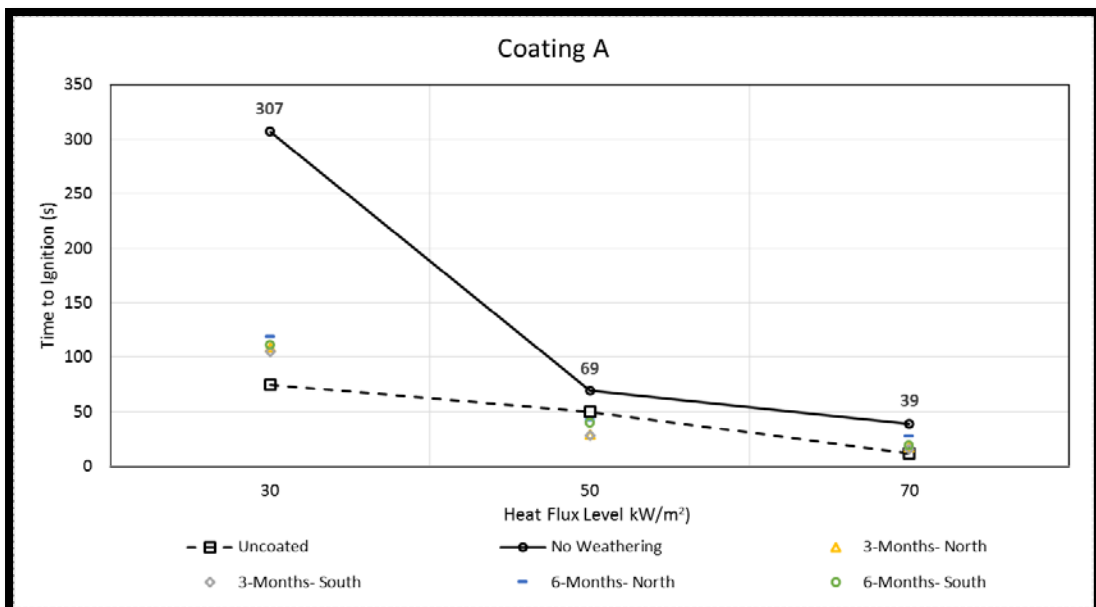


Figure 4.11.b. TTI comparison diagram for coating A

According to figure 4.11.b, all TTI data-points for weathered specimens were lower than baseline (which represents the non-weathered specimens). This shows the weathering effect on coatings.

Numerous flashings were seen in all three heat flux levels, and all weathering periods during the fire test. Based on ASTM E1354 standard, flashing is defined as a transitory flaming which lasts less than 4 seconds.

Table 21. Effects on TTI- coating A

Time-to-Ignition (TTI)	
Parameter	Effects
Weathering Period	The 3-months and 6-months weathered specimens did not show a significant difference in TTI in lower HF levels (30 kW/m <sup>2</sup> ). According to Table 20, the TTI average difference was more than 10% between 3-months and 6-months weathered specimens (in HF levels of 50kW/m <sup>2</sup> and 70 kW/m <sup>2</sup> ).
Heat Flux Level	In lower heat flux (30 kW/m <sup>2</sup> ), the TTI is high (307 s), but as the heat flux increases, TTI values become more similar for coated and uncoated specimens. Note that non-weathered specimens at HF=30 kW/m <sup>2</sup> were the only place with high TTI in comparison to other (weathered or non-weathered) specimens. This caused by the change of sequence in intumescence mechanism in higher heat flux levels (section 4.3).
Weathering Orientation	There was no noticeable difference in TTI values between the southern and northern specimens except for HF of 70 kW/m <sup>2</sup> . 6-months weathered specimens in southern section showed more vulnerability (-51%) in comparison to northern side samples (-31%) in combustibility tests (Table 20).

#### 4.2.3.2 Coating B

Numerous flashings were observed during Coating B tests. In all three heat flux levels for non-weathered specimens, flameout and then piloted re-ignition was seen.

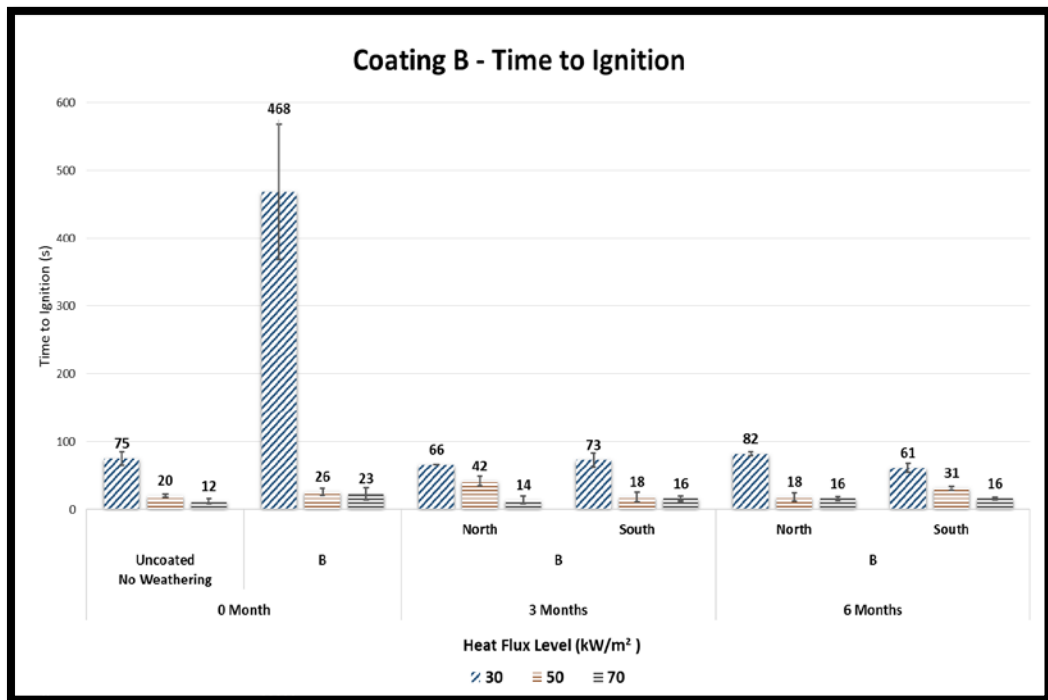


Figure 4.12.a. TTI comparison bar-chart for coating B

Coating B showed a wide range of instability during the testing period. In the first step, the most visible effects of weathering was seen in Coating B specimens among all. As mentioned before, large number of cracks led to several fractures while cutting (Coating B) specimens.

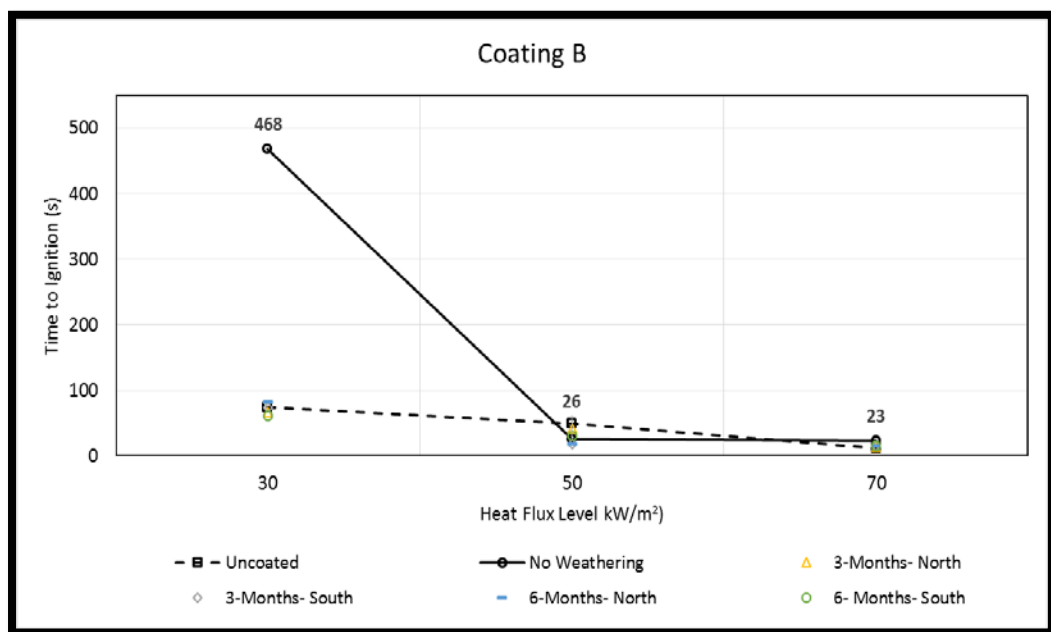


Figure 4.12.b. TTI comparison diagram for coating B

Table 22. Effects on TTI- coating B

Time-to-Ignition (TTI)	
Parameter	Effects
Weathering Period	As shown in Table 20, the 3-months and 6-months weathered specimens did not show a significant difference in TTI in 30 kW/m <sup>2</sup> and 50 kW/m <sup>2</sup> HF levels. In HF of 50 kW/m <sup>2</sup> , weathering orientation was the main parameter to validate the difference; -31% for southern specimens in comparison to +19% in northern samples, only for 6-months weathered (no change in 3-months weathered specimens) was seen.
Heat Flux Level	In lower heat flux (30 kW/m <sup>2</sup> ) for non-weathered specimens, the TTI was high (468 s), but as the heat flux increases, TTI values become more similar for coated and uncoated specimens. The change in intumescence mechanism is obvious in non-weathered specimens. In HF of 50 kW/m <sup>2</sup> , Coating B showed a different behavior in comparison to the other two HF levels. According to Table 20, changes in this HF level was positive (except the 6-months weathered southern specimens), where the rest of values in other two HF levels are negative.
Weathering Orientation	There is no notable difference in TTI values between the southern and northern specimens except in HF of 50 kW/m <sup>2</sup> . 6-months weathered specimens in southern section showed less resistance against ignition in comparison to northern side samples in this HF level.

Observations during tests showed that heat flux level rise had a noticeable role in intumescence mechanism for Coating B. Snapshots from the combustibility tests are shown in section 4.3.

#### 4.2.3.3 Coating C

For Coating C, the flameout-piloted re-ignition was seen for non-weathered and 3-months weathered samples. The reason to have bigger standard deviation (mostly for heat flux level = 30 kW/m<sup>2</sup>) was the intumescence forming; it gradually swelled so that (in some cases), the intumescence was about to touch the spark igniter. With regard to this matter, some of the re-ignition processes in heat flux level = 30 kW/m<sup>2</sup> were piloted, and some were not. This made the difference in TTI values as piloted ignition occurred faster than the non-piloted ignition.

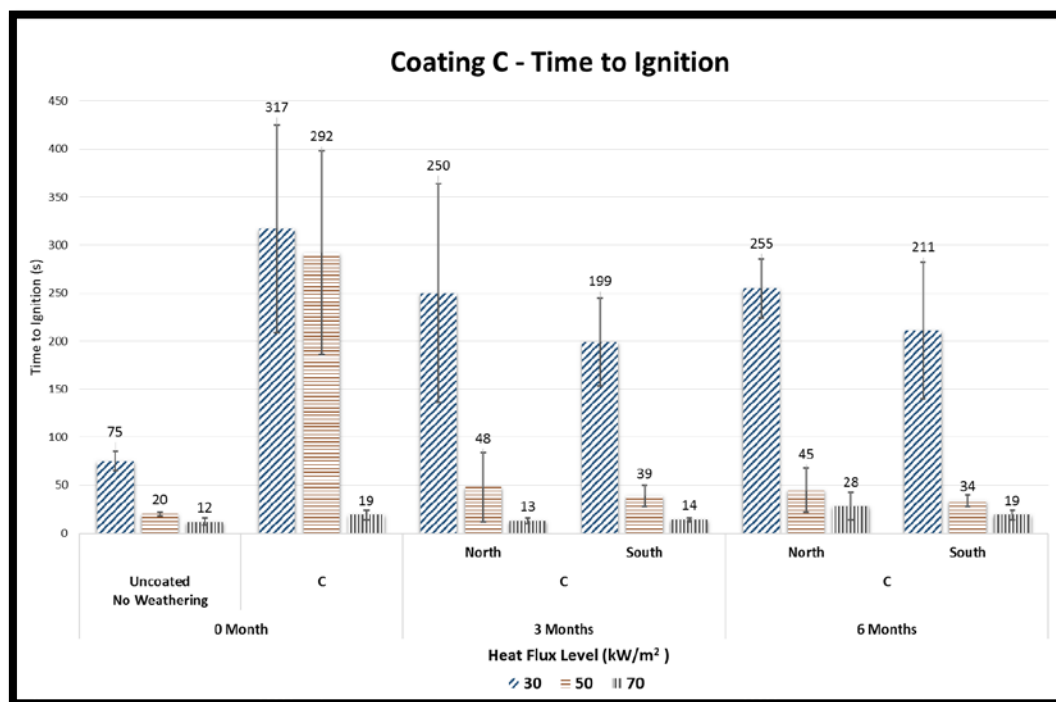


Figure 4.13.a. TTI comparison bar-chart for coating C

Some weathered specimens which did not ignite during the whole fire test. These specimens included: one (out of three) 3-months-weathered at HF=30 kW/m<sup>2</sup>, one (out of three) 6-months-weathered at HF=30 kW/m<sup>2</sup>, and two (out of four) 6-months-weathered specimens at HF=50 kW/m<sup>2</sup> for Coating C. Following the procedures provided in ASTM E1354 standard, such tests were stopped after 10 minutes.

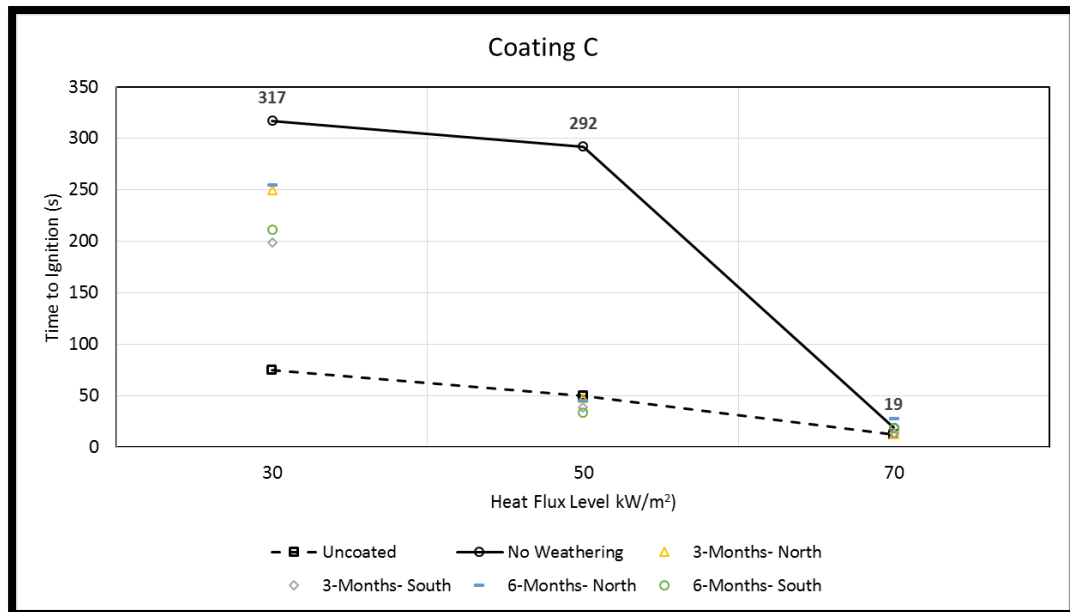


Figure 4.13.b. TTI comparison diagram for coating C

Table 23. Effects on TTI- coating C

Time-to-Ignition (TTI)	
Parameter	Effects
Weathering Period	For non-weathered specimens at heat flux level=50 kW/m <sup>2</sup> , specimens showed a similar behavior to the ones in HF=30 kW/m <sup>2</sup> , but after weathering, the instability in intumescence mechanism was observed. In HF of 70 kW/m <sup>2</sup> , TTI values had a noticeable change; (based on Table 20) from +47% (3-months) to -32% (6-months) in northern specimens, and from 0 (3-months) to -26% (in 6-months) in comparison to non-weathered samples.
Heat Flux Level	TTI showed a consistent behavior in lower heat flux (30 kW/m <sup>2</sup> ). According to the great difference in values between different HF levels (in Table 20), the change in intumescence mechanism occurred. Coating C showed the most variations in TTI at HF = 50 kW/m <sup>2</sup> (average of -85% in this HF).
Weathering Orientation	It was more likely not to see the ignition in the southern section samples than the northern ones for 3-months and 6-months weathered specimens at HF=70 kW/m <sup>2</sup> . Table 20 shows the difference in 3-months (+47% in north to 0% in south) and 6-months (-32% in north to -26% in south). Weathering orientation did not affect the specimens at the other two HF levels.

## 4.2.4 Average Heat Release Rate (AHRR)

### 4.2.4.1 Coating A

The plotted comparison diagrams for AHRR come in the appendix B.

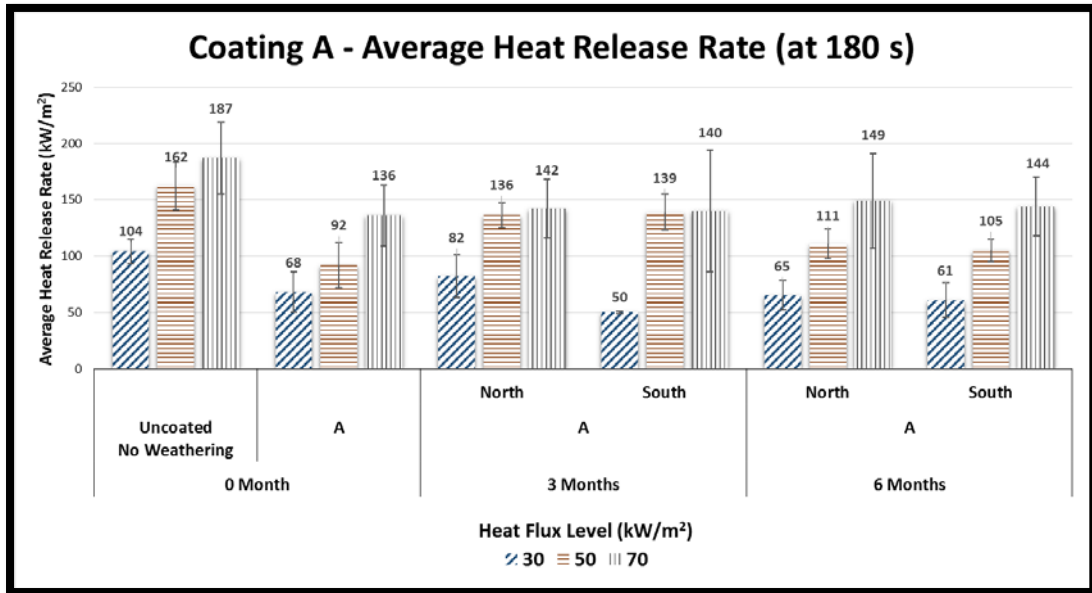


Figure 4.14. AHRR comparison bar-chart for coating A

Along with no significant difference (regard to the four parameters in Table 24) was seen for AHRR, the PHRR values were also independent of these parameters except the weathering period; for non-weathered specimens, the PHRR had greater values in comparison to the ones with a same heat flux level and different weathering period. Also, for all three heat flux levels in 3-months and 6-months weathered specimens (both north and south), the time to PHRR appeared sooner in comparison to the non-weathered samples. The result are summarized in Table 25.

Table 24. AHRR average decrease/increase percentage during tests

Coating	HF [kW/m <sup>2</sup> ]	Change in Comparison to	0 Month [%]	3-Months		6-Months	
				North [%]	South [%]	North [%]	South [%]
A	30	Baseline	-35	-21	-52	-38	-41
		Non-Weathered	-	+21	-26	-4	-10
	50	Baseline	-43	-16	-14	-31	-35
		Non-Weathered	-	+48	+51	+21	+14
	70	Baseline	-27	-24	-25	-20	-23
		Non-Weathered	-	+4	+3	+9	+6
B	30	Baseline	-51	-10	-7	-10	-4
		Non-Weathered	-	+19	+23	+19	+26
	50	Baseline	-50	-5	-14	-5	-20
		Non-Weathered	-	+806	+718	+806	+659
	70	Baseline	-74	-12	-11	-12	+3
		Non-Weathered	-	+98	+101	+98	+131
C	30	Baseline	-24	-71	-78	-64	-82
		Non-Weathered	-	-41	-55	-27	-63
	50	Baseline	-89	-83	-90	-86	-83
		Non-Weathered	-	-67	-80	-73	-67
	70	Baseline	-56	-77	-79	-78	-80
		Non-Weathered	-	-10	-17	-15	-21

Table 25. Effects on AHRR- coating A

Average Heat Release Rate (AHRR)	
Parameter	Effects
Weathering Period	Based on Figure 4.14, no noticeable difference was seen for AHRR during weathering period at high HF level (70 kW/m <sup>2</sup> ). Based on Table 24, changes at the other two HF levels are significant. For instance, from +51% (in 3-months) to +14% (in 6-months) in southern specimens at HF=50 kW/m <sup>2</sup> .
Heat Flux Level	The AHRR increased as the heat flux level was increased, regardless of the weathering period. However, the changes in HF of 70 kW/m <sup>2</sup> were less in comparison to other two HF levels (Table 24).
Weathering Orientation	As shown in Table 24, the weathering orientation of specimens did not have an impact on AHRR except for the 3-months weathered specimens at HF level of 30 kW/m <sup>2</sup> .

## 4.2.4.2 Coating B

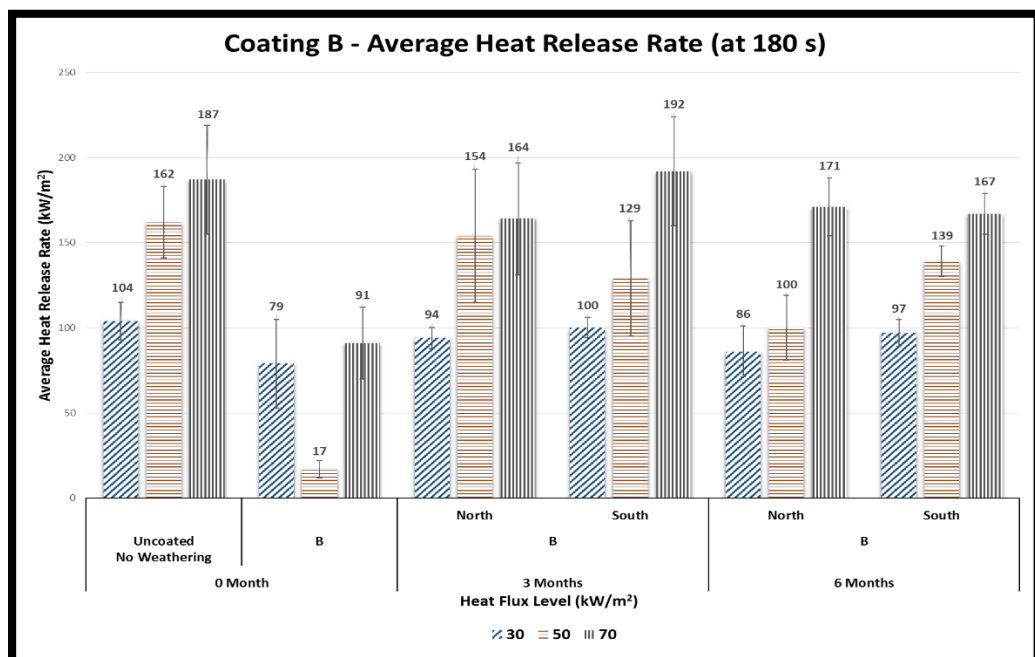


Figure 4.15. AHRR comparison bar-chart for coating B

Table 26. Effects on AHRR- coating B

Average Heat Release Rate (AHRR)	
Parameter	Effects
Weathering Period	The non-weathered specimens (especially at HF=50 kW/m <sup>2</sup> ) had less AHRR value in comparison to 3-months and 6-months weathered samples. Changes in AHRR values were greatly affected after weathering especially at HF of 50 kW/m <sup>2</sup> .
Heat Flux Level	As mentioned for TTI, the non-weathered specimens at the heat flux level=50 kW/m <sup>2</sup> went through flameout/re-ignition (piloted/non-piloted) several times. In addition, as the intumescence at this heat flux was more likely to touch the intumescence, the spark igniter's was relocated to prevent this matter. Other than this specific case, there was an increase in AHRR as the heat flux level increased. As shown in Table 24, weathered specimens increased 600% to 800% in comparison to non-weathered samples (at HF=50 kW/m <sup>2</sup> ). Weathering period did not affect the other two HF levels.
Weathering Orientation	There was different behavior for 3-months and 6-months weathered specimens regard to the weathering orientation, although the values for same heat flux were not significantly different. This means except HF=50 kW/m <sup>2</sup> , southern specimens had a larger average AHRR in comparison to northern specimens. As an example, +131% (south) and 98% (north) increase in comparison to non-weathered specimens in 6-months weathered samples at HF=70 kW/m <sup>2</sup> (Table 24).

## 4.2.4.3 Coating C

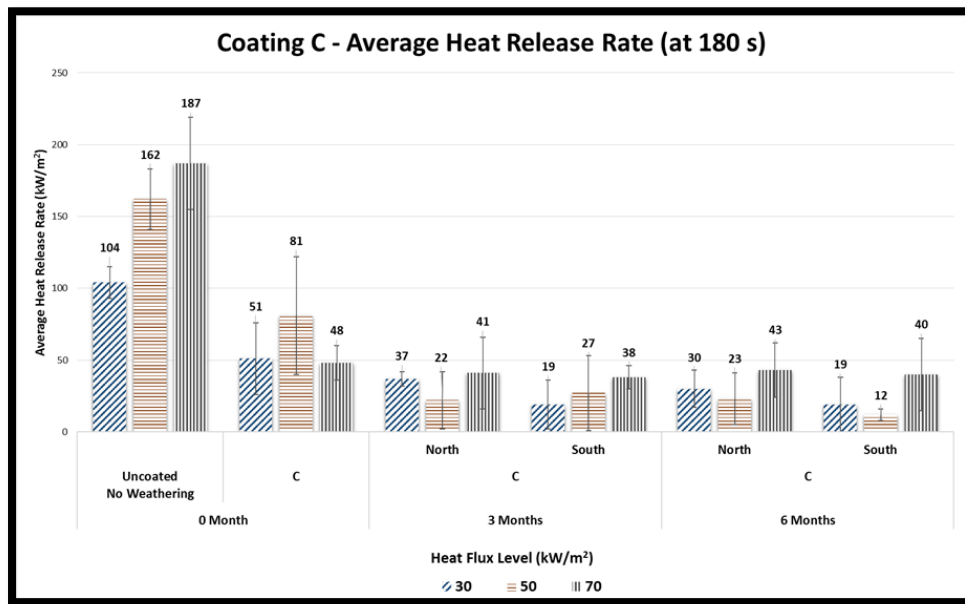


Figure 4.16. AHRR comparison bar-chart for coating C

Table 27. Effects on AHRR- coating C

Average Heat Release Rate (AHRR)	
Parameter	Effects
Weathering Period	3-months and 6-months weathered specimens reached lower AHRR values in comparison to non-weathered samples. According to Table 24, changes in AHRR after weathering are not noticeable.
Heat Flux Level	Coating C had a similar situation to Coating B in terms of intumescence growth; to prevent the spark igniter being touched by the intumescence, it was relocated for several times. Heat flux level=70 kW/m <sup>2</sup> was the only place where PHRR appeared; far from the weathering period. Moreover, several flameout/ re-ignitions occurred at heat flux level=50 kW/m <sup>2</sup> (for all weathering periods). Regarding the plotted heat release rate diagrams (in appendix B 3.3.2), the HRR gradually increased during the fire test for coating C.
Weathering Orientation	Regard to Figure 4.16, the specimens' weathering orientation did have a notable impact on the AHRR value except for the 6-months weathered samples at HF=30 kW/m <sup>2</sup> (-27% for north and -63% for south in comparison to non-weathered specimens).

## 4.2.5 Peak Heat Release Rate (PHRR)

Table 28. PHRR average decrease/increase percentage during tests

Coating	HF [kW/m <sup>2</sup> ]	Change in Comparison to	0 Month [%]	3-Months		6-Months	
				North [%]	South [%]	North [%]	South [%]
A	30	Baseline	-27	-5	-4	-16	-21
		Non-Weathered	-	+30	+31	+15	+8
	50	Baseline	-37	-15	-19	-15	-26
		Non-Weathered	-	+36	+29	+35	+18
	70	Baseline	-26	-8	-21	-3	-8
		Non-Weathered	-	+24	+7	+30	+24
B	30	Baseline	-20	+10	-9	+10	-17
		Non-Weathered	-	+38	+15	+38	+5
	50	Baseline	-42	+1	-1	+1	-12
		Non-Weathered	-	+74	+71	+74	+53
	70	Baseline	-33	-8	+2	-8	0
		Non-Weathered	-	+37	+51	+37	+48
C	30	Baseline	-42	-20	-86	-34	-83
		Non-Weathered	-	+38	-75	+15	-70
	50	Baseline	-37	-37	-88	-29	-25
		Non-Weathered	-	0	-82	+13	+19
	70	Baseline	-43	-23	-16	-23	-41
		Non-Weathered	-	+36	+49	+36	+4

4.2.5.1 Coating A

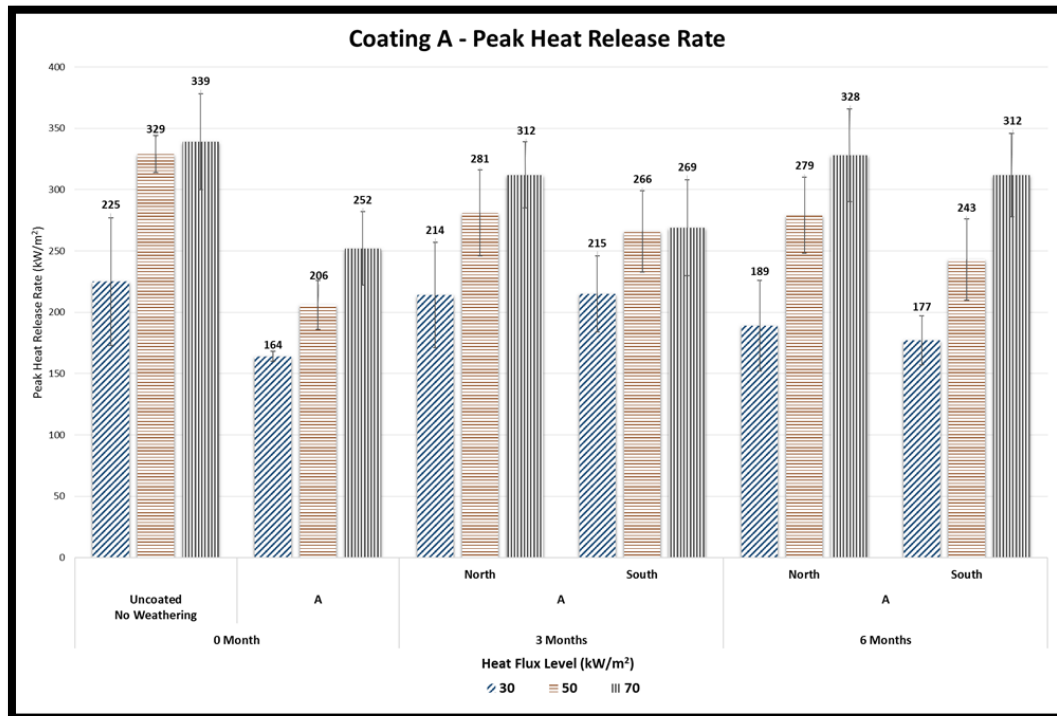


Figure 4.17. PHRR comparison bar-chart for coating A

Table 29. Effects on PHRR- coating A

Peak Heat Release Rate (PHRR)	
Parameter	Effects
Weathering Period	Table 28 shows that except for southern side specimens at HF of 30 kW/m <sup>2</sup> , the rest of values are consistent, and weathering period did not affect them at all.
Heat Flux Level	Comparing the increase/decrease percentage values in Table 28, and according to Figure 4.17. PHRR values did not significantly differ base on heat flux level rise.
Weathering Orientation	Except for 3-months weathered specimens at HF of 70 kW/m <sup>2</sup> (+24% for north and +7% for south), the changes in the rest of specimens according to the weathering orientation is negligible.

## 4.2.5.2 Coating B

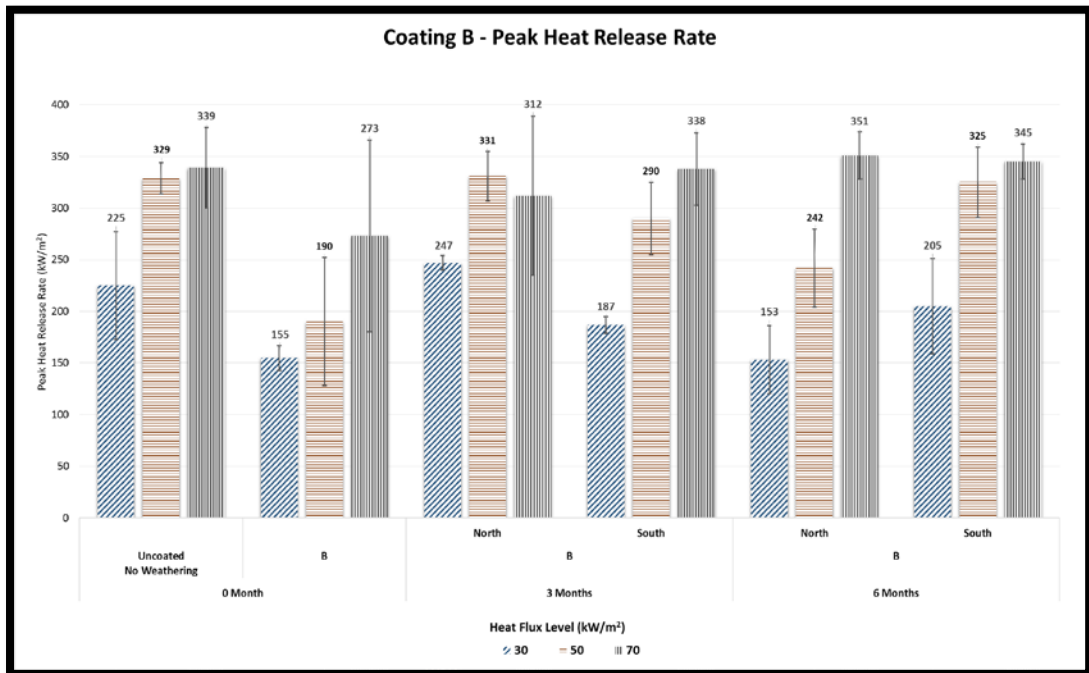


Figure 4.18. PHRR comparison bar-chart for coating B

Table 30. Effects on PHRR- coating B

Peak Heat Release Rate (PHRR)	
Parameter	Effects
Weathering Period	Based on Table 28 and figure 4.18, weathering period did not affect the PHRR. The only noticeable effect was seen in weathered samples at HF=50 kW/m <sup>2</sup> in southern section.
Heat Flux Level	PHRR changes more at HF=50 kW/m <sup>2</sup> in comparison to the other two HF levels (Table 28). According to Figure 4.18, the PHRR values were increased by the HF level increase (except for 3-months weathered northern specimens at HF=50 kW/m <sup>2</sup> ).
Weathering Orientation	Weathering orientation effect varied based on HF level for Coating C. At low HF (30 kW/m <sup>2</sup> ), southern side specimens showed less change in comparison to northern side ones (Table 28), but southern specimens at HF=70 kW/m <sup>2</sup> affected more than northern samples in that HF level. No significant difference was seen in specimens which were tested at 50 kW/m <sup>2</sup> based on their weathering orientation.

4.2.5.3 Coating C

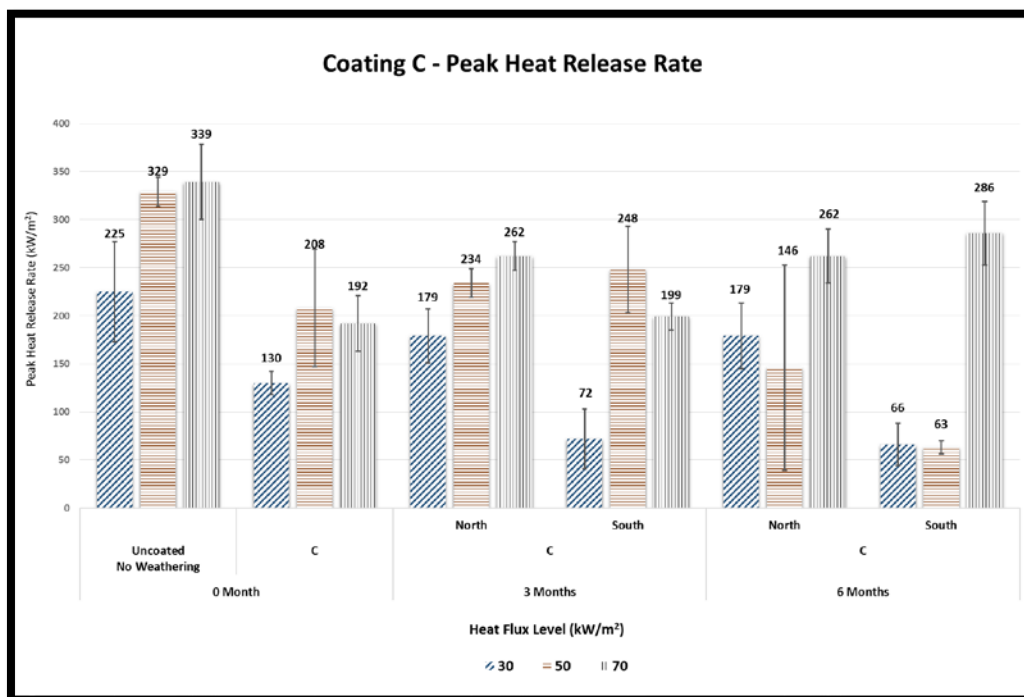


Figure 4.19. PHRR comparison bar-chart for coating C

Table 31. Effects on PHRR- coating C

Peak Heat Release Rate (PHRR)	
Parameter	Effects
Weathering Period	Base on Table 28, changes in PHRR comparison percentage values are negligible considering the weathering period. The PHRR values were decreased after weathering in comparison to baseline data.
Heat Flux Level	As shown in Figure 4.19, PHRR values increased as the HF level increases (mostly) except for specimens at HF of 50 kW/m <sup>2</sup> . In this HF level, multiple flameout/re-ignition was seen. Changes in HRR are presented in section 3.2.1 of Appendix B.
Weathering Orientation	In low HF level, weathering orientation affected the PHRR significantly. For instance (based on Table 28), 6-months weathered specimens percentage change were +15% for north and -70% for south (at HF=30 kW/m <sup>2</sup> ). The rest of specimens (except 3-months weathered at HF=50 kW/m <sup>2</sup> ) were not noticeably affected by the weathering orientation.

## 4.2.6 Effective Heat of Combustion

Table 32. EHC average decrease/increase percentage during tests

Coating	HF [kW/m <sup>2</sup> ]	Change in Comparison to	0 Month [%]	3-Months		6-Months	
				North [%]	South [%]	North [%]	South [%]
A	30	Baseline	+23	-7	-8	-8	-10
		Non-Weathered	-	-24	-25	-25	-27
	50	Baseline	-2	+3	+2	-4	0
		Non-Weathered	-	+5	+5	-2	+2
	70	Baseline	+36	+28	+19	-9	-9
		Non-Weathered	-	-6	-13	-34	-34
B	30	Baseline	+35	+1	+7	+1	+5
		Non-Weathered	-	-25	-21	-25	-22
	50	Baseline	-5	+56	-7	+56	+18
		Non-Weathered	-	+64	-2	+64	+24
	70	Baseline	-3	-19	-7	-17	-10
		Non-Weathered	-	-17	-4	-15	-8
C	30	Baseline	+30	-8	-45	-6	-55
		Non-Weathered	-	-29	-58	-28	-66
	50	Baseline	-9	-27	-70	-23	-19
		Non-Weathered	-	-20	-67	-16	-11
	70	Baseline	-7	-14	-16	-14	-13
		Non-Weathered	-	-7	-10	-7	-6

## 4.2.6.1 Coating A

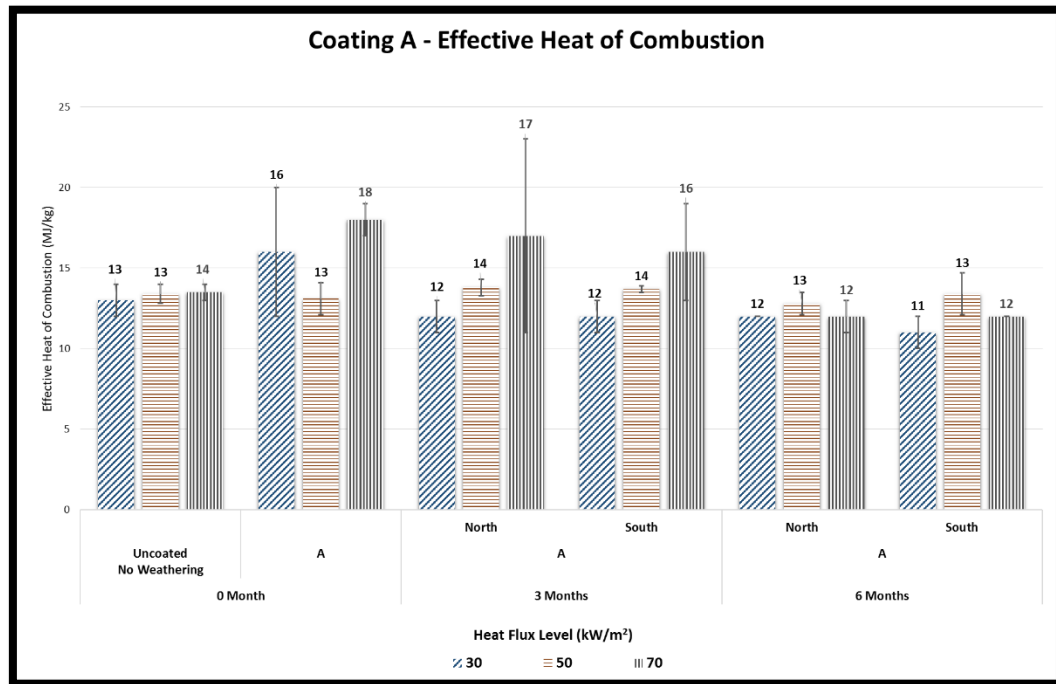


Figure 4.20. EHC comparison bar-chart for coating A

Table 33. Effects on EHC- coating A

Effective Heat of Combustion (EHC)	
Parameter	Effects
Weathering Period	As shown in Figure 4.20, changes in EHC values according to weathering period is not significant (except for HF=70 kW/m <sup>2</sup> ). Table 32 also validates this statement.
Heat Flux Level	At high HF level (70 kW/m <sup>2</sup> ), EHC values were slightly increased in comparison to uncoated specimens. Also, changes in low HF level (30 kW/m <sup>2</sup> ) were greater in comparison to the other two HF levels. For instance, regard with Table 32, -27% for southern 6-months weathered specimens at HF=30 kW/m <sup>2</sup> in comparison to +2% for southern 6-months weathered specimens at HF=50 kW/m <sup>2</sup> .
Weathering Orientation	Based both on Figure 4.20 and Table 32, weathering orientation did not affect the EHC values.

4.2.6.2 Coating B

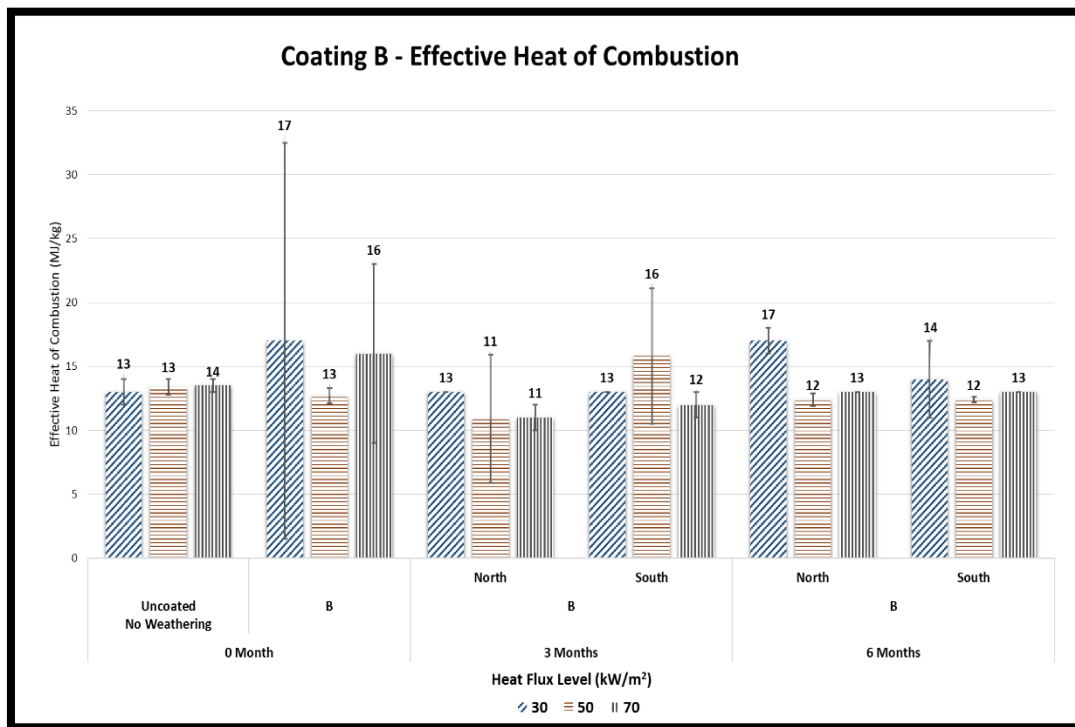


Figure 4.21. EHC comparison bar-chart for coating B

Table 34. Effects on EHC- coating B

Effective Heat of Combustion (EHC)	
Parameter	Effects
Weathering Period	The weathering period did not affect low and high HF levels (Table 32). The only significant change in comparison to non-weathered specimens was southern specimens at HF of 50 kW/m <sup>2</sup> (-2% for 3-months weathered and +24 for 6-months weathered).
Heat Flux Level	According to Figure 4.21, there was no uniform behavior in HF level increase/decrease for Coating B. EHC had the greatest value at HF of 30 kW/m <sup>2</sup> (except for 3-months weathered southern specimens at HF=50 kW/m <sup>2</sup> ). Base on Table 32, EHC valued decreased in comparison to non-weathered specimens except for northern samples at HF of 50 kW/m <sup>2</sup> (both 3-months and 6-months weathered).
Weathering Orientation	Both Figure 4.21 and Table 32 confirmed that the weathering orientation did not affect the EHC values and changes in percentage except for specimens at HF=50 kW/m <sup>2</sup> .

4.2.6.3 Coating C

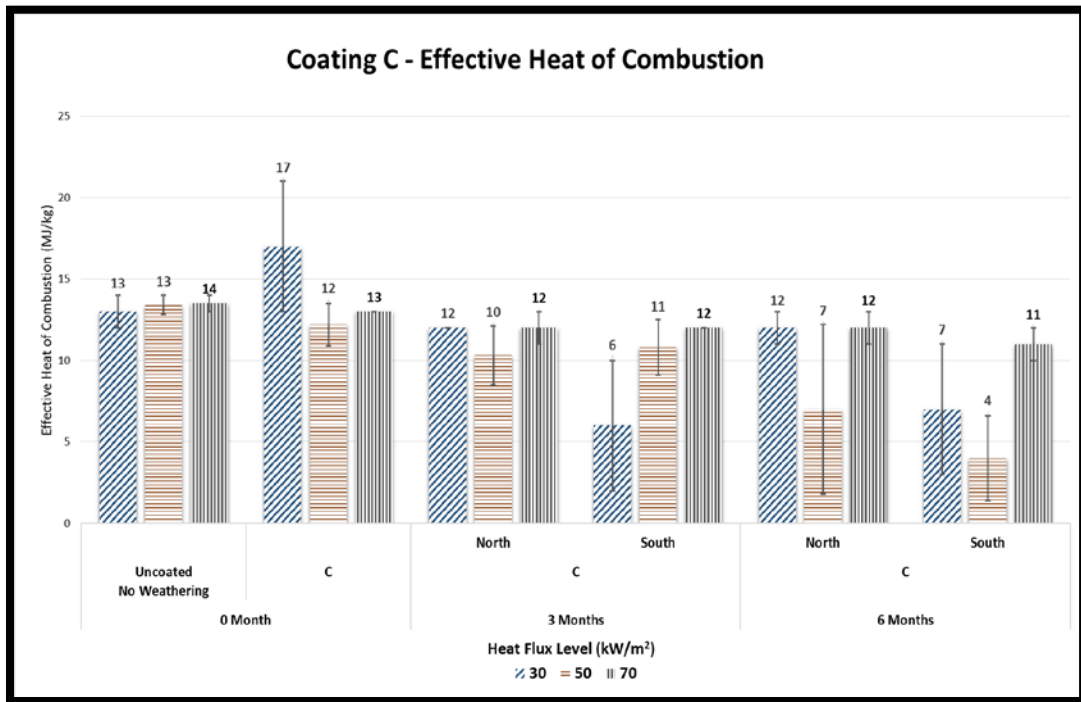


Figure 4.22. EHC comparison bar-chart for coating C

Table 35. Effects on EHC- coating C

Effective Heat of Combustion (EHC)	
Parameter	Effects
Weathering Period	According to Table 32 and Figure 4.22, weathering period affected the specimens mostly at HF levels of 30 kW/m <sup>2</sup> and 50 kW/m <sup>2</sup> .
Heat Flux Level	Same as the weathering period parameter, specimens at HF levels of 30 kW/m <sup>2</sup> and 50 kW/m <sup>2</sup> were affected more in comparison to those at 71 kW/m <sup>2</sup> . Table 32 validates that the changes in percentage at the first two HF levels are greater. As an instance, 6-months weathered southern specimens changed -66% at HF=30 kW/m <sup>2</sup> , where the change at HF=70 kW/m <sup>2</sup> for such samples was -6% in comparison to non-weathered specimens.
Weathering Orientation	As shown in Figure 4.22, weathering orientation affected the EHC values for specimens at HF of 30 kW/m <sup>2</sup> . Also, the percentage changes showed that specimens at southern section were more vulnerable in comparison to northern ones (at HF=30 kW/m <sup>2</sup> ). The noticeable difference in southern section specimens was also seen for 3-months weathered samples at HF of 50 kW/m <sup>2</sup> (-67% in south and -20% in north in comparison to non-weathered specimens).

### 4.3 Intumescence Mechanism during Combustibility Tests

One of the most important observations during the combustibility tests was the intumescence formation. As discussed in previous sections, weathering and heat flux affect the intumescence formation as the intumescence did not follow the regular sequence, which is shown in Figure 4.23.

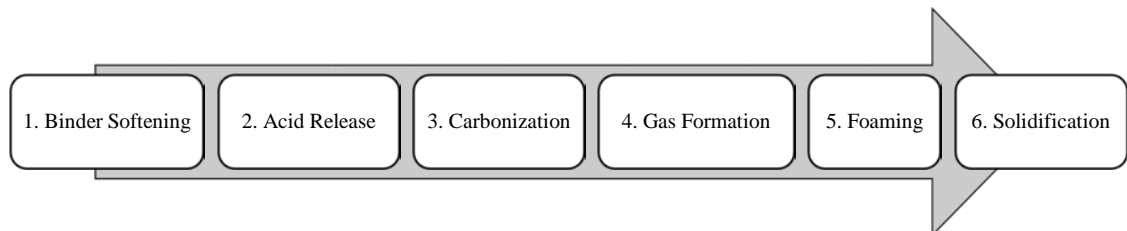


Figure 4.23. Main steps in intumescence mechanism

Based on Figure 4.23, different stages which were seen during the combustibility tests can be explained:

1. Bubbling: Occurred at step 3 (carbonization), and pyrolysis gases (the fuel flow) can be seen afterward,
2. Char Formation: Occurred at step 5 (foaming), and is defined a time where the carbonaceous layer (char) covered the surface of the specimen.
3. Intumescence: Occurred at step 6 (solidification), where the carbonaceous layer was starting to swell. In other words, the growth of the layer was observable.

Figure 4.24 shows the intumescence formation of a Coating A, 3-month weathered specimen with a southern weathering orientation and a HF exposure of 50 kW/m<sup>2</sup>. 6 seconds after opening the shutters, bubbling is started, and it took nearly 26 seconds for the bubbles covered the whole surface. However, the mechanism was stopped at bubbling stage (carbon char formation), and ignition occurred before any intumescence growth was seen.



(1) 6s

(2) 16s

(3) 26s

(4) 30s

Figure 4.24. Coating A- south- 3-months weathered- HF=50 kW/m<sup>2</sup>

In Figure 4.20, a Coating A, 3-month weathered specimen with southern weathering orientation at HF=70 kW/m<sup>2</sup>. Bubbling and pyrolysis gases can be clearly seen after 5 seconds, and char was partially formed after 10 seconds (although the char did not cover the whole surface). 5 second later, ignition was occurred, and a continuation in bubbling was seen until the char covered the surface. Again, no intumescence growth was seen.



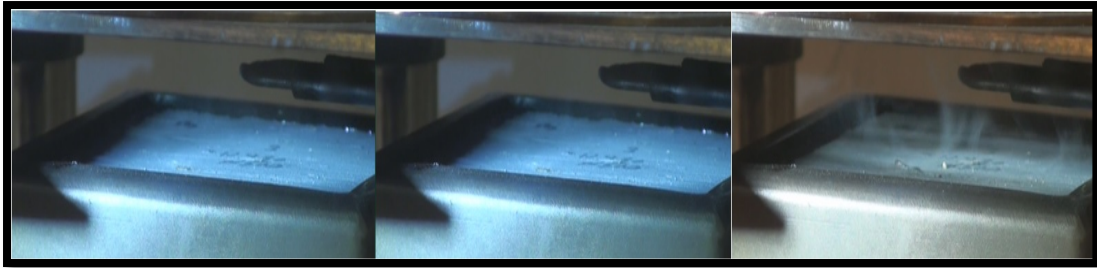
(1) 5s

(2) 10s

(3) 15s

Figure 4.25. Coating A- south- 3-months weathered- HF=70 kW/m<sup>2</sup>

As mentioned before, Coating B showed more instability in comparison to the other two coatings. This instability was especially seen in weathered (3 and 6 months) coatings at heat flux levels higher than 30 kW/m<sup>2</sup> (at the 50 kW/m<sup>2</sup> and 70 kW/m<sup>2</sup> HF levels). Figures 4.26.a and 4.26.b show a Coating B, 3-month weathered specimen with southern weathering orientation at HF=30 kW/m<sup>2</sup>. After 15 seconds, no sign of bubbling or gas release was seen. Limited bubbling and pyrolysis gas release was started around t=35s, and bubbling was partially expanded on one side (without carbon foam formation and covering the whole surface), and ignition occurred.



(1) 15s

(2) 25s

(3) 35s

Figure 4.26.a. Coating B- south- 3-months weathered- HF=30 kW/m<sup>2</sup>

Most of the 3-months and 6-months weathered, Coating B specimens showed a similar behavior in all three heat flux levels. The break in intumescence formation mechanism occurred sooner as the heat flux level was increased for Coating B specimens.



(1) 45s

(2) 55s

(3) 65s

Figure 4.26.b Coating B- south- 3-months weathered- HF=30 kW/m<sup>2</sup>

Another Coating B specimen is seen in Figure 4.27. It can be noticed from picture (2) that ignition occurred while bubbling, and bubbles covered the surface about 5 seconds after the ignition, in figure (3). Although bubbling was partially occurred, no intumescence was seen.



(1) 5s

(2) 10s

(3) 15s

Figure 4.27. Coating B- south- 3-months weathered- HF=50 kW/m<sup>2</sup>

A Coating C, 6-month weathered specimen with northern weathering orientation at  $HF=70 \text{ kW/m}^2$  is shown in Figures 28.a and 28.b. As mentioned before, two important points were observed in coating C specimens: 1) multiple flame-out/re-ignitions (which can clearly be seen in reduced AHRR values in Figure 4.16); and 2) intumescence growth as the intumescence touched the spark igniter and in some cases, tests were continued without the igniter.

In addition, two more important observations were: 1) intumescence was seen in all Coating C specimens (regardless of weathering orientation, weathering period, and heat flux level); and 2) at the heat flux level ( $50 \text{ kW/m}^2$ ), most of 6-months weathered, southern-orientated specimens did not ignite.

As shown in Figure 23.a, intumescence formed even in high heat flux level, and the growth was continued even after the ignition (Figure 4.23.b).

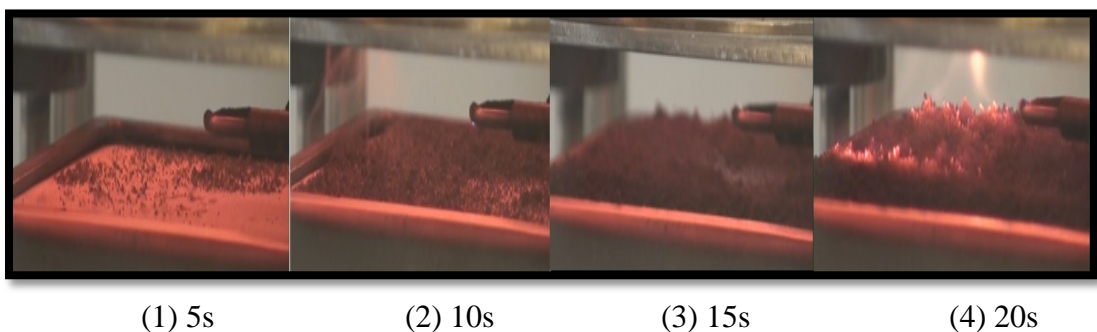


Figure 4.28.a. Coating C- north- 6-months weathered-  $HF=70 \text{ kW/m}^2$

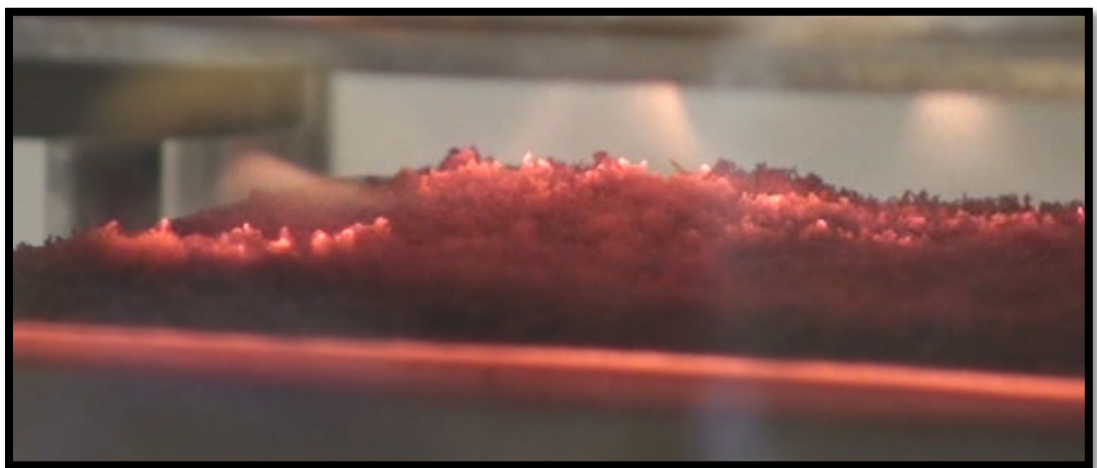


Figure 4.28.b. Coating C- north- 6-months weathered-  $HF=70 \text{ kW/m}^2$

As a result, higher heat flux levels (50 kW/m<sup>2</sup> and 70 kW/m<sup>2</sup>) clearly affected coatings A and B in this study (regardless of weathering period and weathering orientation more than Coating C specimens. Intumescence mechanism break in higher heat flux levels can also be explained by the meaningful difference in TTI values for all coatings (Figures 4.11.a, 4.12.a, and 4.13.a).

#### 4.4 SDT Thermal Tests

A set of simultaneous DSC and TGA (SDT) tests were performed at the UNC Charlotte's Materials Characterization Laboratory (MCL). Note that the collected coating from the specimens' surface were tested, not the entire specimen (including plywood substrate and the coating). For Coating A, collecting sample from the specimen's surface was not possible after weathering period due to possible absorption/desorption, mold, and presence of bugs; so the result was the average on two test performed on non-weathered specimens. Results from the TGA tests can be seen in Table 24.

As shown in Table 36, the final mass percentage for Coatings B and C were decreased as a result of weathering. Although there is no significant difference in values between 3-months and 6-months weathered coatings, the difference between 3-months and no-weathering specimens are significant. Differences are discussed in detail in next sub-sections.

In addition, based on the obtained data, no notable difference can be seen regard to the orientation; north or south. Note that a complete thermal analysis for coatings demands a gas analysis alongside.

Table 36. Results obtained from the SDT tests

Coating	Temperature Range [°C]	Average Initial Mass [mg]	Weathering Period				
		Remained Mass Percentage [%]	0	3		6	
				North	South	North	South
A	30 to 769 (Ambient to the temperature equivalent to heat flux level=50 kW/m <sup>2</sup> in the fire test)	$M_{i,avg.}^*$	4.84	Data not Available			
		$M_F^{**}$	17.18				
B		$M_{i,avg.}$	8.61	7.42	9.93	9.18	7.26
		$M_F$	24.08	37.34	32.36	29.22	27.85
C		$M_{i,avg.}$	6.82	8.12	8.64	9.65	8.26
		$M_F$	50.06	47.27	48.17	47.03	45.56

\*  $M_{i,avg.}$ : Average Initial Mass in mg

\*\*  $M_F$ : Remained Mass Percentage

#### 4.4.1 Coating A

The TGA report for Coating A can be seen in Figure 4.29. Coating A lost the glossiness during weathering, and parts of the coating were substituted by mold. From Figure 4.29, non-weathered specimens lost the water content in the first 150°C of the thermal test. The four curvatures in the diagram shows that there were at least four decomposed components within this temperature range.

There was no data for 3-months and 6-months weathered from tests to compare. The remaining SDT test diagrams for Coating A are presented in appendix C1. The diagram is plotted based on average values from two SDT tests in same conditions.

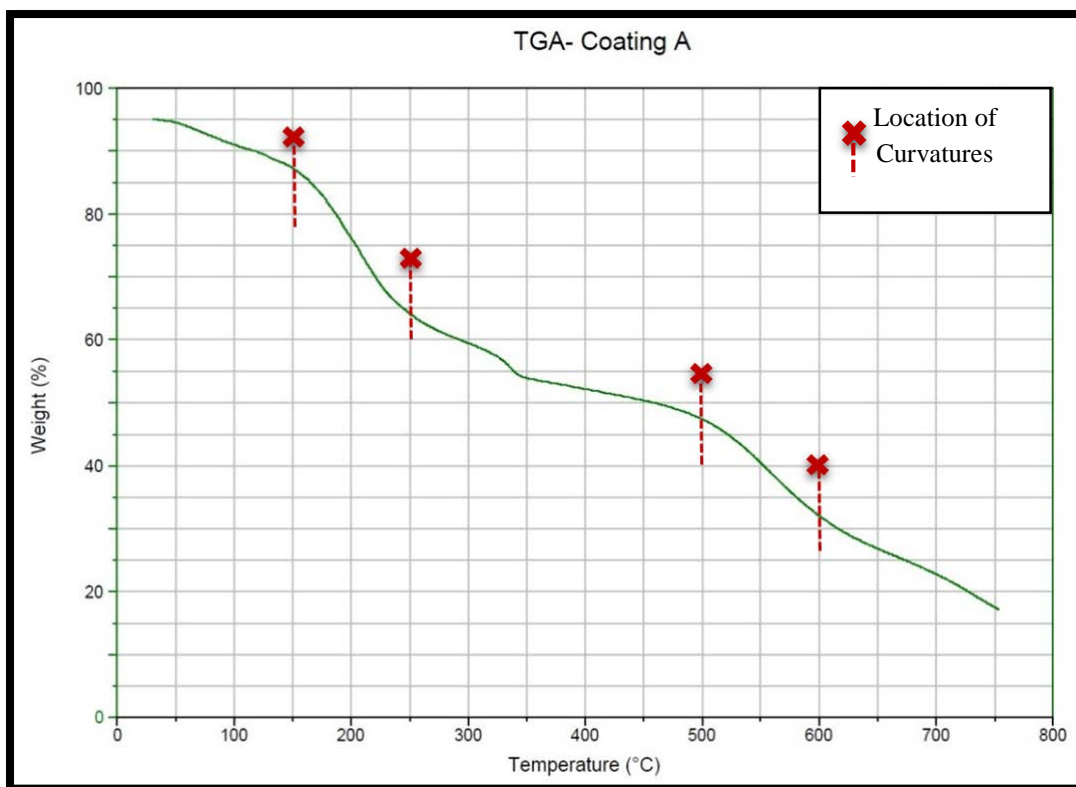


Figure 4.29. SDT result for coating A

#### 4.4.2 Coating B

Figure 4.30 shows the mass loss was increased for Coating B during the weathering. The figure also indicates that specimens lost the water content in the first 150°C of testing.

The presence of four curvatures in this temperature range shows that at least four components were decomposed within this range. The remaining SDT test diagram for Coating B are presented in appendix C2. The diagram is plotted based on average values from two SDT tests in same conditions.

Based on Table 32, weathering orientation did not affect the final mass percentage (less than 5% for 3-months weathered and less than 2% for 6-months weathered specimens). In addition, differences in weathering period were also negligible for Coating B.

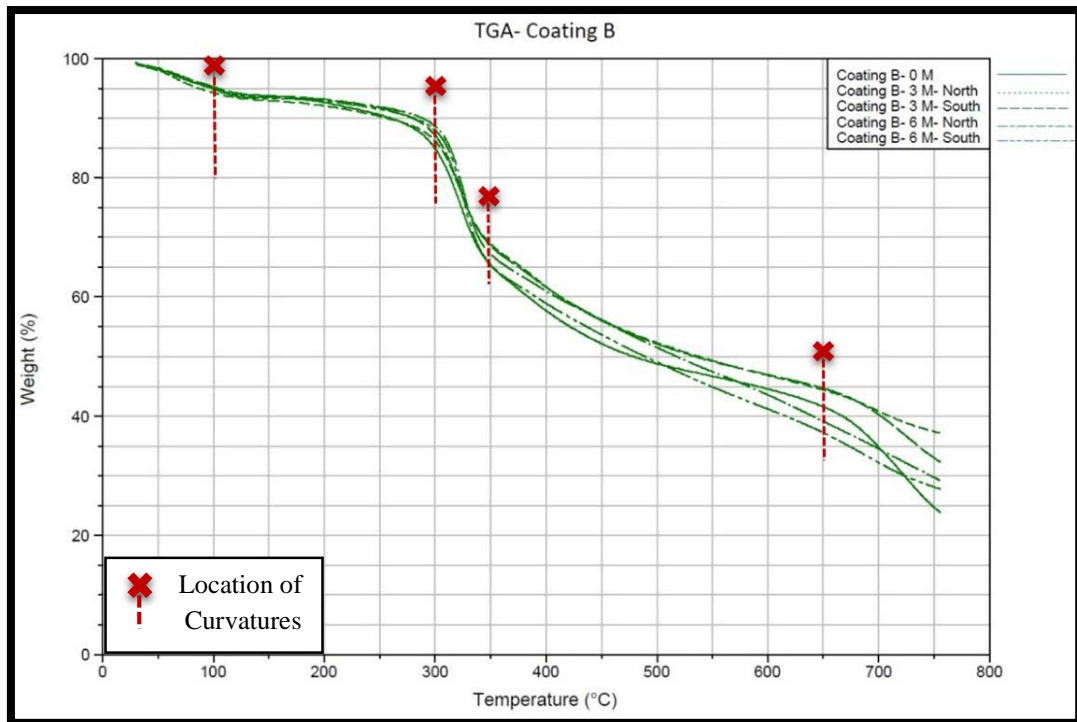


Figure 4.30. SDT results for coating B

#### 4.4.3 Coating C

Similar to the fire test results, Coating C showed better resistance in the thermal tests, as well. As shown in Figure 4.31, there is no major mass loss up to 200 °C. Presence of three curvatures within the temperature range indicates that there were at least three decomposed components.

As shown in Table 36, there was no significant difference in mass loss based on the weathering orientation of the specimens (less than 2%). In addition, weathering period did not affect the specimens, either. Comparison among specimens which were weathered in different time intervals showed less than 5% difference in final mass.

The remaining SDT test diagrams for Coating C are presented in appendix C3. The diagram is plotted based on average values from two SDT tests in same conditions.

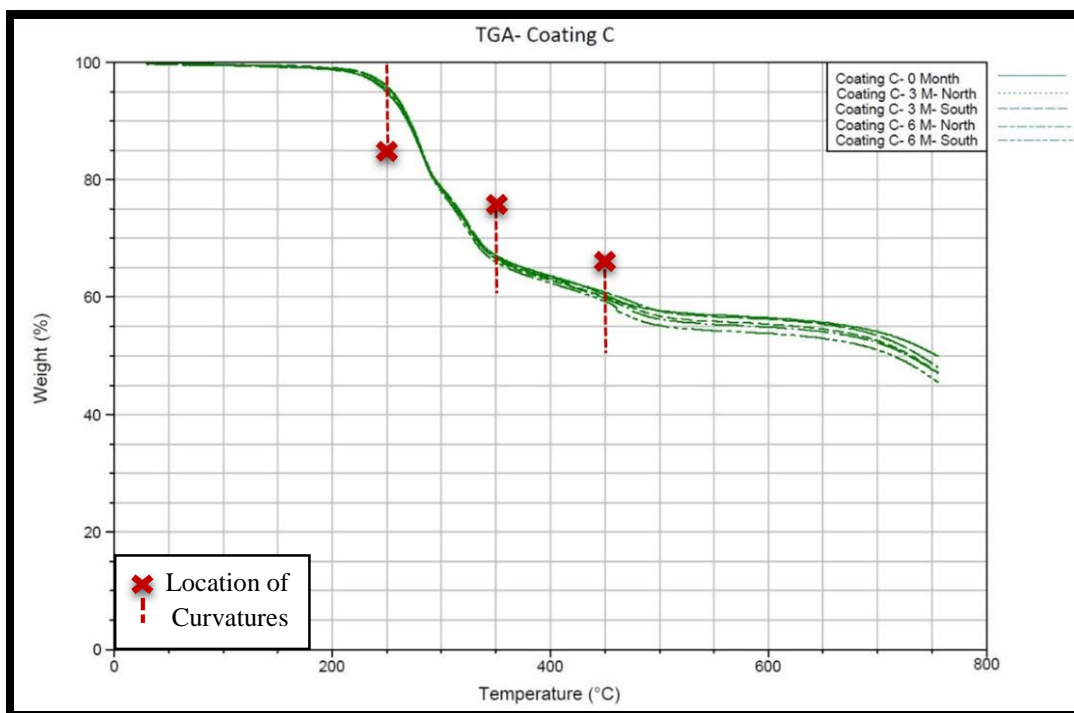


Figure 4.31. SDT results for coating C

Figure 2.32 shows the no-weathered specimens which was collected from the surface using a stainless steel spatula. The residues for each sample were also collected. No intumescence/ char was seen during the thermal tests in the pans. The residues were powdery ash, with lighter color for Coating B, and darker color for Coating C. No noticeable change in color or shape of residues was observed regard to the weathering orientation (north/south), and weathering period.

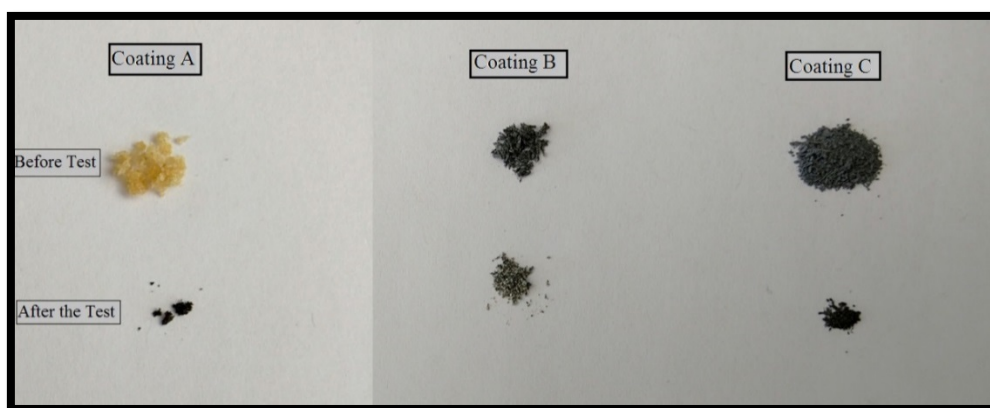


Figure 4.32. Collected coatings from surface of specimens

Figure 4.33 shows the non-weathered specimens after the fire test with the cone calorimeter at heat flux level=30 kW/m<sup>2</sup>.



Figure 4.33. Comparison of the specimens at the end of the fire test

## CHAPTER FIVE: CONCLUSIONS AND RECOMMENDATIONS

### 5.1 Conclusions

The following conclusions can be made based on the finding from the combustibility tests:

1) The TTI values in different time intervals (0, 3, and 6 months) showed that the primary weathering factors (solar irradiation, moisture, and temperature) clearly affected the performance of coatings. TTI values were reduced more at  $HF=50 \text{ kW/m}^2$  in all three coatings in comparison to the other two heat flux levels. The variation of TTI values in different weathering intervals clearly addressed the first concern that the weathering reduced the ignition resistance of the coatings.

2) No significant changes in PHRR and EHC values was seen during the combustibility tests for Coating A and Coating C. These results revealed that it is *not* likely that the coating layer would act as an additional combustible fuel to the structure ignition after the weathering period, *and increases the potential* for fire growth for these two coatings. However, Coating B (especially in HF of  $50 \text{ kW/m}^2$ ) showed variations in PHRR and EHC values. In conclusion, the probability for a layer act as a combustible fuel to the structure is also depends on the coating type.

3) No uniform behavior was seen in terms of the weathering orientation. For some properties (such as  $t_{\text{intu.}}$  and  $H_{\text{intu.}}$ ), no adequate data was gathered for comparison. Weathering orientation specifically affected the TTI and EHC for Coating C (at HF of  $70 \text{ kW/m}^2$ ) and Coating B (at HF of  $50 \text{ kW/m}^2$ ).

4) The heat flux increase in the combustibility tests had great effects on performance of the coatings. Most specimens showed a different behavior at higher heat flux levels (50 kW/m<sup>2</sup> and 70 kW/m<sup>2</sup>) after being exposed to weathering conditions. The difference was in intumescence formation stages, where most of the weathered Coating A were stopped at step 5 (char formation or foaming), and weathered Coating B specimens were stopped at step 3 (bubbling or carbonization) regardless of their weathering orientation. This indicated that coatings which were tested were designed for the flux levels lower than 50 kW/m<sup>2</sup>. However, the *threshold* in which the sequence of intumescence mechanism was changed is *not known yet*.

5) The SDT results did not show an observable difference (less than 5%) in pyrolysis kinetics for the coatings during the thermal degradation tests after different weathering periods (3-months or 6-months) or weathering orientation.

## 5.2 Significance of Research

Several studies have been conducted with a steel substrate, and some on impregnated coatings, but there was a gap present for intumescent coatings. Along with providing a better understanding of such effects, this study may lead to a standard procedure establishment for application of coatings on wooden substrates and the effect of weathering on their performance.

This was the first comprehensive study focused on the effect of weathering on fire performance of intumescent coatings on wooden structures. Findings of this study indicated that weathering had a more noticeable effect on the fire resistance of the tested intumescent coatings. Obtained results can contribute to optimize the fire performance of intumescent fire retardant coatings.

In addition, it gave a better understanding of weathering effects on coatings as one of the passive fire protection methods used both for the continuation of this project, and in survival of the structures in WUI fires.

### 5.3 Recommendations for Future Research

This study was part of a bigger project. The project was planned for 5 years from 2014 to 2019, and the first three sets of tested specimens were considered for the first year. The study is ongoing unless the specimens will not be testable in the remained time. No statistical analysis methods (e.g. ANOVA) were used for the finding of this study, and it is recommended that such analysis should be performed for the next steps.

As an example, Coating A specimens were affected more by weathering, as the surface of the specimens lost glossiness, covered with mold, and multiple crack were appeared. Regarding future work with intumescent fire retardant coatings, it is recommended that the tests will be continued with the new procedure (which the tests stopped 3 minutes after the PHRR observation), and further the effects of weathering should be studied during the remained period of the project.

There are standards available for the application of intumescent coatings on steel structures (such as ASTM E2924: Standard Practice for Intumescent Coatings), but no such standard for wooden structures. It is recommended that similar procedures or standards should be developed.

The coatings used in this study were claimed to be able to resist the weathering exposure conditions up to 5 years. Some of the manufacturers provided the inspection requirements after a certain time. It is recommended that manufacturers also provide assessment guides and procedures (if needed) for re-coating.

One important observation during this study was the effect of heat flux on the performance of the intumescent coatings. So far, the heat flux level threshold value in which the intumescence cannot be formed is still unknown. This threshold depends on the chemical composition of each coating along with weathering effects. It is recommended that this threshold be provided value to clarify the application range and limitation of each coating.

## REFERENCES

- [1] Ahrens, M. (2013). *Brush, Grass, and Forest Fires*: National Fire Protection Association, Report, pp. 6.
- [2] ASTM Standard E84, 2015, "Surface Burning Characteristics of Building Materials," ASTM International, West Conshohocken, PA 2015, DOI: 10.1520/E0084-15A.
- [3] ASTM Standard E1354, 2015, "Standard Test Method for Heat and Visible Smoke Release Rates for Materials and Products Using an Oxygen Consumption Calorimeter," ASTM International, West Conshohocken, PA, 2015, DOI: 10.1520/E1354-15A.
- [4] ASTM Standard G113, 2014, "Standard Terminology Relating to Natural and Artificial Weathering Tests of Nonmetallic Materials," ASTM International, West Conshohocken, PA, 2014, DOI: 10.1520/G0113-14.
- [5] Azwa, Z., Yousif, B., Manalo, A., & Karunasena, W. (2013). A review on the degradability of polymeric composites based on natural fibres. *Materials & Design*, 47, 424-442.
- [6] Babrauskas, V. (1984). Development of the cone calorimeter—a bench-scale heat release rate apparatus based on oxygen consumption. *Fire and Materials*, 8(2), 81-95.
- [7] Babrauskas, V., & Peacock, R. D. (1992). Heat release rate: the single most important variable in fire hazard. *Fire safety journal*, 18(3), 255-272.
- [8] Beyler, C. L., & Hirschler, M. M. (2002). Thermal decomposition of polymers. *SFPE handbook of fire protection engineering*, 7, 113-123.
- [9] Bhatnagar, M. (1996). *Epoxy resins (overview)* (pp. 1): CRC Press: Boca Raton, FL, USA.
- [10] Bisschoff, J. (2000). *Oxygenated Hydrocarbon Compounds as Flame Retardants for Polyester Fabric*. MS Thesis, University of Pretoria, Pretoria, South Africa.
- [11] Boake, T. M. (2015). *Architecturally Exposed Structural Steel: Specifications, Connections, Details*, 82-91.
- [12] Bourbigot, S., & Duquesne, S. (2007). Fire retardant polymers: recent developments and opportunities. *Journal of Materials Chemistry*, 17(22), 2283-2300.
- [13] Brown, M. E. (2001). *Introduction to thermal analysis: techniques and applications* (Vol. 1): Springer Science & Business Media, 8-11.

- [14] Calkin, D. E., Cohen, J. D., Finney, M. A., & Thompson, M. P. (2014). How risk management can prevent future wildfire disasters in the wildland-urban interface. *Proceedings of the National Academy of Sciences*, 111(2), 746-751.
- [15] CEI International, I. (2012). Wet and Dry Film Thickness Formulae. from <https://www.geionline.com/wet-film-formulae>  
[Last access date: November 12th, 2015]
- [16] Cohen, J. D. (1995). Structure ignition assessment model (SIAM). Paper presented at the Weise, David R.; Martin, Robert E., technical coordinators. *Proceedings of the Biswell symposium: fire issues and solutions in urban interface and wildland ecosystems*, 85-87
- [17] Cohen, J. D. (2000a). Preventing Disaster: Home Ignitability in the Wildland-Urban Interface. *Journal of Forestry*, 98(3), 15-21.
- [18] Cohen, J. D. (2000b). What is the wildland fire threat to homes? School of Forestry, Presented as the Thompson Memorial Lecture, Northern Arizona University, Flagstaff, AZ, 7-10
- [19] Cohen, J. D. (2010). The wildland-urban interface fire problem. *Fremontia*, 38(2-3), 16-22.
- [20] Cohen, J. D., & Butler, B. W. (1996). Modeling potential structure ignitions from flame radiation exposure with implications for wildland/urban interface fire management. Paper presented at the Thirteenth Fire and Forest Meteorology Conference, Lorne, Australia, pp. 82.
- [21] Community, Chemical Free. (2015). Flame Retardants (Halogenated/BrominatedHFR/BFR). from <http://www.chemfree.com/chemicals/flameretardantshalogenatedbrominated-hfrbfr/>  
[Last access date: November 12th, 2015]
- [22] Corrosionpedia. (2015). Weathering Test. from <https://www.corrosionpedia.com/definition/1396/weathering-test>  
[Last access date: November 12th, 2015]
- [23] Crooks, R. (2011). What Is AC Grade Plywood? , from <http://homeguides.sfgate.com/ac-grade-plywood-99041.html>  
[Last access date: November 12th, 2015]
- [24] Daniliuc, A., Deppe, B., Deppe, O., Friebel, S., Kruse, D., & Philipp, C. (2012). New trends in wood coatings and fire retardant. *European Coatings Journal*, 7(08), 2012, 21-24.
- [25] Dasari, A., Yu, Z.-Z., Cai, G.-P., & Mai, Y.-W. (2013). Recent developments in the fire retardancy of polymeric materials. *Progress in Polymer Science*, 38(9), 1357-1387.

- [26] Davis, R. D. (2014). Cone Calorimeter. from [http://www.nist.gov/el/facilities\\_instruments/conecal.cfm](http://www.nist.gov/el/facilities_instruments/conecal.cfm)  
[Last access date: November 12th, 2015]
- [27] Diamantes, D. (2010). Principles of Fire Prevention: Cengage Learning, 122-133.
- [28] Enright, P. A., & Fleischmann, C. M. (1999). Uncertainty of Heat Release Rate Calculation of the ISO5660–1 Cone Calorimeter Standard Test Method. *Fire Technology*, 35(2), 153-169.
- [29] Firewise. (2012). Defensible Space. from [http://www.napafirewise.org/DS%20Download/defensable-space-live/15\\_defensiblespace.html](http://www.napafirewise.org/DS%20Download/defensable-space-live/15_defensiblespace.html)  
[Last access date: November 12th, 2015]
- [30] Firewise. (2014). What Exactly is The Home Ignition Zone?, from <http://firewise.org/wildfire-preparedness/be-firewise/home-and-landscape/what-exactly-is-the-home-ignition-zone.aspx>  
[Last access date: November 12th, 2015]
- [31] Foundation, Nuffield. (2012). Observing the motion of the sun. from <http://www.nuffieldfoundation.org/practical-physics/observing-motion-sun>  
[Last access date: November 12th, 2015]
- [32] FPS, 3MTM DireDamTM. (2011). Intumescent Coating WB 1000 Training Module: Thinner is Better. from <http://www.fire.tc.faa.gov/pdf/systems/Nov12Meeting/Paragon-1112-Containers-WB1000.pdf>, 5-6.  
[Last access date: November 12th, 2015]
- [33] Francis, R. (2009). Dry Film Thickness Measurements: How Many Are Enough? *Journal of protective coatings & linings.*, 71(12), pp. 22.
- [34] FTT. (2015). Cone Calorimeter (ISO 5660 ASTM E 1354)- The most comprehensive bench scale fire test. In *Fire Testing Technology (Ed.2), Brochure*, (pp. 6).
- [35] FTT & GBH International, (2014). Cone Calorimeter Standard Operating Procedure (SOP) (pp. 5): *Fire Testing Technology (FTT) & GBH International*.
- [36] Georlette, P. (2001). Applications of halogen flame retardants. *Fire retardant materials*, 264-292.
- [37] Gollner, M., Caton, Cohler. (2015). Pathways for Building Fire Spread at the Wildland Urban Interface: Department of Fire Protection Engineering, University of Maryland, College Park, Maryland USA, 18-44.

- [38] Green, J. (1997). 25 Years of Flame Retarding Plastics. *Journal of fire sciences.*, 15(1), pp. 52.
- [39] Harada, T., Matsunaga, H., Kataoka, Y., Kiguchi, M., & Matsumura, J. (2009). Weatherability and combustibility of fire-retardant-impregnated wood after accelerated weathering tests. *Journal of Wood Science*, 55(5), 359-366.
- [40] Hastie, J. W., & Bonnell, D. (1980). Molecular chemistry of inhibited combustion systems: National Bureau of Standards, 22-26.
- [41] Hinojosa, R. (2009). Field testing of wet film thickness and dry film thickness of waterproof coatings. *Interface*, pp. 22.
- [42] Holmes, C. A., & Knispel, R. O. (1981). Exterior Weathering Durability of Some Leach-Resistant Fire-Retardant Treatments for Wood Shingles: A Five-Year Report: DTIC Document, 1-4.
- [43] Horacek, H., & Grabner, R. (1996). Advantages of flame retardants based on nitrogen compounds. *Polymer Degradation and Stability*, 54(2), 205-215.
- [44] Huggett, C. (1980). Estimation of rate of heat release by means of oxygen consumption measurements. *Fire and Materials*, 4(2), 61-65.
- [45] Hull, T. R., & Kandola, B. K. (2009). Fire retardancy of polymers: New strategies and mechanisms: Royal Society of Chemistry, pp. 136.
- [46] Hurley, M. J., Gottuk, D. T., Hall Jr, J. R., Harada, K., Kuligowski, E. D., Puchovsky, M., et al. (2015). *SFPE handbook of fire protection engineering (Vol. III)*: Springer, pp 3298.
- [47] ICC. (2015). International Wildland-Urban Interface Code (pp. 19-20): International Code Council (ICC). From: <http://codes.iccsafe.org/app/book/toc/2015/I-Codes/2015%20IWUIC%20HTML/index.html>  
[Last access date: November 12th, 2015]
- [48] Jimenez, M., Bellayer, S., Revel, B., Duquesne, S., & Bourbigot, S. (2013). Comprehensive study of the influence of different aging scenarios on the fire protective behavior of an epoxy based intumescent coating. *Industrial & Engineering Chemistry Research*, 52(2), 729-743.
- [49] Kilinc, F. S. (2013). *Handbook of fire resistant textiles*: Elsevier, pp. 332.
- [50] Koo, E., Pagni, P. J., Weise, D. R., & Woycheese, J. P. (2010). Firebrands and spotting ignition in large-scale fires. *International Journal of Wildland Fire*, 19(7), 818-843.
- [51] Labuschagné, F. J. W. J., Focke, W.W., and Mentz, J.C. . (2001). South Africa Patent No. 2002/4876 University of Pretoria, Pretoria, South Africa.

- [52] Lawrence, C. (2014). *High performance textiles and their applications*: Elsevier, pp. 161.
- [53] LeVan, S. L., & Holmes, C. A. (1986). Effectiveness of fire-retardant treatments for shingles after 10 years of outdoor weathering, 1-11.
- [54] Lyon, R. E., & Janssens, M. L. (2005). *Polymer Flammability*: U.S. Department of Transportation, Federal Aviation Administration, Office of Aviation Research, Washington, DC, pp. 3
- [55] Manzello, S. L., Shields, J. R., Hayashi, Y., & Nii, D. (2008). Investigating the vulnerabilities of structures to ignition from a firebrand attack. *Fire Safety Science*, 9, 143-154.
- [56] Masys, A. (2015). *Disaster Management: Enabling Resilience*: Springer, pp. 291.
- [57] Matafonova, G., & Batoev, V. (2012). Recent progress on application of UV excilamps for degradation of organic pollutants and microbial inactivation. *Chemosphere*, 89(6), 637-647.
- [58] McGreer, M. (2001). *Atlas weathering testing guidebook*. Chicago: Atlas Material Testing Technology LLC, 5-25.
- [59] Mell, W. E., McDermott, R. J., Forney, G. P., Hoffman, C., & Ginder, M. (2010). Wildland fire behavior modeling: perspectives, new approaches and applications. Paper presented at the Proc. Third Fire Behaviour and Fuels Conf., 2-4.
- [60] Morgan, A. B., & Wilkie, C. A. (2007). *Flame retardant polymer nanocomposites*: John Wiley & Sons, 13-15.
- [61] Mount, R. A. (1994). *Handbook of fire retardant coatings and fire testing services*, 1994. Lancaster; Basel: Technomic Pub. Co.
- [62] Mouritz, A. P., & Gibson, A. G. (2007). *Fire properties of polymer composite materials* (Vol. 143): Springer Science & Business Media, pp. 8.
- [63] NII, National Institute of Industrial Research, Board of Consultants & Engineers. (2009). *The complete technology book on wood and its derivatives*. Kamla Nagar, Delhi: National Institute of Industrial Research, pp. 305.
- [64] National Fire Protection Association. (2015). *NFPA 101: Life Safety Code*.
- [65] National Fire Protection Association. (2014). *NFPA 130: Standard for fixed guideway transit and passenger rail systems*.

- [66] National Fire Protection Association. (2012). NFPA 287: Standard test methods for measurement of flammability of materials in cleanrooms using a fire propagation apparatus (fpa).
- [67] National Fire Protection Association. (2011). NFPA 556: Guide on methods for evaluating fire hazard to occupants of passenger road vehicles: National Fire Protection Association (NFPA).
- [68] NFPA. (2008). Deadliest/large-loss fires, 25 largest fire losses in US history. Quincy, MA: National Fire Protection Association (NFPA).
- [69] NFPA. (2013). Largest Loss Wildland Fires. from <http://www.nfpa.org/research/reports-and-statistics/outdoor-fires/largest-loss-wildland-fires>  
[Last access date: November 12th, 2015]
- [70] NIFC. (2014). Human-caused fires and acres (2001-2013). from [https://www.nifc.gov/fireInfo/fireInfo\\_stats\\_human.html](https://www.nifc.gov/fireInfo/fireInfo_stats_human.html)  
[Last access date: November 12th, 2015]
- [71] NIFC. (2015a). Communicator's Guide for Wildland Fire Management. from [https://www.nifc.gov/prevEdu/comm\\_guide/TOC.html](https://www.nifc.gov/prevEdu/comm_guide/TOC.html)  
[Last access date: November 12th, 2015]
- [72] NIFC. (2015b). Historically Significant Wildland Fires. from [https://www.nifc.gov/fireInfo/fireInfo\\_stats\\_histSigFires.html](https://www.nifc.gov/fireInfo/fireInfo_stats_histSigFires.html)  
[Last access date: November 12th, 2015]
- [73] NWCG. (2015). National Wildland Coordination Group- Glossary. from <http://www.nwcg.gov/term/glossary/wildland>  
[Last access date: November 12th, 2015]
- [74] NPS. (2012). Wildfire Causes. from <http://www.nps.gov/fire/wildland-fire/learning-center/fire-in-depth/wildfire-causes.cfm>  
[Last access date: November 12th, 2015]
- [75] Papaspyrides, C. D., & Kiliaris, P. (2014). Polymer Green Flame Retardants: A Comprehensive Guide to Additives and Their Applications: Newnes.
- [76] Pearce, E. (2012). Flame-retardant polymeric materials: Springer Science & Business Media, pp. 114 & 414.
- [77] Quarles, S. L., Valachovic, Y., Nakamura, G. M., Nader, G., & DeLasaux, M. (2010). Home survival in wildfire-prone areas: building materials and design considerations. ANR Publication, 8393.

- [78] Quill, J., & Fowler, S. (2015). Test Method Development for Outdoor Exposure and Accelerated Weathering of Vinyl Siding Specimens. In C. C. White, J. Martin & J. T. Chapin (Eds.), *Service Life Prediction of Exterior Plastics* (pp. 135-150): Springer International Publishing.
- [79] Ripling, E., Mostovoy, S., & Corten, H. (1971). Fracture mechanics: a tool for evaluating structural adhesives. *The Journal of Adhesion*, 3(2), 107-123.
- [80] Roach, K. (2014). Balancing passive, active fire protection. from <http://www.csemag.com/single-article/balancing-passive-active-fire-protection/6201f8f2c81dd5cd87307b7e0075161d.html>  
[Last access date: November 12th, 2015]
- [81] Roberts, T. A., Shirvill, L. C., Waterton, K., & Buckland, I. (2010). Fire resistance of passive fire protection coatings after long-term weathering. *Process Safety and Environmental Protection*, 88(1), 1-19.
- [82] Saxena, N., & Gupta, D. (1990). Development and evaluation of fire retardant coatings. *Fire Technology*, 26(4), 329-341.
- [83] Schartel, B. (2010). Phosphorus-based flame retardancy mechanisms—old hat or a starting point for future development? *Materials*, 3(10), 4710-4745.
- [84] Schartel, B., & Hull, T. R. (2007). Development of fire-retarded materials— Interpretation of cone calorimeter data. *Fire and Materials*, 31(5), 327-354.
- [85] Schulz, U. (2009). Accelerated testing: nature and artificial weathering in the coatings industry: Vincentz Network GmbH & Co KG.
- [86] Searle, N. D. (2009). Natural and artificial weathering of sealants. *Handbook of Sealant Technology* (CRC Press, New York, 2009), 93-142.
- [87] SpecialChem. (2015). Flame Retardants for Polymers. from <http://polymer-additives.specialchem.com/selection-guide/flame-retardants-center#content>  
[Last access date: November 12th, 2015]
- [88] Stevens, M. P. (1999). *Polymer chemistry : an introduction*. New York: Oxford University Press.
- [89] Sundström, B. (2007). The Development of a European Fire Classification System for Building Products-Test Methods and Mathematical Modelling. Department of Fire Safety Engineering, Lund University, Lund, Sweden, Doctoral Thesis, pp. 5.
- [90] Thewes, V. (2009). Intumescent Coatings Expand in Fires to Protect Substrates. *European Coatings Journal*, 5(2009), pp. 2.
- [91] Twilley, W. H., & Babrauskas, V. (1988). User's guide for the cone calorimeter. NASA STI/Recon Technical Report N, 89, 22086, 5-17.

- [92] Urbas, J., & Luebbers, G. E. (1995). The intermediate scale calorimeter development. *Fire and materials*, 19(2), 65-70.
- [93] Urbas, J., & Shaw, J. R. (1993). Testing wall assemblies on an intermediate-scale calorimeter. *Fire Technology*, 29(4), 332-349.
- [94] USFA. (2014). Wildland Urban Interface Terminology. From [https://www.usfa.fema.gov/downloads/pdf/coffee-break/cr/cr\\_2014\\_3.pdf](https://www.usfa.fema.gov/downloads/pdf/coffee-break/cr/cr_2014_3.pdf) [Last access date: November 12th, 2015]
- [95] Vahabi, H., Sonnier, R., & Ferry, L. (2015). Effects of ageing on the fire behaviour of flame-retarded polymers: a review. *Polymer International*, 64(3), 313-328.
- [96] Visakh, P., & Arao, Y. (2015). *Flame Retardants: Polymer Blends, Composites and Nanocomposites*: Springer, pp. 224.
- [97] Wright, J. D., & Singer, J. (2014). *Fire and Explosives*: Routledge.
- [98] Wu, S. (1982). *Polymer interface and adhesion*: M. Dekker.

## APPENDIX A: PRELIMINARY DATA

## A1 UNCOATED SPECIMENS

Table 37. Raw data from the fire tests for uncoated specimens

Parameter	Heat Flux [kW/m <sup>2</sup> ]	TTI [s]	PHRR [kW/m <sup>2</sup> ]	t <sub>p</sub> [s]	AHRR <sub>180s</sub> [kW/m <sup>2</sup> ]	THR [MJ/m <sup>2</sup> ]	EHC [MJ/kg]	FIGRA [kW/s]	FPI [s.m <sup>2</sup> /kW]	AMLR <sub>10-90</sub> [g/m <sup>2</sup> .s]
Weathering [Month]	30	75±10	225 ± 52	517± 64	104 ± 11	62 ± 26	12.8 ± 1.4	0.74 ± 0.59	0.35 ± 0.11	10.2 ± 1.7
	50	20±2	329 ± 15	330±40	162 ± 21	83 ± 1	13.4 ± 0.6	1.00 ± 0.09	0.06	17.0 ± 1.5
	70	12±4	339 ± 39	315± 38	187 ± 32	86 ± 2	13.5 ± 0.5	1.10 ± 0.25	0.03 ± 0.01	17.6 ± 2.6

## A2 COATING A

Table 38. Raw data from the fire tests for coating A

Parameter	Flammability Properties											Intumescence Properties	
	Heat Flux [kW/m <sup>2</sup> ]	TTI [s]	PHRR [kW/m <sup>2</sup> ]	AHRR <sub>180</sub> s[kW/m <sup>2</sup> ]	THR [MJ/m <sup>2</sup> ]	EHC [MJ/kg]	FIGRA [kW/s]	FPI [s.m <sup>2</sup> /kW]	AMLR <sup>10-90</sup> [g/m <sup>2</sup> .s]	T <sub>intu.</sub> [s]	H <sub>intu.</sub> [mm]		
0	30	307±	164±4	68±18	92±25	15.7±3.5	0.2±0.01	1.87±0.27	7.3±0.5	23±2	13.2±2.1		
	50	69±14	206±20	92±20	99±20	13.1±1.0	0.39±0.06	0.34±0.08	9.5±4.2	17±2	11.5±2.0		
	70	39±8	252±30	136±27	166±6	18.4±1.3	0.62±0.07	0.15±0.02	4.8±0.5	9±1	10.9±1.5		
3	30	109±29	214±43	82±19	75±11	11.9±0.6	0.36±0.06	0.53±0.22	10.4±0.8	67±12	NA		
	50	29±6	281±35	136±11	84±6	13.8±17.3	0.72±0.09	0.10±0.01	14.6±1.5	26±6	NA		
	70	17±3	312±27	142±26	158±68	17.3±5.6	0.81±0.20	0.06±0.01	9.8±7.3	13±1	NA		
6	30	105±23	215±31	50±1	65±5	11.7±0.7	0.34±0.04	0.48±0.05	9.1±0.7	60±6	2.0±0.2		
	50	28±7	266±33	139±16	80±4	13.7±0.2	0.68±0.11	0.10±0.03	14.0±0.7	23±4	NA		
	70	16±1	269±39	140±54	139±46	16.0±3.3	0.70±0.21	0.06±0.01	5.9±2.6	12±2	3.7±3.4		
NA	30	119±16	189±37	65±13	72±4	11.7±0.2	0.36±0.10	0.64±0.12	8.7±0.8	60±4	NA		
	50	42±17	279±31	111±13	80±3	12.8±0.7	0.62±0.08	0.16±0.08	13.0±0.6	24±3	NA		
	70	27±3	328±38	149±66	84±9	12.2±0.6	0.95±0.28	0.08±0.02	18.0±3.2	14±6	3.0±1.1		
N	30	111±19	177±20	61±15	68±8	11.5±1.0	0.28±0.02	0.63±0.10	8.7±0.4	65±4	2.3		
	50	40±13	243±33	105±10	78±5	13.4±1.3	0.53±0.12	0.17±0.07	11.8±1.6	29±5	NA		
	70	19±5	312±34	144±26	84±7	12.2±0.2	0.89±0.08	0.06±0.01	17.6±1.8	15±3	NA		
S	Weathering [Month]												
	Orientation												
	6												

## A3 COATING B

Table 39. Raw data from the fire tests for coating B

Parameter	Flammability Properties											Intumescence Properties	
	Heat Flux [kW/m <sup>2</sup> ]	TTI [s]	PHRR [kW/m <sup>2</sup> ]	AHRR <sub>180</sub> s[kW/m <sup>2</sup> ]	THR [MJ/m <sup>2</sup> ]	EHC [MJ/kg]	FIGRA [kW/s]	FPI [s.m <sup>2</sup> /kW]	AMLR <sub>10-90</sub> [g/m <sup>2</sup> .s]	T <sub>intu.</sub> [s]	H <sub>intu.</sub> [mm]		
	Orientation												
	0			3				6					
Weathering [Month]													
	30	506±100	179 ± 12	79 ± 26	88 ± 20	17.3± 3.3	0.17±0.01	2.82±0.48	8.1 ± 1.2	64 ± 12	12.9 ± 1.2		
	50	26 ± 5	190 ± 62	17 ± 5	101 ± 6	12.7± 0.6	0.32±0.10	0.15±0.06	9.6 ± 2.5	22 ± 4	16.2		
	70	24 ± 10	228 ± 30	83 ± 18	94 ± 9	13.1± 0.5	0.44±0.05	0.11±0.05	11.5 ± 1.0	14 ± 2	10.6 ± 2.4		
	30	66	247 ± 7	94 ± 6	84 ± 1	12.9± 0.1	0.41±0.01	0.27±0.01	10.00± 0.9	Not Seen	NA		
	50	42 ± 7	331 ± 24	154 ± 39	85 ± 2	20.9± 5.0	0.92±0.15	0.13±0.03	11.6± 3.3	31	NA		
	70	14 ± 6	312 ± 77	164 ± 33	40 ± 13	10.9± 1.4	5.12±3.50	0.05±0.01	16.2± 3.9	Not Seen	NA		
	30	61 ± 7	205 ± 46	97 ± 8	78 ± 10	13.7± 2.7	0.37±0.07	0.31±0.07	9.2± 0.7	Not Seen	NA		
	50	31 ± 3	325 ± 34	139 ± 9	87 ± 5	12.4± 0.2	0.77±0.02	0.10±0.02	14.7± 1.4	Not Seen	NA		
	70	16 ± 2	345 ± 17	167 ± 12	84 ± 5	12.6± 0.3	1.04±0.08	0.05	17.5± 0.7	Not Seen	NA		
	30	66	247 ± 7	94 ± 6	84 ± 1	12.9± 0.1	0.41±0.01	0.27±0.01	10.0± 0.9	Not Seen	NA		
	50	42 ± 7	331 ± 24	154 ± 39	85 ± 2	20.9± 0.5	0.92±0.15	0.13±0.03	11.6± 3.3	31	NA		
	70	14 ± 6	312 ± 77	164 ± 33	51 ± 25	11.2± 1.3	4.10±3.51	0.05±0.01	16.4± 3.2	Not Seen	NA		
	30	73 ± 10	187 ± 8	100 ± 6	73 ± 4	13.5± 0.1	0.36±0.02	0.39±0.07	9.9± 0.6	Not Seen	NA		
	50	18 ± 7	290 ± 35	129 ± 34	85 ± 11	15.8± 5.3	0.73±0.07	0.06±0.02	14.7± 1.3	Not Seen	3.10		
	70	16 ± 4	338 ± 35	192 ± 32	73 ± 30	12.1± 1.3	4.42±3.51	0.05±0.01	18.7± 2.6	Not Seen	3.00		

## A4 COATING C

Table 40. Raw data from the fire tests for coating C

Parameter	Flammability Properties											Intumescence Properties	
	Heat Flux [kW/m <sup>2</sup> ]	TTI [s]	PHRR [kW/m <sup>2</sup> ]	AHRR <sub>180</sub> s[kW/m <sup>2</sup> ]	THR [MJ/m <sup>2</sup> ]	EHC [MJ/kg]	FIGRA [kW/s]	FPI [s.m <sup>2</sup> /kW]	AMLR <sup>10-90</sup> [g/m <sup>2</sup> .s]	T <sub>intu.</sub> [s]	H <sub>intu.</sub> [mm]		
NA	30	317±108	130 ± 12	51 ± 25	101 ± 23	16.6± 3.9	0.11±0.01	2.41±0.72	5.4±0.2	46 ± 18	13.4 ± 2.5		
	50	292±106	208 ± 61	81 ± 41	76 ± 4	12.2± 1.3	0.32±0.15	1.43±0.57	11.7±0.3	42 ± 6	12.7 ± 0.8		
	70	19 ± 5	192 ± 29	48 ± 12	100 ± 17	12.5± 0.4	0.30±0.06	0.10±0.04	8.8±3.3	11 ± 1	9.2 ± 1.8		
N	30	255 ± 31	179 ± 34	30 ± 13	73 ± 7	11.8± 0.9	0.19±0.04	1.47±0.41	7.8±0.6	42 ± 3	15.9 ± 4.9		
	50	56 ± 21	208 ± 1	27 ± 23	68 ± 20	9.8± 2.8	0.29±0.02	0.27±0.10	9.8±1.0	24 ± 1	11.4 ± 3.2		
	70	28 ± 14	262 ± 28	43 ± 19	80 ± 6	11.6± 0.9	0.41±0.01	0.11±0.06	10.6±0.7	12 ± 2	9.1 ± 1.5		
S	30	211 ± 71	32 ± 22	23 ± 15	18 ± 11	7.0± 4.4	0.06±0.01	8.67±8.34	4.9±2.2	49 ± 2	17.4 ± 2.1		
	50	34 ± 6	38 ± 26	16 ± 12	12 ± 12	4.0± 2.6	0.18±0.15	0.56±0.49	5.7±1.9	26 ± 3	12.0 ± 2.0		
	70	19 ± 5	286 ± 33	40 ± 25	84 ± 2	11.3± 0.8	0.51±0.03	0.07±0.02	12.2±1.0	13 ± 3	9.1 ± 2.3		
N	30	250±114	149 ± 28	37 ± 5	68 ± 9	12.0± 3.0	0.17±0.04	1.79±0.94	7.4±0.4	50 ± 5	16.6 ± 4.0		
	50	48 ± 36	234 ± 15	22 ± 20	69 ± 11	10.3± 1.8	0.49±0.20	0.21±0.17	10.2±0.6	22 ± 1	12.4 ± 2.0		
	70	13 ± 3	262 ± 15	41 ± 25	82 ± 3	11.6± 0.9	0.47±0.04	0.05±0.01	11.9±0.8	11 ± 1	8.2.0 ± 2.5		
S	30	199 ± 46	39 ± 31	19 ± 17	8 ± 6	5.7 ± 4.1	0.06±0.04	4.99±3.88	4.9±2.9	53 ± 4	16.3 ± 3.7		
	50	39 ± 11	248 ± 45	27 ± 26	73 ± 12	10.8± 1.7	0.40±0.07	0.16±0.06	10.7±1.1	19 ± 1	11.8 ± 1.2		
	70	14 ± 2	199 ± 14	38 ± 8	80 ± 4	11.7± 0.2	0.34±0.04	0.07±0.01	10.3±0.8	11 ± 1	9.1±1.4		
Weathering [Month]													
0													
3													
6													
Orientation													

## APPENDIX B: FIRE TEST DIAGRAMS

### B.1 Types of Diagrams

For each coating (A, B, and C), three comparison bar-charts and two comparison diagrams have been plotted and presented in this appendix. A simple guideline for the plotted comparison diagrams come in Table 28.

Table 41. Guideline for plotted comparison diagrams

Number	Weathering Period [Month]	Orientation	Pattern
1	0	NA	Solid line
2	3	North	Short dash
3	3	South	Long dash
4	6	North	Dash-dot
5	6	South	Dash-double dot

#### B1.1 Mass Loss

The normalized mass of samples during the whole test is plotted versus time (s).

#### B1.2 Heat Release Rate (HRR)

The average heat release rate ( $\text{kW/m}^2$ ) of samples during the whole test is plotted versus time (s). Note that the data used for conclusion are the average values between 0 s and 180 s, as it stated in ASTM E1354 standard.

#### B1.3 Peak Heat Release Rate (PHRR)

The peak heat release rate ( $\text{kW/m}^2$ ) of samples during the whole test is plotted versus time (s). A reminder that the performed fire tests lasted either 3 minutes after the peak heat release rate observation, or 10 minutes total (based on ASTM E1354), in the revised procedure. The revised testing procedure was used for uncoated, 3-months weathered, and 6-months weathered specimens.

#### B1.4 Effective Heat of Combustion (EHC)

The average effective heat of combustion ( $\text{MJ/kg}$ ) of samples during the whole test is plotted versus time (s).

### B1.5 Average Mass Loss Rate (AMLR)

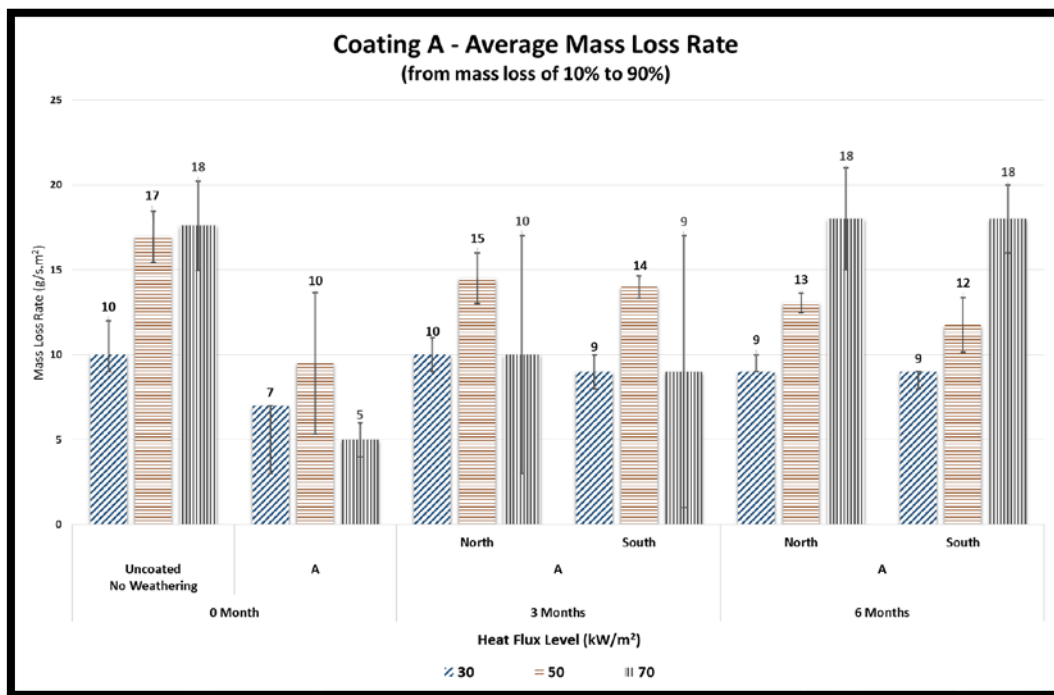
Regard to ASTM E1354, the specimen mass loss used to plot comparison bar-charts is defined as the “average specimen mass loss rate ( $\text{g}/\text{m}^2\text{-s}$ ), computed over the period starting when 10 % of the ultimate specimen mass loss occurred and ending at the time when 90 % of the ultimate specimen mass loss occurred”.

Table 42. AMLR average decrease/increase percentage during tests

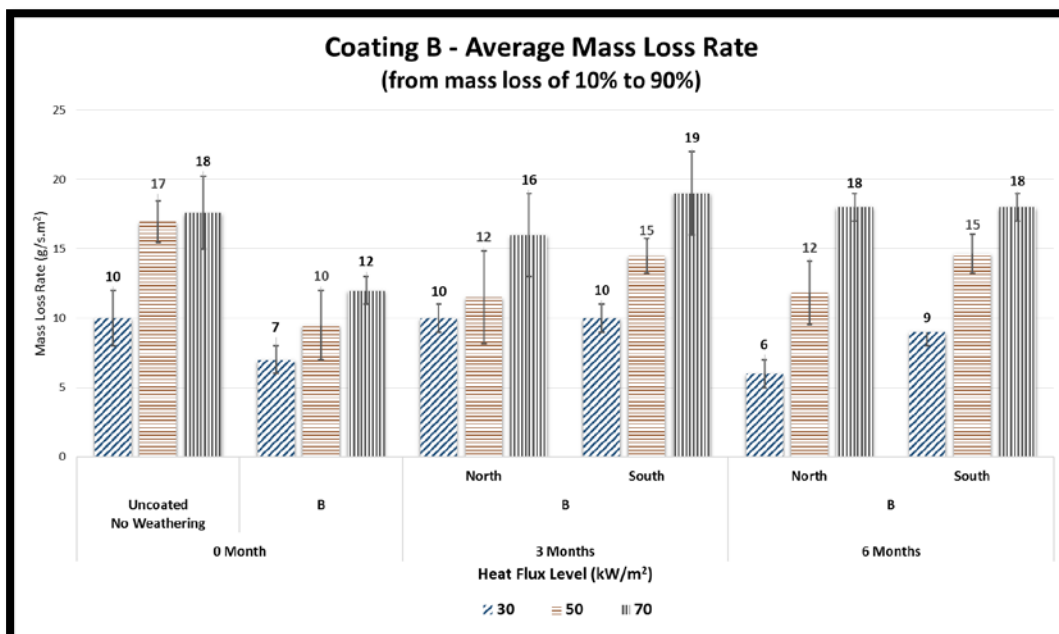
Coating	HF [kW/m <sup>2</sup> ]	Change in Comparison to	0 Month [%]	3-Months		6-Months	
				North [%]	South [%]	North [%]	South [%]
A	30	Baseline	-28	+2	-11	-15	-15
		Non-Weathered	-	+42	+25	+19	+19
	50	Baseline	-44	-14	-18	-23	-31
		Non-Weathered	-	+54	+47	+37	+24
	70	Baseline	-73	-44	-66	+2	0
		Non-Weathered	-	+104	+23	+275	+257
B	30	Baseline	-21	-2	-10	-2	-3
		Non-Weathered	-	+23	+14	+23	+22
	50	Baseline	-43	-32	-14	-32	-14
		Non-Weathered	-	+21	+53	+21	+53
	70	Baseline	-35	-8	-1	-7	+6
		Non-Weathered	-	+41	+52	+43	+63
C	30	Baseline	-47	-23	-52	-27	-52
		Non-Weathered	-	+44	-9	+37	-9
	50	Baseline	-31	-42	-66	-40	-37
		Non-Weathered	-	-16	-51	-13	-9
	70	Baseline	-50	-40	-31	-32	-41
		Non-Weathered	-	+20	+39	+35	+17

## B2 Comparison Bar Charts

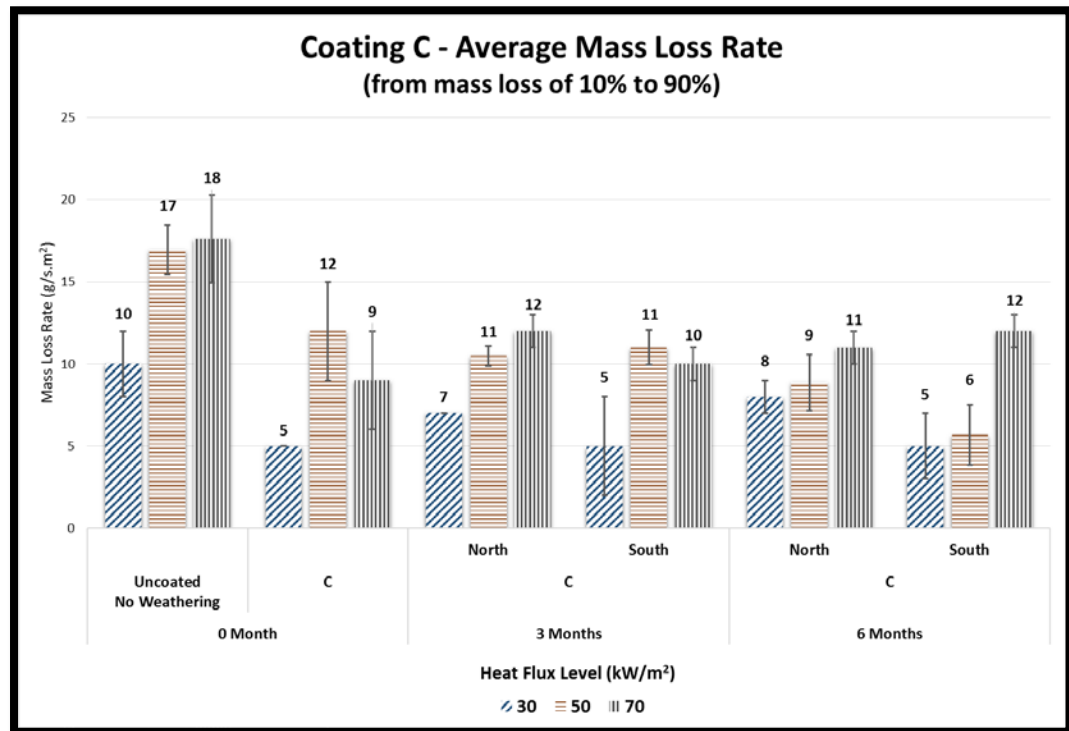
### B2.1 Coating A



### B2.2 Coating B



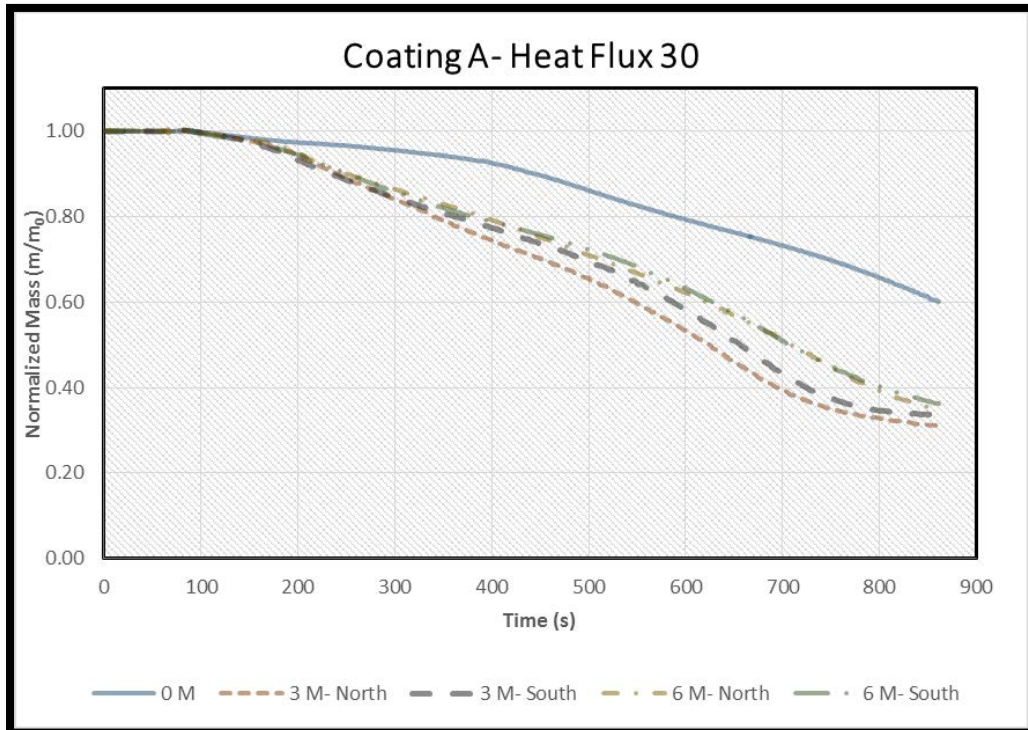
## B2.3 Coating C

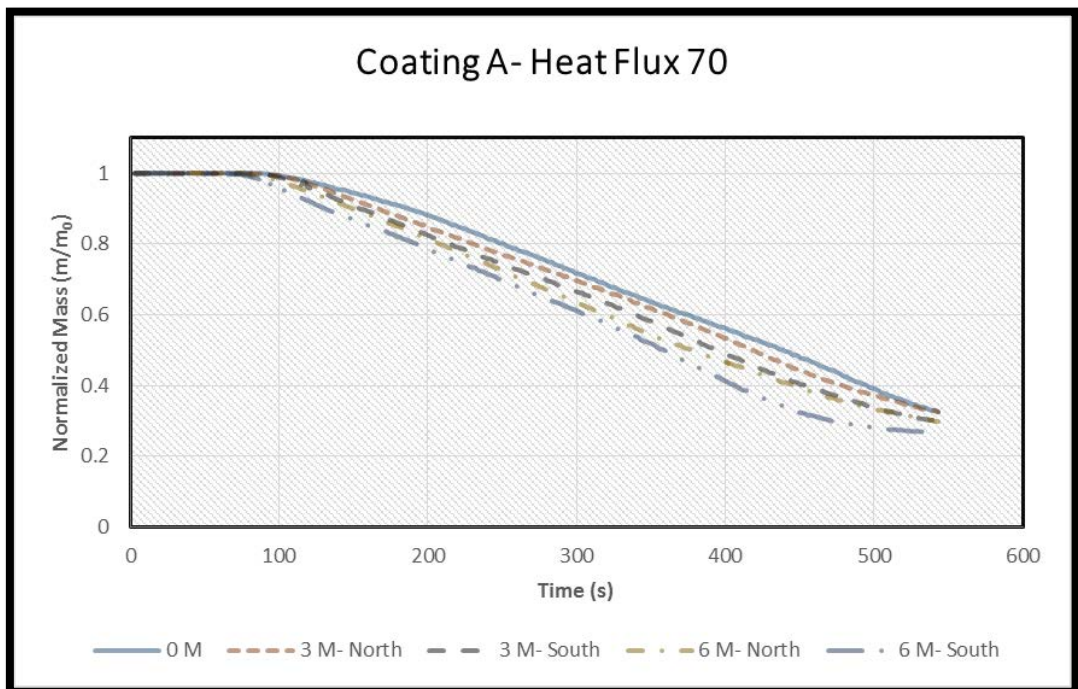
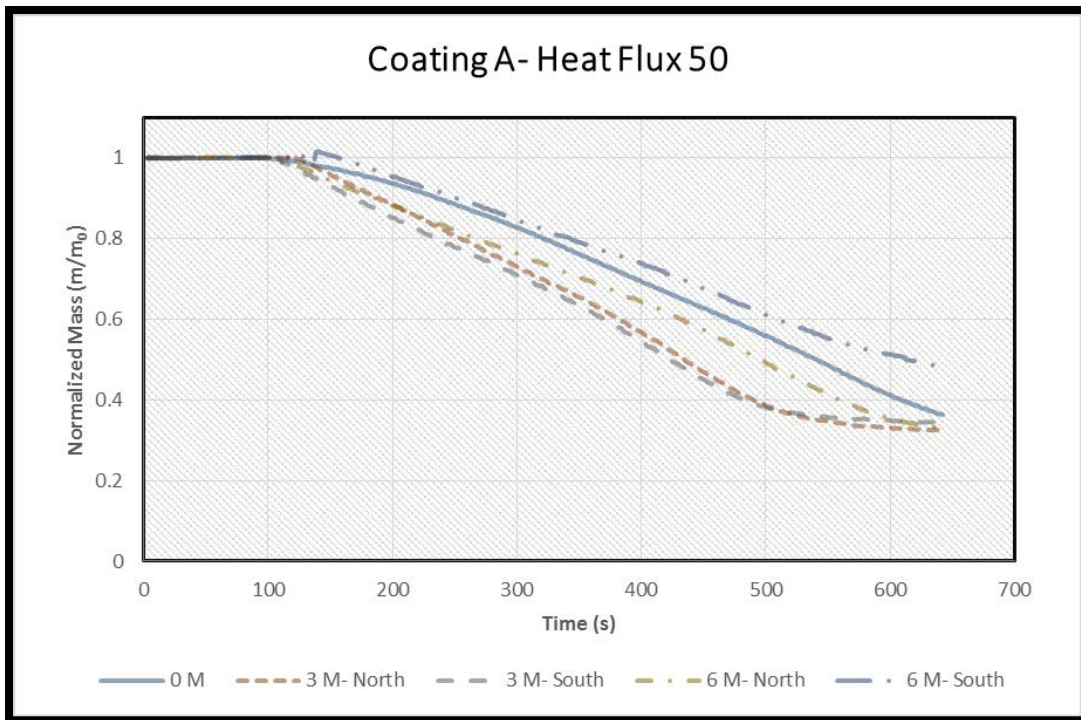


## B3 Comparison Diagrams

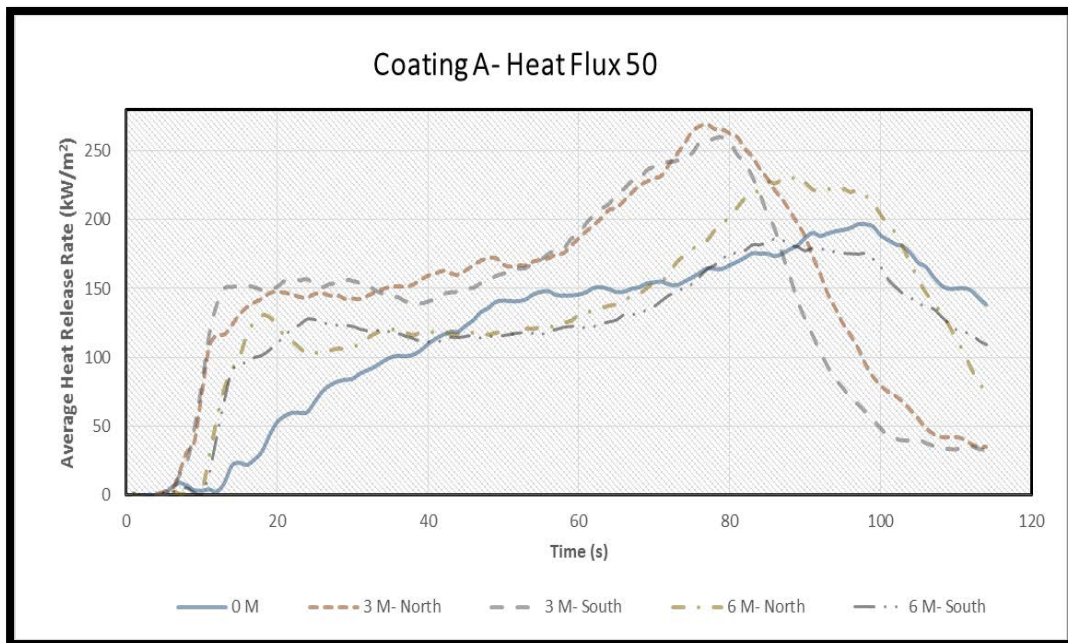
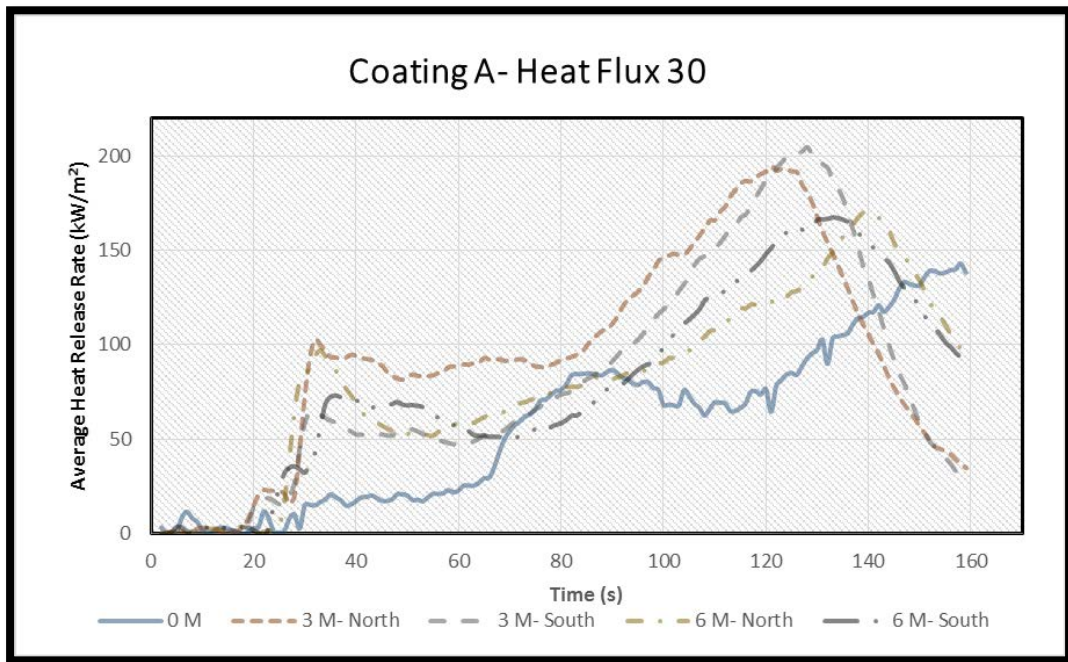
## B3.1 Coating A

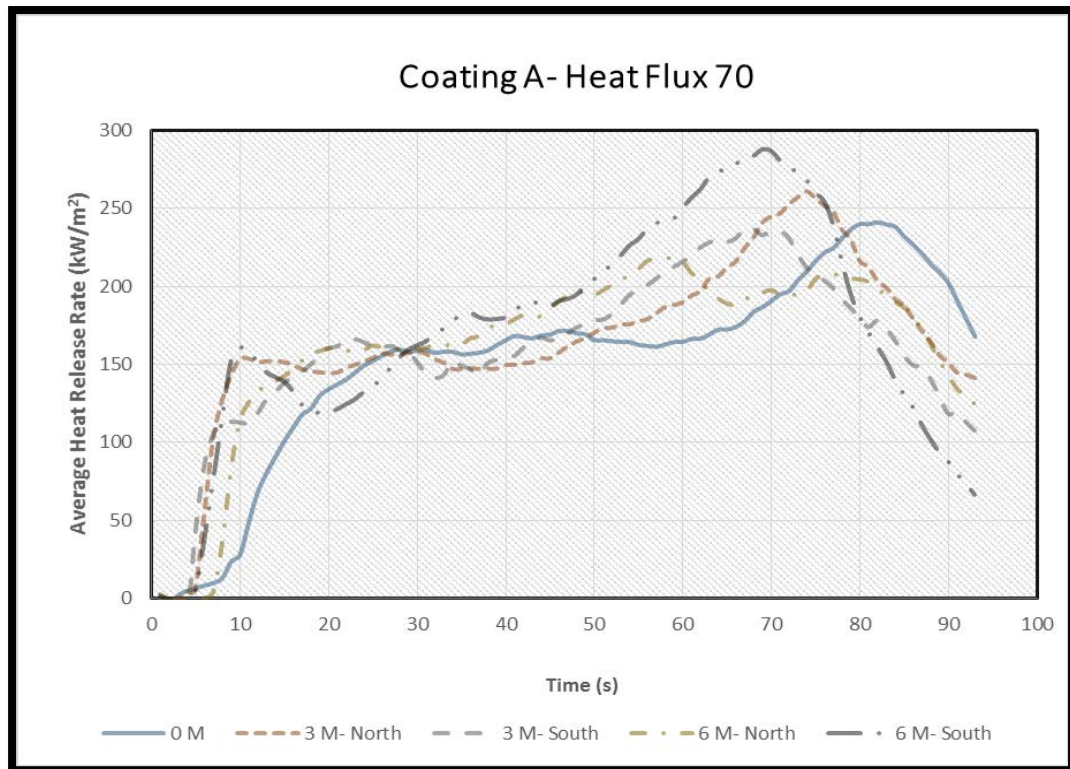
## B3.1.1 Mass Loss





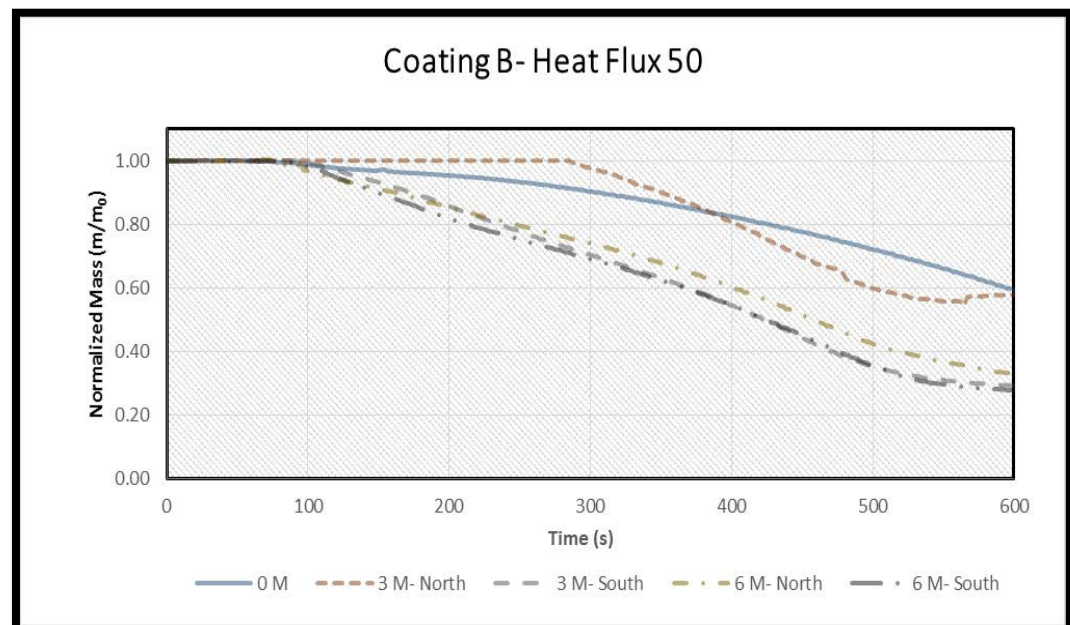
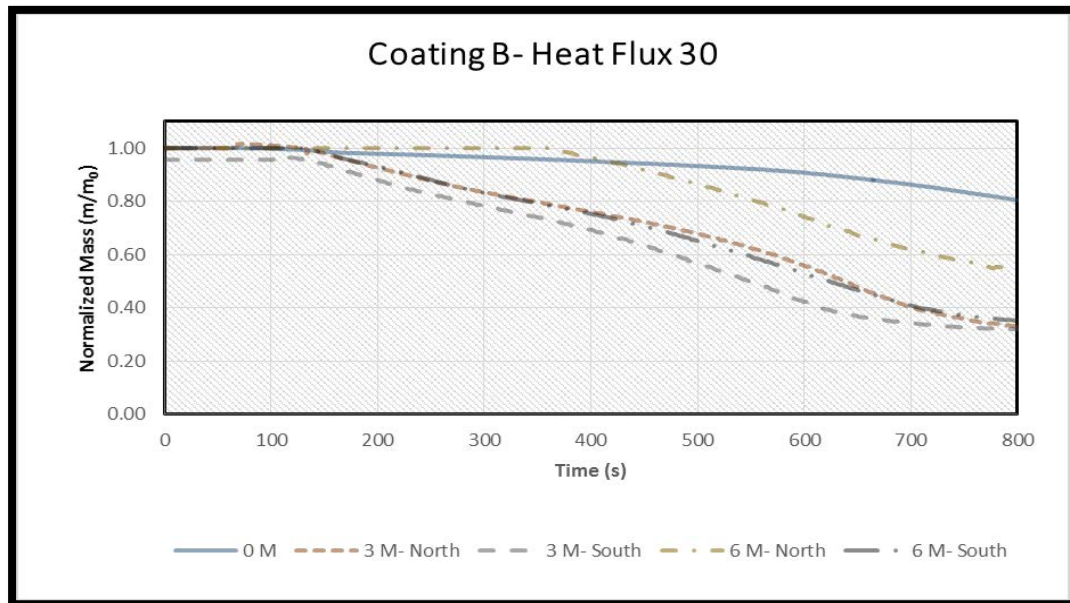
B3.1.2 Heat Release Rate

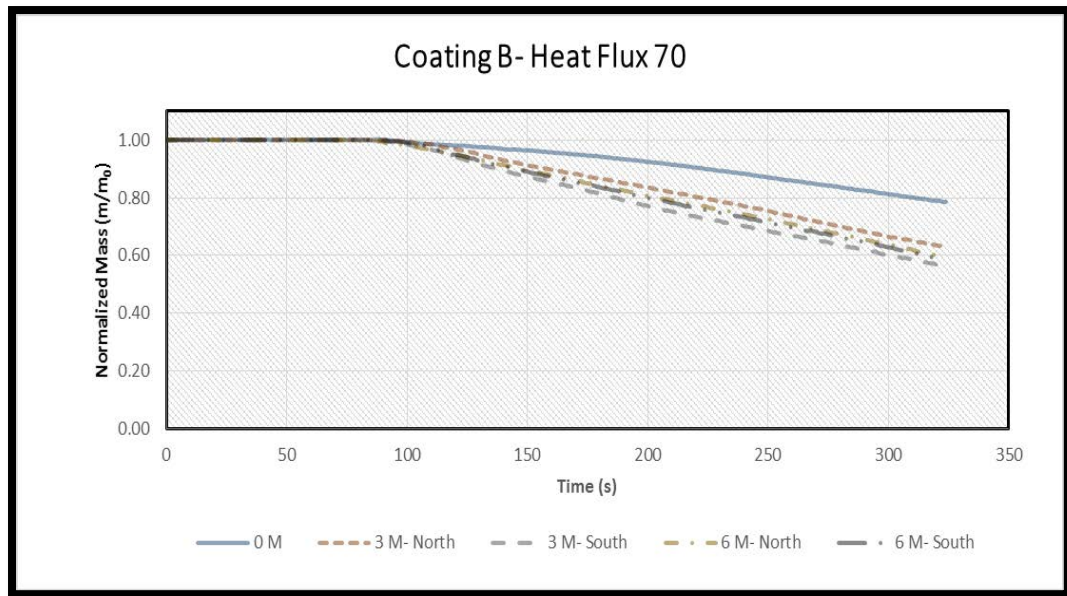




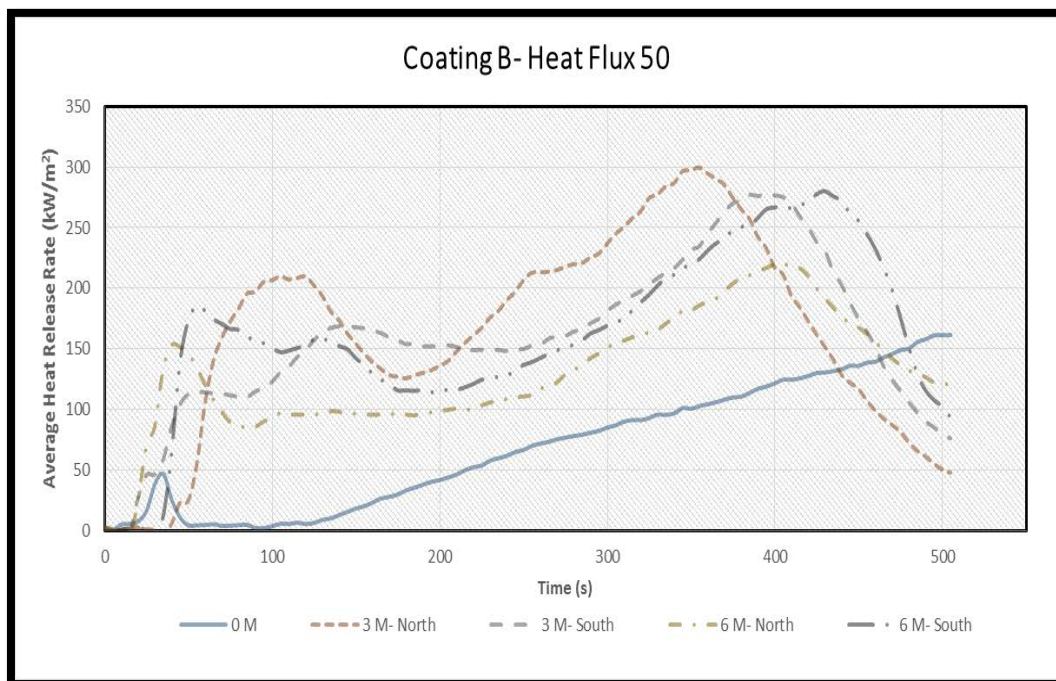
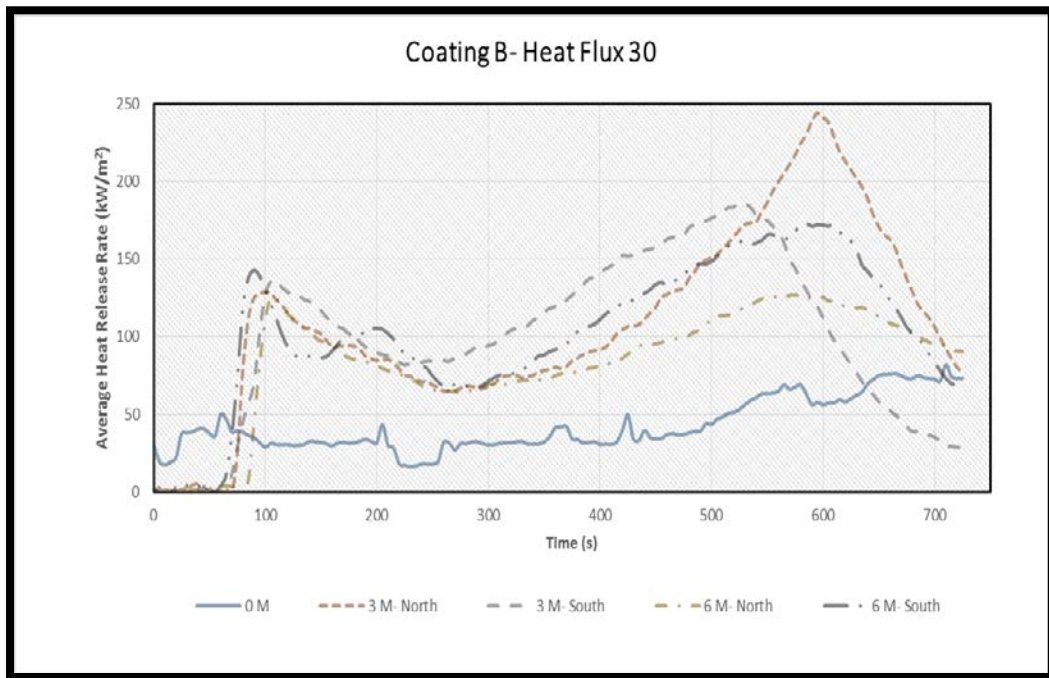
## B3.2 Coating B

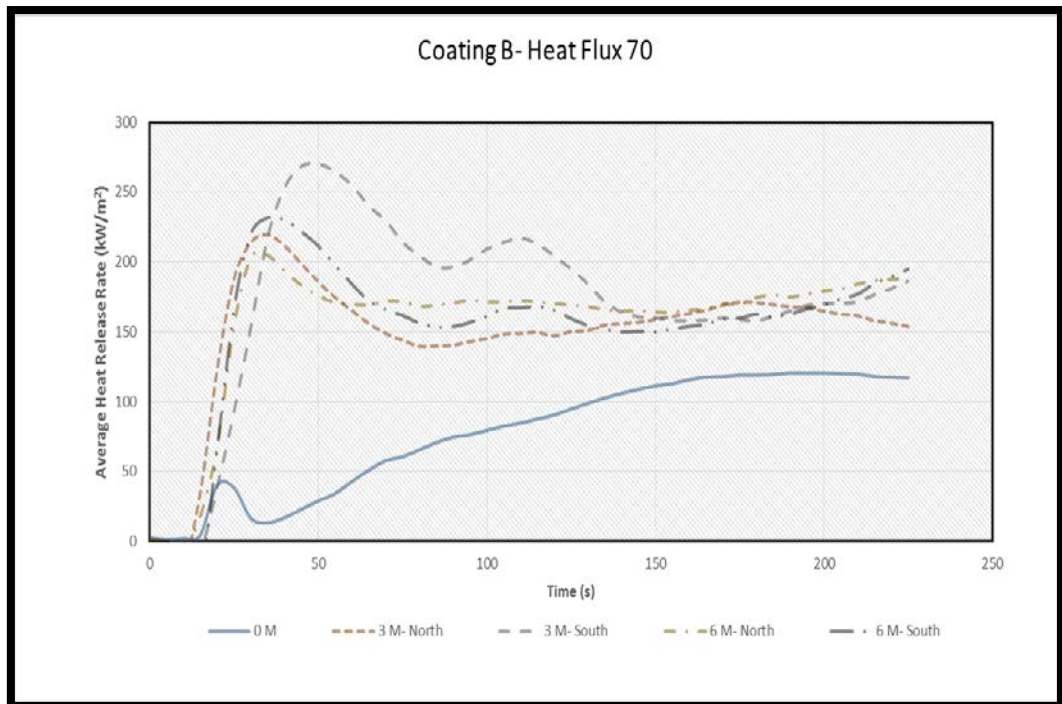
## B3.2.1 Mass Loss





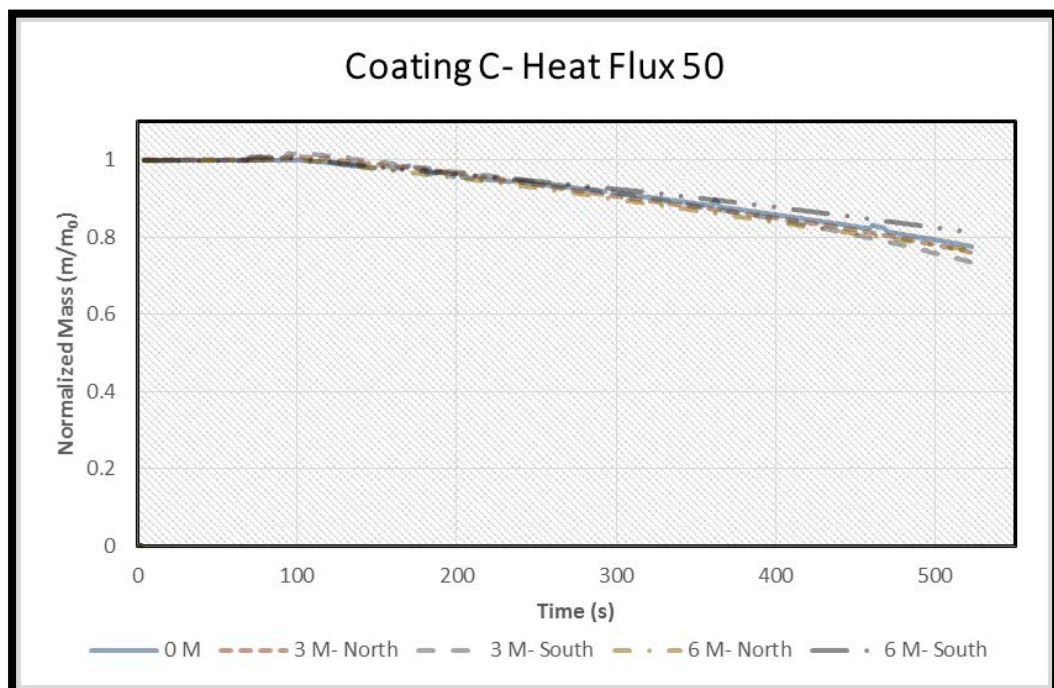
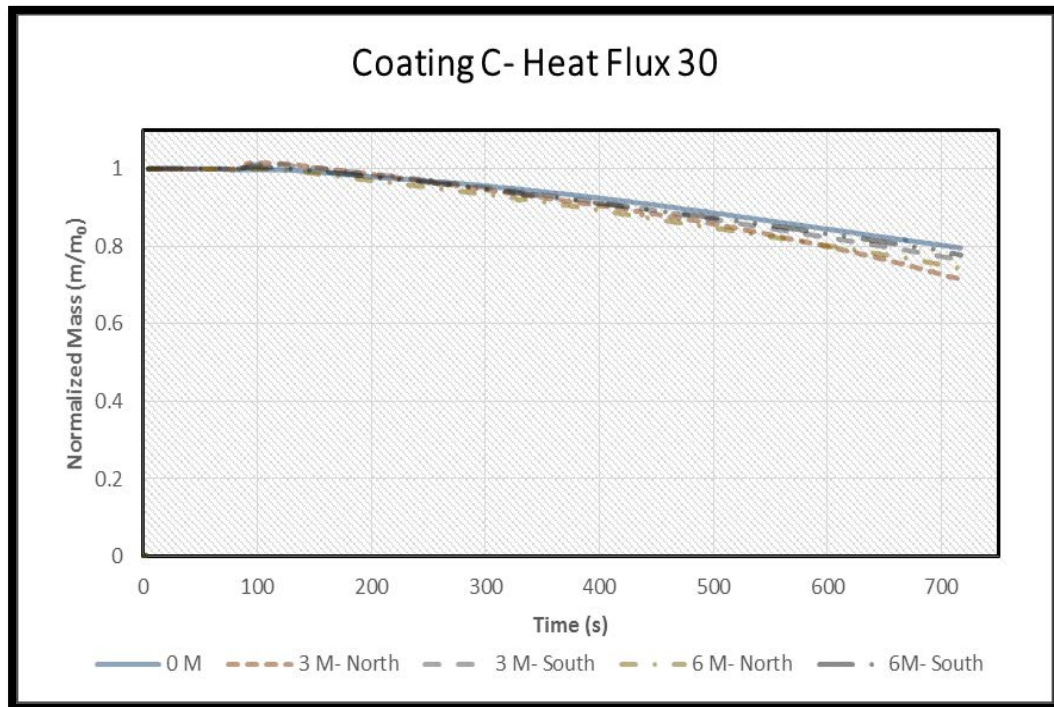
### B3.2.2 Heat Release Rate

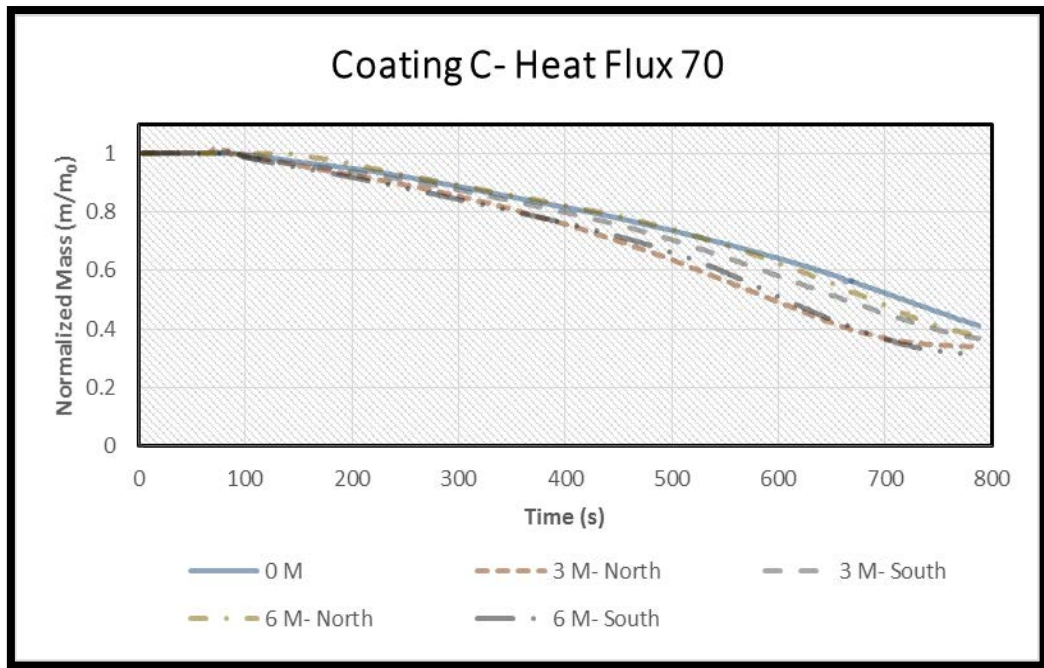




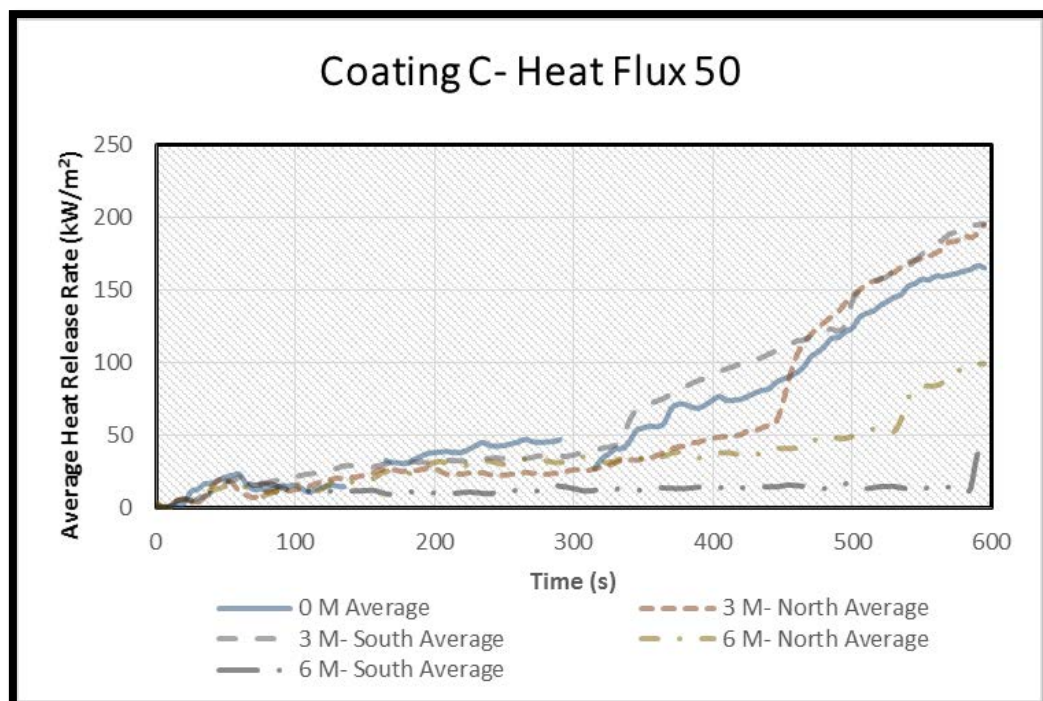
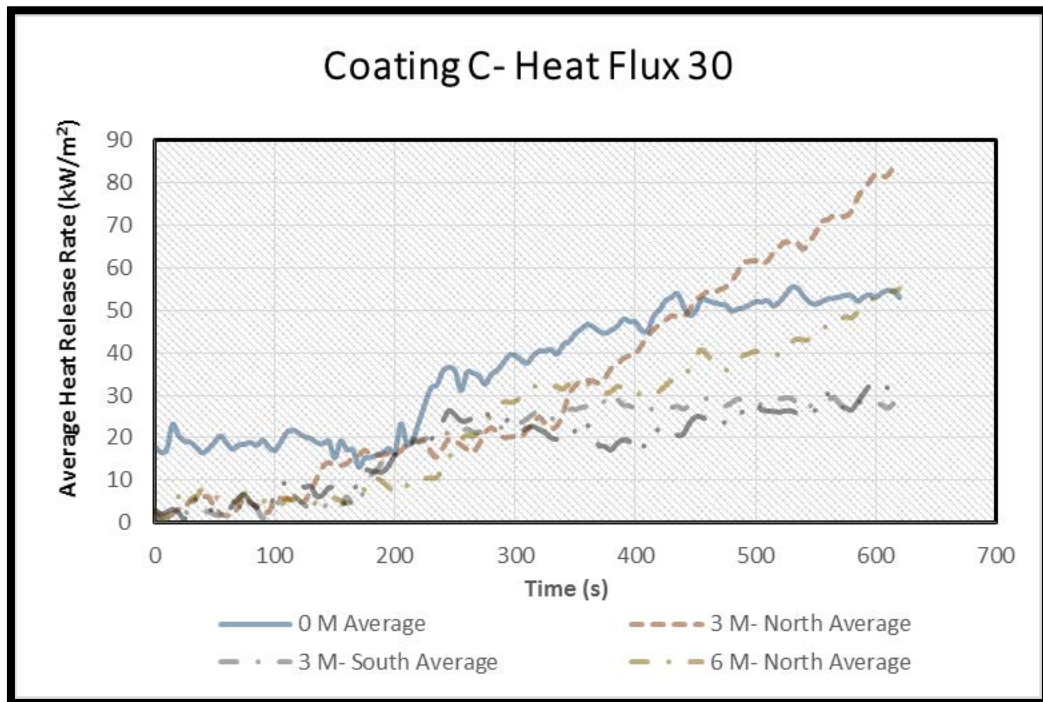
## B3.3 Coating C

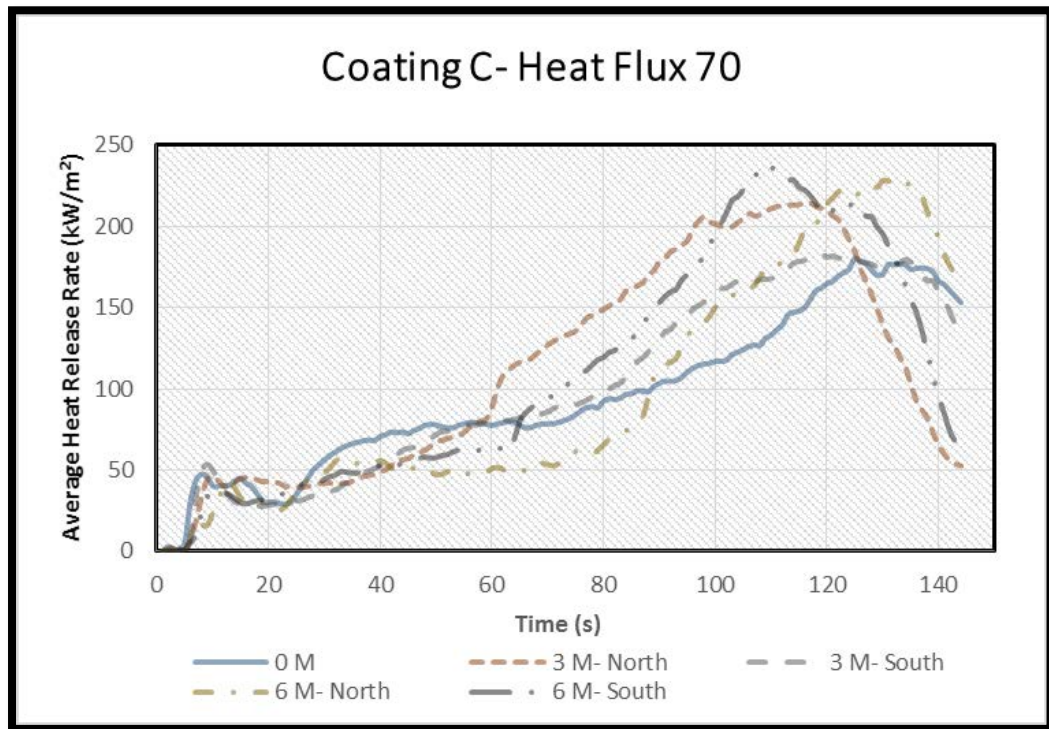
## B3.3.1 Mass Loss





## B3.3.2 Heat Release Rate





## APPENDIX C: SIMULTANEOUS DSC/TGA DIAGRAMS

The reports in this appendix have been generate by TA Instrument's software, namely "TA Universal Analysis, V4.5A".

### C.1 Types of Diagrams

In order to ease the reading, the initial, combined TGA and DSC diagrams have been separated.

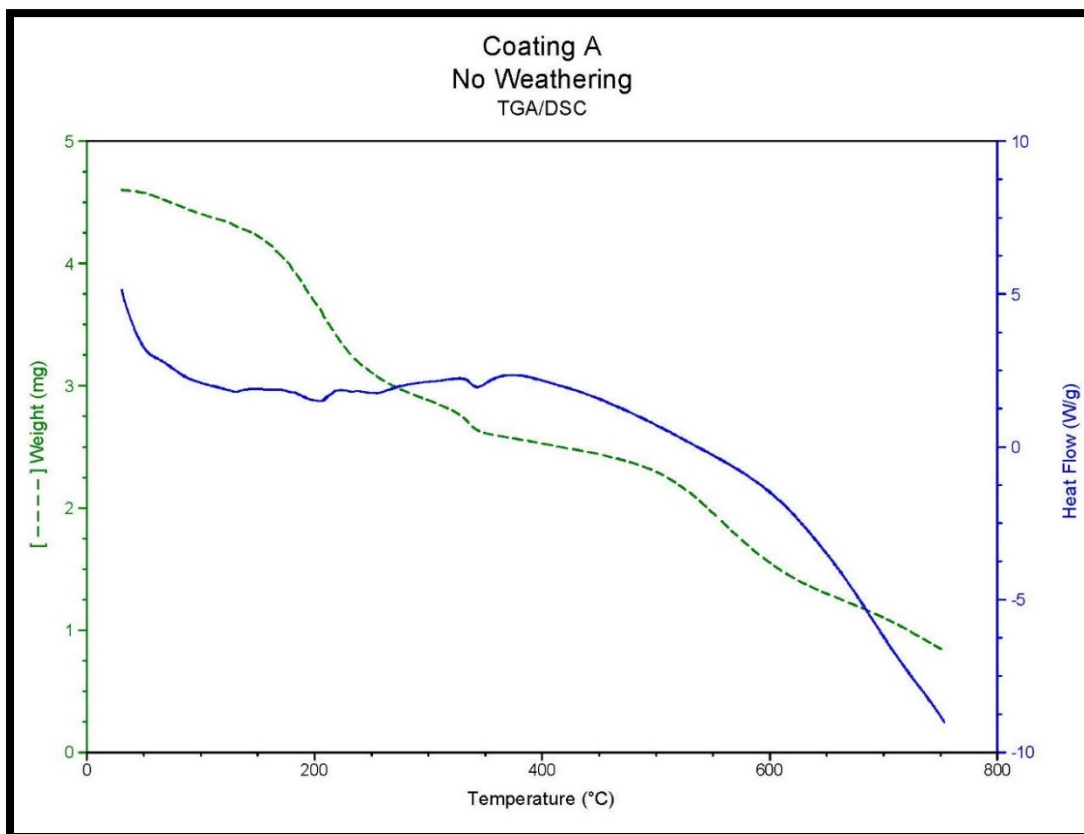
#### C1.1 Mass Loss

The mass of samples during the whole test is plotted once versus time (s), and once vs. temperature ( $^{\circ}\text{C}$ ). The time interval for recording/plotting is 1 s. Note that the normalized mass (mass percentage) vs. temperature came in the chapter 4 of this study. These diagrams are TGA results.

#### C1.2 Heat Flow

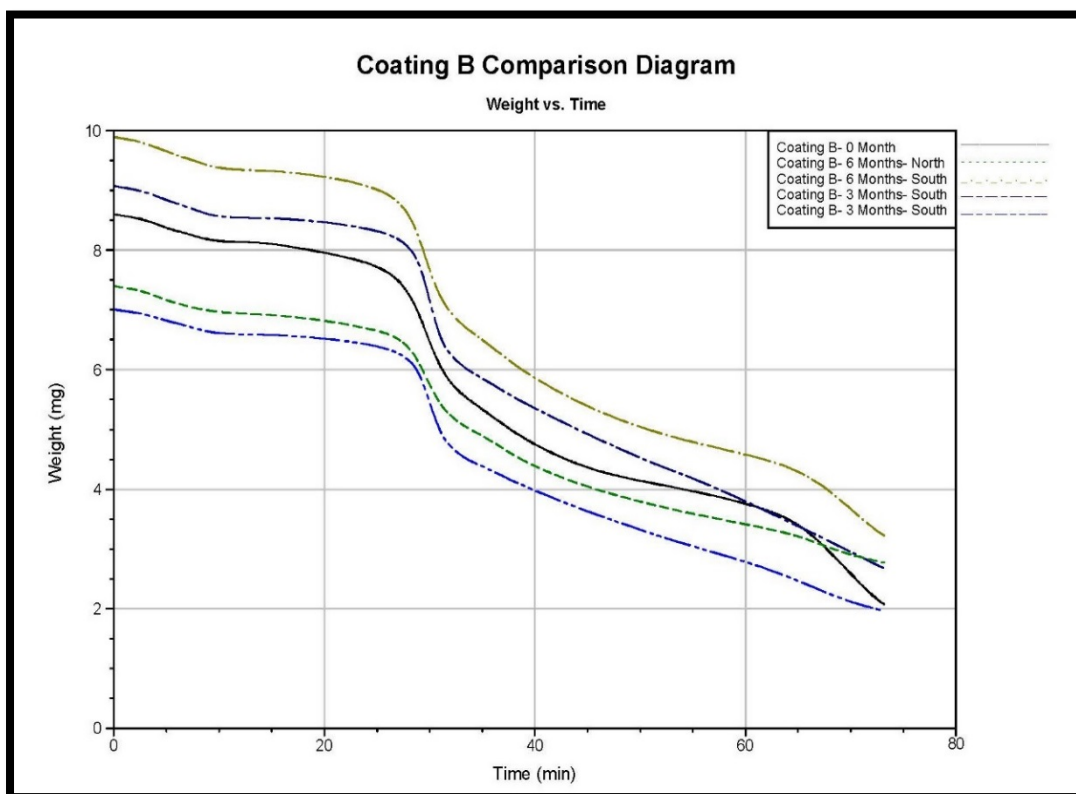
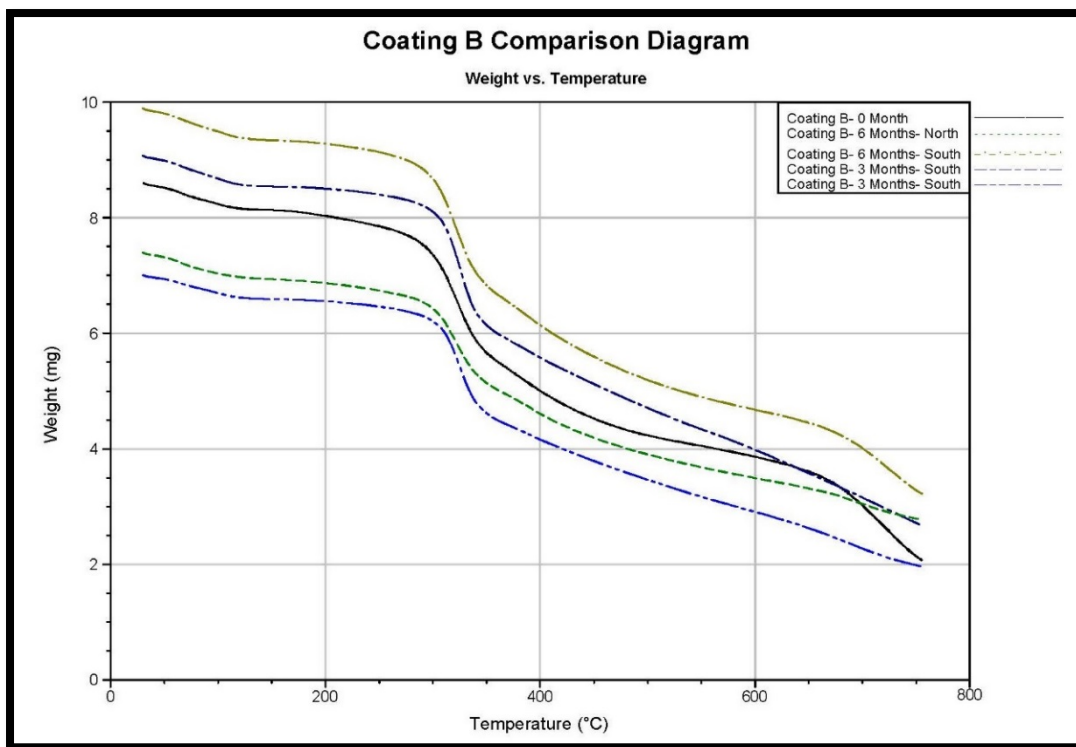
The heat flow of samples during the whole test is plotted once versus time (s), and once vs. temperature ( $^{\circ}\text{C}$ ). These diagrams are DSC results.

## C2 Coating A

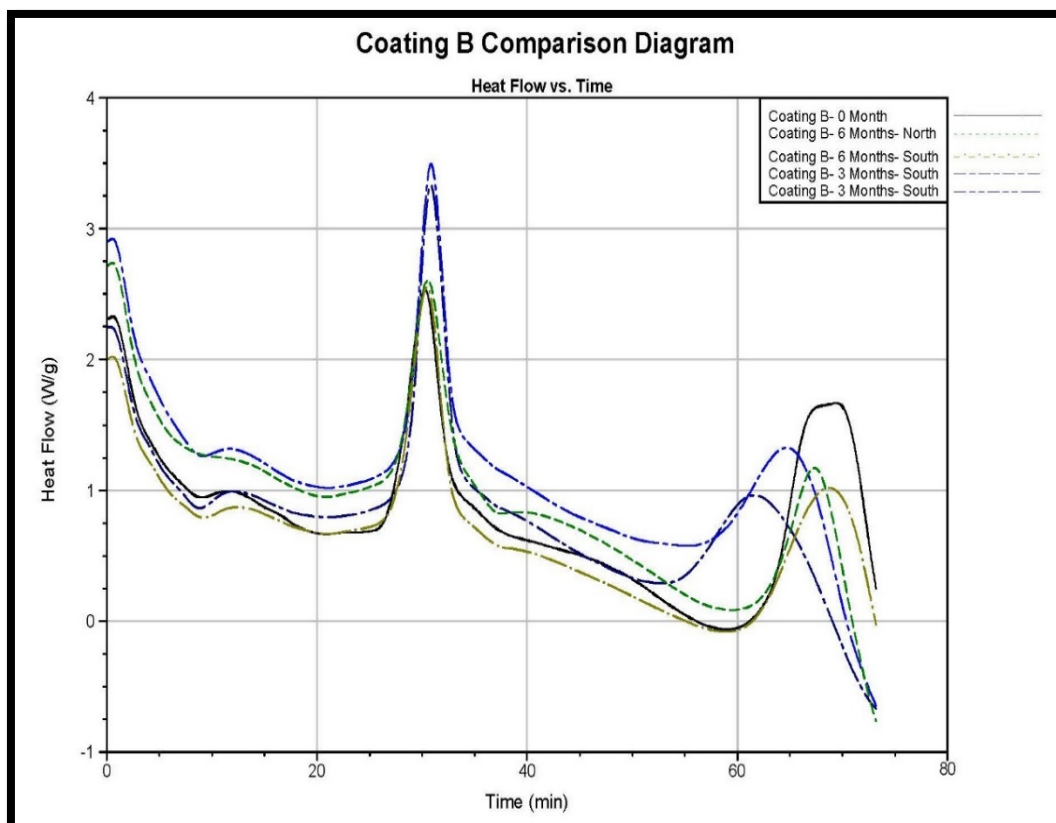
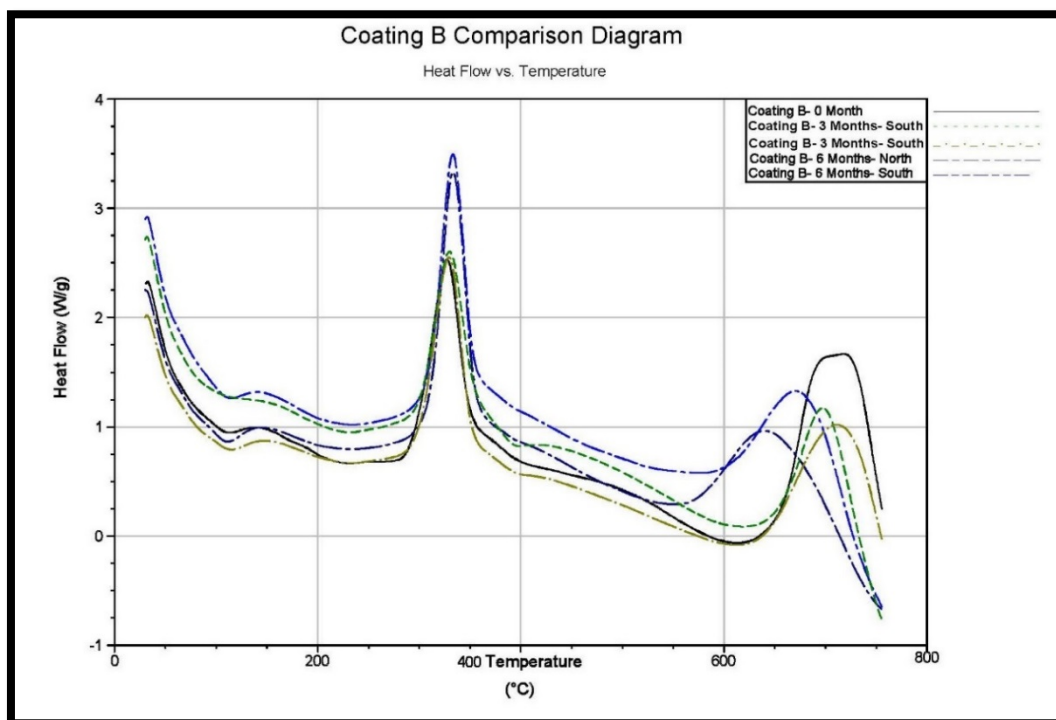


## C3 Coating B

## C3.1 TGA- Mass Loss

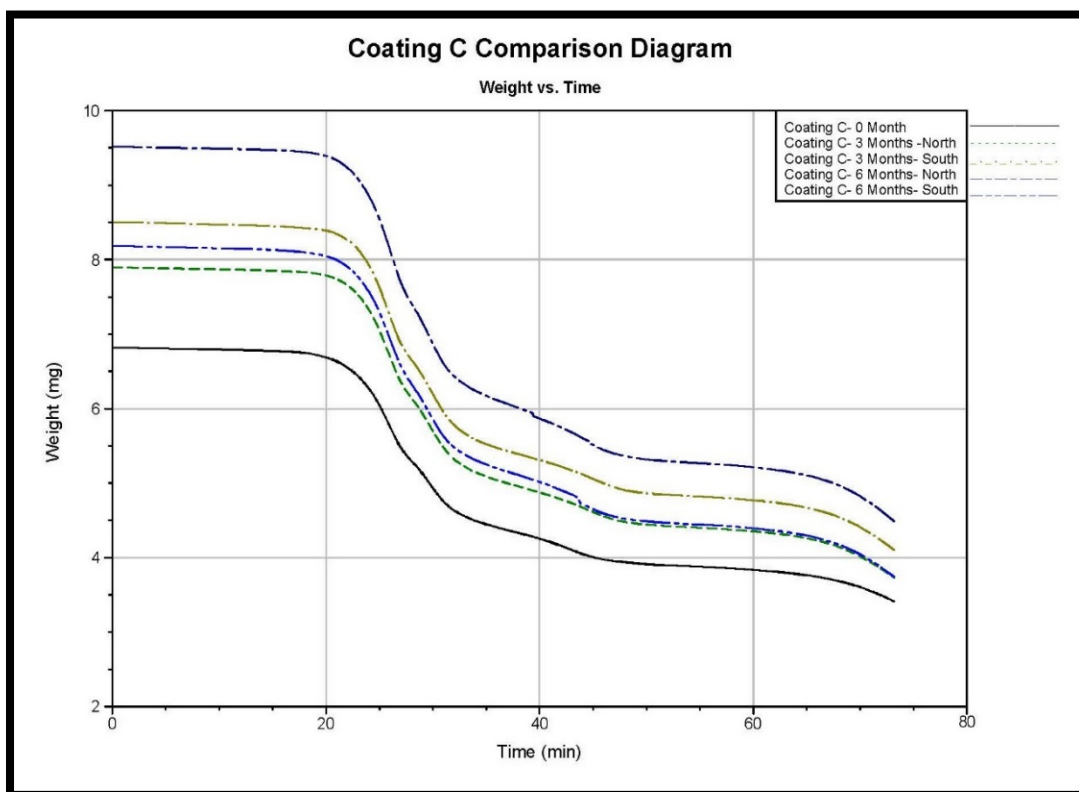
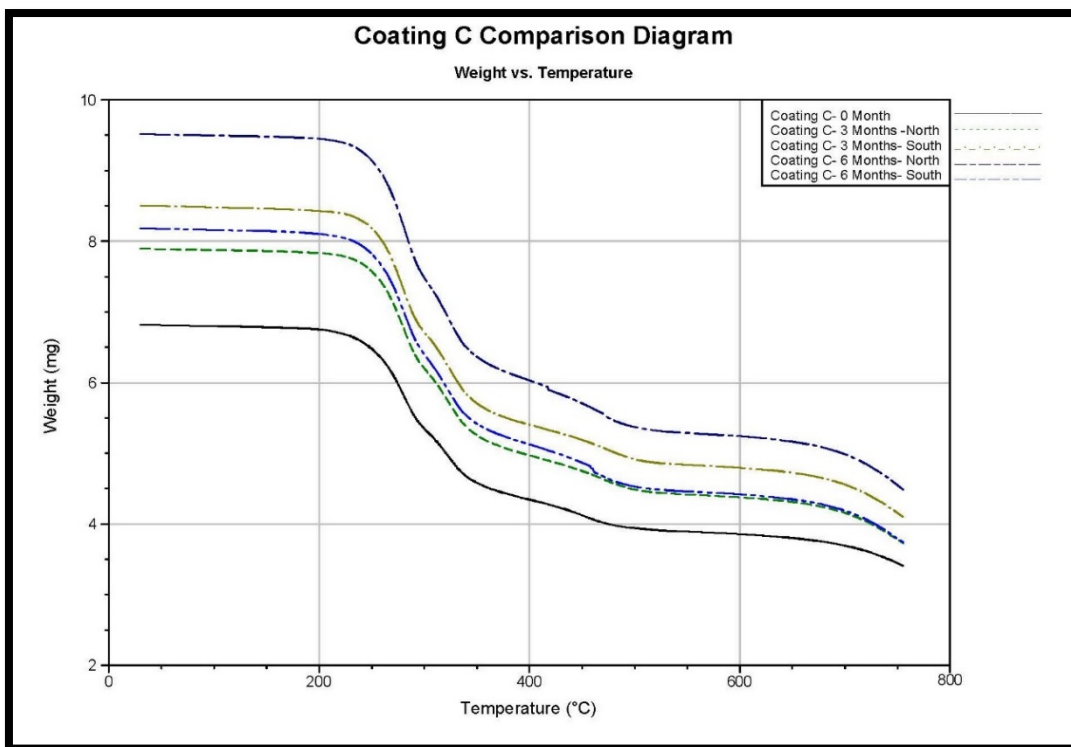


### C3.2 DSC- Heat Flow

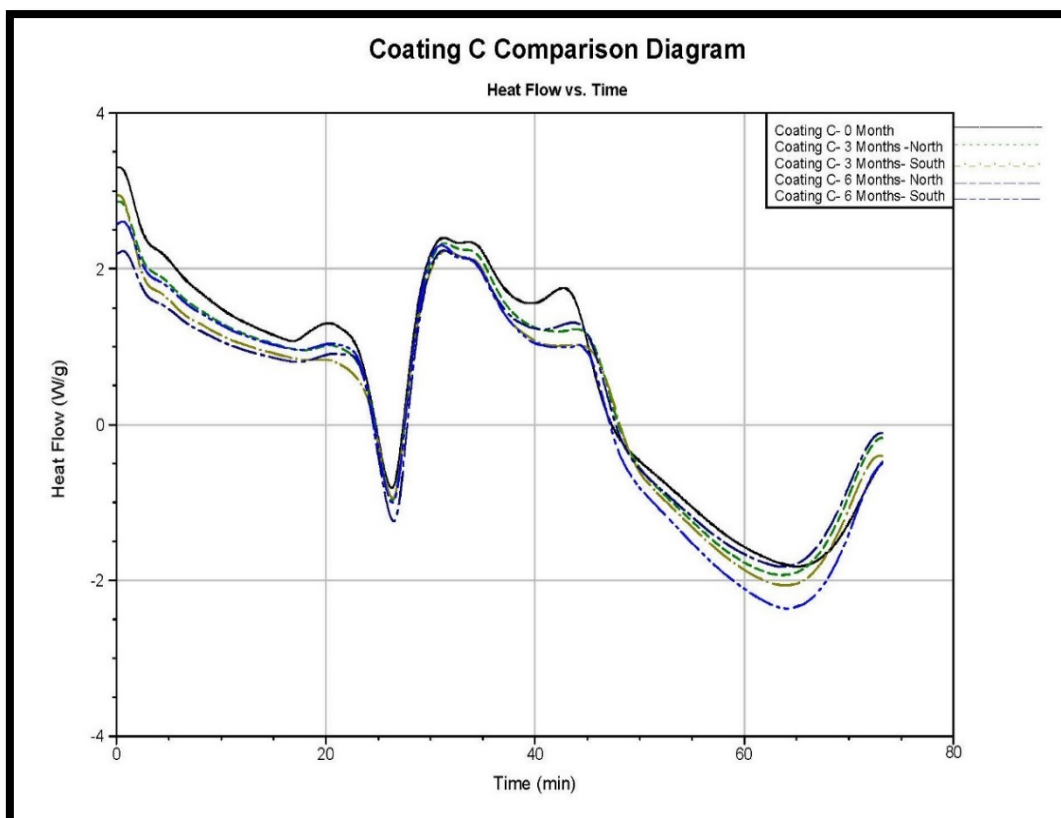
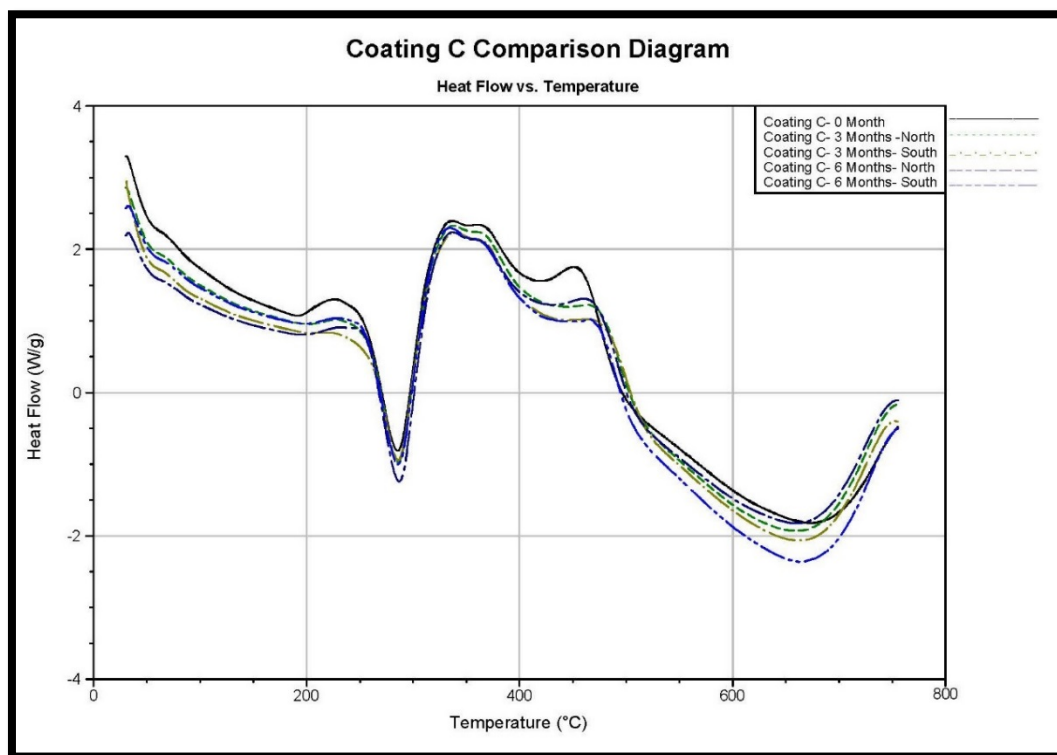


## C4 Coating C

## C4.1 TGA- Mass Loss



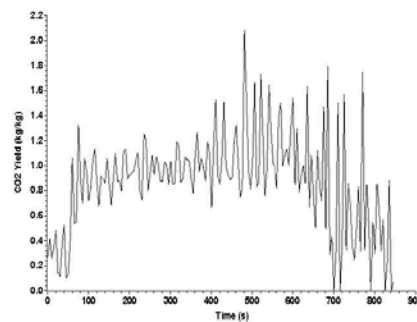
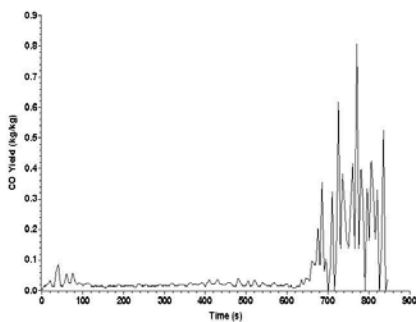
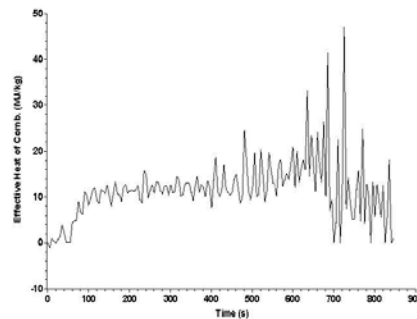
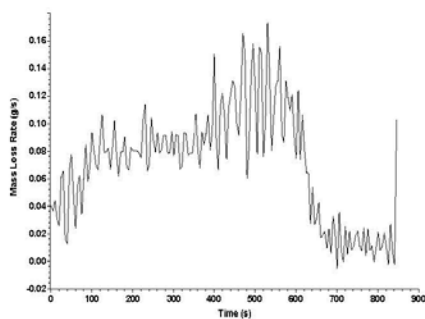
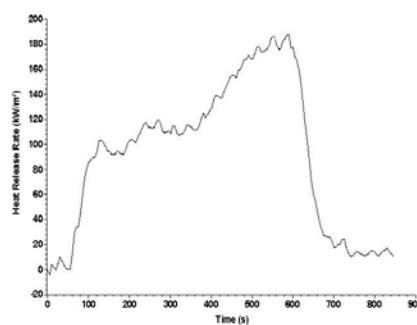
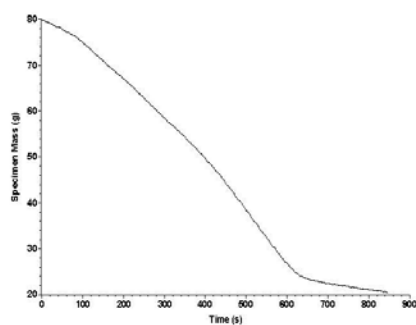
## C4.2 DSC- Heat Flow





## Cone Calorimeter Test Report

Laboratory Name UNC Charlotte Flammability Lab  
 Operator Babak Bahrani  
 File Name A121B  
 Report Name A121\*- No Weathering  
 Sample Description FirePoly FP100 water-based intumescent coating, no weathering  
 Material Name/ID A121\*



The test results relate to the behaviour of the test specimens of a product under the particular conditions of the test; they are not intended to be the sole criterion for assessing the potential fire hazard of the product in use.

## APPENDIX E: THE MATLAB CODE

This MATLAB code has been written to obtain the intumescent height using image processing.

```
function videomarks()
dirName = pwd;
files = dir(fullfile(dirName, '*.MPG'));
i=1;
filen=size(files);
for k=1:filen(1)
    videoFReader = vision.VideoFileReader(files(i).name);
    sn=size(files(i).name);
    newfolder(1:sn(2)-4)=files(i).name(1:sn(2)-4);
    mkdir(newfolder);
    framerate=videoFReader.info.VideoFrameRate;

    videoFrame=step(videoFReader);
    fprintf(1,'Pick Two Corner Points\n');
    imshow(videoFrame)

    [x,y]=ginput(2);
    box=[round(y(1)),round(y(2)),round(x(1)),round(x(2))];
    videoFrame(box(1)-2:box(1)+2, :, :)=1;
    videoFrame(box(2)-2:box(2)+2, :, :)=1;
    videoFrame(:, box(3)-2:box(3)+2, :)=1;
    videoFrame(:, box(4)-2:box(4)+2, :)=1;
    h=imshow(videoFrame);

    prompt = 'The height\n'; [height] = input(prompt);
    prompt = 'Start Time\n'; [skiptime] = input(prompt);
    prompt = 'Total Time\n'; [tot] = input(prompt);
    prompt = 'time interval\n'; [dt] = input(prompt);
    [ prompt = 'column\n'; [col] = input(prompt);
    prompt = 'row\n'; [rows] = input(prompt);

    set(gcf, 'visible', 'off')

    ny=round((box(2)-box(1))/rows);
    nx=round((box(4)-box(3))/col);

    % skip the starting time
    for j=1:skiptime*framerate
        videoFrame=step(videoFReader);
    end

    for i=1:round(tot/dt)
        for j=1:dt*framerate
            videoFrame=step(videoFReader);
        end
        for mm=1:rows+1
            videoFrame(box(1)+(mm-1)*ny-1:box(1)+(mm-1)*ny+1, :, :)=1;
        end
        for nn=1:col+1
            videoFrame(:, box(3)+(nn-1)*nx-1:box(3)+(nn-1)*nx+1, :)=1;
        end
        h=imshow(videoFrame);

        for mm=1:rows+1
            text(100,box(1)+(mm-1)*ny,num2str((rows-mm+1)*height/rows));
        end

        figname=num2str(i*dt);
        saveas(gcf,fullfile(newfolder, figname), 'jpg' );
    end
end
end
```